

Final Report

Federal Agency and Organization to Which Proposal is Submitted: U.S. Department of Energy

Federal Grant No. DE-FE-0026142

Project Title: Low Cost Air Separation Process for Gasification Applications

Principal Investigator: Dr. Gökhan O. Alptekin
TDA Research, Inc.
12345 W. 52nd Avenue
Wheat Ridge, CO 80033-1916
(303) 422-7819

Submitting Official: Same

Submission Date: July 30, 2019

DUNS Number: 181947730-0000

Recipient Organization: TDA Research, Inc.
12345 W. 52nd Avenue
Wheat Ridge, CO 80033-1916
(303) 422-7819

Project/Grant Period: October 1, 2015 to May 31, 2019

Reporting Period End Date: May 31, 2019

Report Term or Frequency Quarterly

COTR: Diane R. Madden
DOE Office of Fossil Energy NETL
626 Cochran's Mill Road
P.O. Box 10940
Pittsburgh, PA 15236-0940

Contracting Officer: David Staudt
DOE Office of Fossil Energy NETL
626 Cochran's Mill Road
P.O. Box 10940
Pittsburgh, PA 15236-0940

Signature of Submitting Official:



Low Cost Air Separation Process for Gasification Applications

Final Report

**Dr. Gökhan O. Alptekin
Dr. Ambalavanan Jayaraman
Margarita Dubovik
David Gribble
Sara Rolfe
Michael Ware**

**TDA Research, Inc.
12345 W. 52nd Avenue
Wheat Ridge, CO 80033-1916
(303) 422-7819**

Dr. Ashok Rao

**Advanced Power & Energy Program
University of California, Irvine
CA 92697-3550
(949) 824-7302 ext. 11345**

Disclaimer

This report was prepared as an account of work sponsored by an agency of the United States Government. Neither the United States Government nor any agency thereof, nor any of their employees, makes any warranty, express or implied, or assumes any legal liability or responsibility for the accuracy, completeness, or usefulness of any information, apparatus, product or process disclosed, or represents that its use would not infringe privately owned rights. Reference therein to any specific commercial product, process, or service by trade name, trademark, manufacturer, or otherwise does not necessarily constitute or imply its endorsement, recommendation, or favoring by the United States Government or any agency thereof. The views and opinions or authors expressed herein do not necessarily state or reflect those of the United States government or any agency thereof.

Abstract

In this project, TDA Research, Inc. (TDA) has further developed TDA's chemical absorbent-based air separation process that can deliver low-cost oxygen to various advanced power generation systems, including oxygen-fired pulverized coal boilers and Integrated Gasification Combined Cycle (IGCC) power plants. TDA's absorbent operates at high temperature and hence eliminates the thermodynamic inefficiencies inherent in the conventional cryogenic air separation units (ASUs). Unlike the sorbents used in commercial Pressure Swing Adsorption (PSA) systems, our sorbent selectively removes oxygen (not nitrogen); which allows the effective utilization of the large amounts of energy in the high pressure oxygen-depleted stream. As a result, the new air separation system is very efficient and delivers a low cost oxygen product.

TDA, in collaboration with University of California, Irvine has increased the technical maturity and commercial viability of the new technology by: 1) demonstrating continuous oxygen generation in a prototype test system, and 2) carrying out a high fidelity process design and economic analysis. With the successful completion of the R&D effort, the technology is now ready for a larger pilot-scale demonstration and the technology readiness has been raised from TRL 4 to TRL 6. TDA's ASU unit provides significant improvement in overall plant performance increasing the net plant efficiency from 32% to 34.05% for the cold gas cleanup Case for GE gasifier while the improvement is lower for the warm gas cleanup case at 35.33% vs 34.46%. The 1st year Cost of Electricity (COE) and the Cost of CO₂ Capture are also lower for the TDA ASU than that for the cryogenic ASU. For an IGCC power plant integrated with a cold gas cleanup system that uses GE gasifiers, the use of our system instead of a cryogenic unit reduces the COE per MWh from \$142 to \$127.1 while the cost of CO₂ capture including TS&M goes from \$47 to \$37 per tonne. However for an IGCC power plant integrated with a warm gas cleanup system the reduction is much smaller, the COE per MWh is \$134 vs \$121.9 while the cost of CO₂ capture including TS&M is \$41 vs \$30 per tonne.

Table of Contents

Abstract.....	4
Table of Contents.....	5
List of Tables	6
List of Figures	6
Executive Summary.....	9
1. Introduction	12
1.1 TDA's Air Separation Process	12
2. Project Objectives	14
2.1 Work Plan.....	15
3. Results	16
3.1 Task 1. Project Management and Planning (PMP)	16
3.2 Task 2. Sorbent Production Scale-up	17
3.3 Task 3. Sorbent Life Tests.....	19
3.4 Task 4. Adsorption, CFD Modeling and Reactor Design.....	23
3.4.1 CFD Modeling and Reactor Design.....	23
3.4.2 Adsorption Modeling	32
3.5 Task 5. Optimization of Cycle Sequence	38
3.6 Task 6. Design of 1 kg/hr Prototype Unit.....	40
3.7 Task 7. Fabrication of 1 kg/hr Prototype Unit.....	42
3.8 Task 8. Testing of the Prototype Unit.....	46
3.9 Task 9. Techno-economic analysis.....	52
3.9.1 TDA's System Design	65
4. Conclusions and Recommendations	69
4.1 Recommendations for Future Work	69
5. References	70
Appendix A	71

List of Tables

Table 1. Comparison of TDA's ASU unit against cryogenic ASU for IGCC power plants.....	11
Table 2. Project Milestone Log.....	16
Table 3. Extrudate Compositions.	19
Table 4. System dimensions	32
Table 5. Model equations used for breakthrough simulation.....	33
Table 6. Process variables used in the full-model optimization.....	38
Table 7. Time at (or above) temperature for reactor R-140 by internal TC location	49
Table 8. Overall Plant Performance – IGCCs with TDA ASU - Cold Gas Cleanup.	55
Table 9. Overall Plant Performance – IGCCs with TDA ASU - Warm Gas Cleanup.	56
Table 10. Overall Plant Performance – IGCCs with Cryogenic ASU - Cold Gas Cleanup.....	57
Table 11. Overall Plant Performance – IGCCs with Cryogenic ASU - Warm Gas Cleanup.....	58
Table 12. Plant Cost Summary (2011 \$1000) – IGCCs with TDA ASU - Cold Gas Cleanup.....	59
Table 13. Plant Cost Summary (2011 \$1000) – IGCCs with TDA ASU - Warm Gas Cleanup. ..	60
Table 14. Plant Cost Summary (2011 \$1000) – IGCC with Cryogenic ASU - Cold Gas Cleanup.	61
Table 15. Plant Cost Summary (2011 \$1000) –IGCC with Cryogenic ASU - Warm Gas Cleanup.	62
Table 16. Process economics for IGCC plants with TDA ASU.	63
Table 17. Process economics for IGCC plants with Cryogenic ASU.....	64
Table 18. Summary of sorbent characteristics.....	66
Table 19. Summary of TDA ASU Plant Costs – Case 1A (\$ 2011 basis) integrated with IGCC plant with GE gasifier and cold gas cleanup.....	67
Table 20. Summary of TDA ASU Plant Costs – Case 2A (\$ 2011 basis) integrated with IGCC plant with E-gas gasifier and cold gas cleanup.....	67
Table 21. Summary of TDA ASU Plant Costs – Case 1B (\$ 2011 basis) integrated with IGCC plant with GE gasifier and warm gas cleanup.....	68
Table 22. Summary of TDA ASU Plant Costs – Case 2B (\$ 2011 basis) integrated with IGCC plant with E-gas gasifier and warm gas cleanup.....	68

List of Figures

Figure 1. Oxygen transfer cycle.	9
Figure 2. Average oxygen capacity of each sorbent batch from TGA data.	9
Figure 3. Optimized PSA cycle sequence and steps.	10
Figure 5. TDA's 1 kg/hr prototype oxygen generation unit.	10
Figure 4. Stable operation with the improved steam generation and temperature. Several interruptions are indicated during the roughly 70-hour test snapshot. In between steam interruptions, the oxygen product purity is at or above 98%.	10
Figure 6. Energy demand of the air separation unit in a 210 MW oxy-fired PC combustion power plant (Nskala et al., 2008).....	12
Figure 7. TDA's air separation system integrated with a coal-fired power plant.	13
Figure 8. Oxygen transfer cycle.	13
Figure 9. Integration of the air separation system to the IGCC plant.	14

Figure 10. Stainless steel calciner.....	17
Figure 11. 2" Extruder	17
Figure 12. Results of TGA screening cycles showing stable oxygen capacity of the sorbents... Figure 13. Average oxygen capacity of each sorbent batch from TGA data.	18
Figure 14. Modified fixed bed reactor system that allows counter current operation used for 6,000 cycle life tests.....	19
Figure 15. P&ID of the fixed bed system with capability for counter current operation.....	20
Figure 16. Results from multiple cycle life tests.....	20
Figure 17. Sorbent life test with the proof-of-concept reactor system. Oxy-combustion plant operating condition: $P_{ads}=100\text{psia}$	21
Figure 18. Sorbent life test with the proof-of-concept reactor system. Oxy-combustion plant operating condition: $P_{ads}=100\text{psia}$	22
Figure 19. Extended sorbent life test under rapid cycle conditions.	22
Figure 20. Example of Fit to Sorption Data.....	23
Figure 21. Values for R^2 and % of saturation at end of fit for all datasets.	24
Figure 22. TDA Bed Temperature Plot	24
Figure 23. Peak Sorbent Temperatures for Calibration Simulation – Various Cases	25
Figure 24. Sorbent Capacity with Time for Validation Modeling vs. Test Data	25
Figure 25. 1kg/h Vessel Geometry.....	26
Figure 26: Middle TC Temperature After 6 Minutes (K) for Low Flow (Top) and Moderate Flow (Bottom) Cases	27
Figure 27. Sorbent Temperature at Middle TC for Select Cases with Higher Flow Rate and External HTC after 6 and 20 minutes	28
Figure 28. Sorbent Bed Temperatures (K) for Case 4-C at 6 minutes (top) and 20 minutes (bottom) for Moderate Gas Flow Rates	29
Figure 29. Example Simulation Results (Temperature Contours) for Cooling with Inner Tube (Top) and Jacket Cooling (Bottom).....	30
Figure 30. Sorbent Temperature for Active Cooling Simulations with Max/Average/Min Temperatures for Jacket Cooling (Red) and Inner Tube Cooling (Green).....	30
Figure 31. Peak and Mass-Weighted Average (MWA) Sorbent Loading for Jacket and Inner Tube Cooling Methods	31
Figure 32. Schematic of the Breakthrough apparatus.....	32
Figure 33. Dead volume experiment	34
Figure 34. Point by point correction.....	35
Figure 35. Experimental breakthrough composition and temperature profiles	35
Figure 36. Experimental Oxygen loading and isotherm fit	36
Figure 37. Experimental and simulated breakthrough composition profile	37
Figure 38. Experimental and simulated breakthrough temperature profile	37
Figure 39. Pareto front Purity vs Recovery for TDA material using a LPP cycle	39
Figure 40. Optimized PSA cycle sequence and steps.	39
Figure 41. Typical cycle sequence for the 1-kg/hr prototype unit.	40
Figure 42. P&ID of the 1-kg/hr prototype unit.	41
Figure 43. Drawing of the sorbent bed for the 1-kg/hr prototype unit.	41
Figure 44. 3-D layout of the 1-kg/hr oxygen production prototype unit.....	42
Figure 45. The completed structural frame assembly for the demo-scale tests system with mounted electronics enclosure and high-temperature tube furnaces.....	42
Figure 46.The electronics enclosure with the main components populated and awaiting field wiring to the instrumentation.	43
Figure 47. A complete Incoloy 800H vessel positioned within one of the Mellen tube furnaces. 43	
Figure 48. The completed structural frame assembly with the high temperature reactors and tube furnaces installed.	44

Figure 49. Fabrication of the Ceramic insulation/support.....	44
Figure 50. High-temperature passive cooling loops.....	44
Figure 51. Prototype unit being moved from TDA's Fabrication shop to the test lab.....	45
Figure 52. The prototype unit as installed at TDA's Golden, CO test facility with power delivered from the 3-phase 480V (wye) connection and the on-board control PC energized.	45
Figure 53. The electronics enclosure with the main components populated and showing field wiring to the instrumentation.	45
Figure 54-Relief header assembly, relief indicating sensor, and outlet plumbing that integrates to dilution duct above drop ceiling.	46
Figure 55. Prototype unit installed at TDA's TM facility.....	46
Figure 56. Impact of absorption time.	47
Figure 57. Bed temperatures in single bed tests.	48
Figure 58. Oxygen purity at different absorption time.	48
Figure 59. Stable operation with the improved steam generation and temperature. Several interruptions are indicated during the roughly 70-hour test snapshot. In between steam interruptions, the oxygen product purity is at or above 98%.	50
Figure 60. Relationship between O ₂ product purity and production rate.	51
Figure 61. Absorption process.	65
Figure 62. Regeneration process.	65
Figure 63. Overview of reactor design.....	66
Figure 64. Overview of 8 bed cycle scheme. Total Cycle time = 8 min.....	67

Executive Summary

In this project, TDA further developed a new chemical absorbent-based air separation process that can deliver low-cost oxygen to various advanced power generation systems, including oxygen-fired pulverized coal boilers and Integrated Gasification Combined Cycle (IGCC) power plants. TDA's absorbent process operates at high temperature and hence eliminates the thermodynamic inefficiencies inherent in the conventional cryogenic air separation plants. Unlike the sorbents used in the commercial Pressure Swing Adsorption (PSA) systems, our sorbent selectively removes oxygen (not nitrogen); which allows the effective utilization of the large amounts of energy in the high pressure oxygen-depleted stream. As a result, the new air separation system is very efficient and delivers a low cost oxygen product.

In two DOE Small Business Innovative Research (SBIR) projects (DE-FG02-05ER84216; FG02-07ER84677), TDA Research Inc. (TDA) demonstrated the efficacy of the new air separation concept integrated with an IGCC plant and an oxy-combustion process. In a previous DOE/NETL sponsored project (DE-FE-0024060) we further advanced the technological maturity via higher fidelity testing and process design. In these projects, we showed that the sorbent can maintain a high oxygen capacity over multiple absorption/regeneration cycles. We evaluated various reactor design options (e.g., fixed-bed, fluidized-bed and moving-bed configurations) and developed a process around a fixed-bed system that removes O_2 via a combination of pressure regeneration bed with low pressure steam). The specific objectives of this DOE/NETL sponsored contract (DE-FE0026142) were to increase the technical maturity and commercial viability of the new technology in collaboration with the University of California, Irvine (UCI), the University of Alberta (UOA) and the Gas Technology Institute (GTI) by: 1) demonstrating continuous oxygen generation in a prototype test system, and 2) carrying out a high fidelity process design and economic analysis.

In this work, we scaled-up the sorbent production and prepared quantities sufficient to support large-scale evaluation using high throughput production equipment. Figure 2 summarizes the performance of each scale-up batch of the sorbent produced for the prototype unit. We completed Manufacturing and Quality Assurance Plans that will provide a basis for commercial production. We carried out over 12,500 absorption/ regeneration cycles to demonstrate sorbent life. We worked with UOA and GTI to optimize the cycle sequence and carried out a detailed

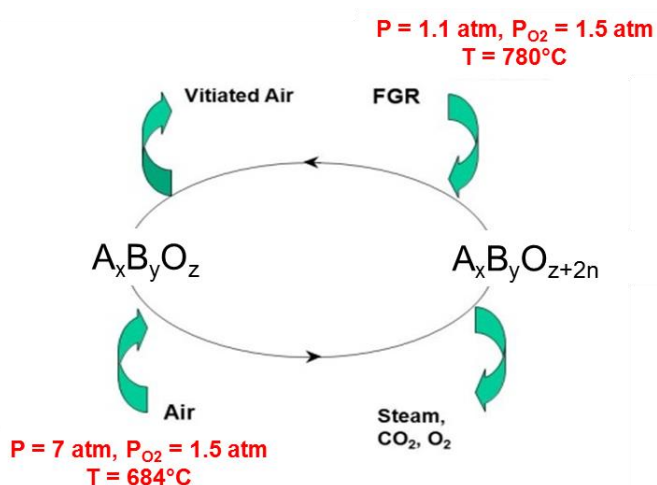


Figure 1. Oxygen transfer cycle.

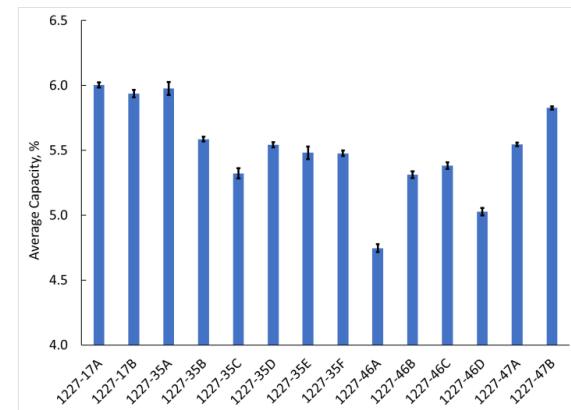


Figure 2. Average oxygen capacity of each sorbent batch from TGA data.

and concentration swing (i.e., purging the regenerating bed with low pressure steam). The specific objectives of this DOE/NETL sponsored contract (DE-FE0026142) were to increase the technical maturity and commercial viability of the new technology in collaboration with the University of California, Irvine (UCI), the University of Alberta (UOA) and the Gas Technology Institute (GTI) by: 1) demonstrating continuous oxygen generation in a prototype test system, and 2) carrying out a high fidelity process design and economic analysis.

design of the sorbent reactors. Figure 3 shows the optimized PSA cycle sequence and steps. We fabricated a prototype unit that consisted of 4 fixed-bed reactors (Figure 4), which allowed us to generate up to 0.7 kg/hr O₂ on instantaneous basis and 0.1

kg/hr on a continuous basis producing 98% oxygen (0.2 kg/hr at 90% purity) (Figure 5). The system is capable of stand-alone operation, treating up to 12 Nm³/hr air at different inlet pressures. In a series of tests, we carried out parametric tests assessing the impact of absorption time, co-current blowdown steps and steam purge rates. We demonstrated the prototype unit operation for over 1,800 hours producing high purity oxygen. We worked with UCI to update the process simulation model developed previously under DOE contract #DE-FE0024060, integrating the new technology with the GE and E-Gas gasification systems and state-of-the-art and emerging carbon capture technologies (i.e., Selexol and TDA's Warm Gas PSA based carbon capture systems). For all cases, we estimated the process efficiency, COE and cost of CO₂ capture, following the DOE/NETL Cost Guidelines. With the successful completion of the R&D effort, the technology is now ready for a larger pilot-scale demonstration and the technology readiness has been raised from TRL 4 to TRL 6.

4-bed Scheme - 2											
	Total Cycle time (a min)			Idle time (0 min)							
Time (min)	Stage 1	Stage 2			Stage 3			Stage 4			
Time (min)	a	b	c	d	b	c	d	b	c	d	
Bed 1	ADS	EQ1D	CoBD	CnBD	PURGE			EQ1R	PRESS		
Bed 2	EQ1R	PRESS		ADS		EQ1D	CoBD	CnBD	PURGE		
Bed 3	PURGE			EQ1R	PRESS		ADS		EQ1D	CoBD	CnBD
Bed 4	EQ1D	CoBD	CnBD	PURGE		EQ1R	PRESS		ADS		

Figure 3. Optimized PSA cycle sequence and steps.



Figure 4. TDA's 1 kg/hr prototype oxygen generation unit.

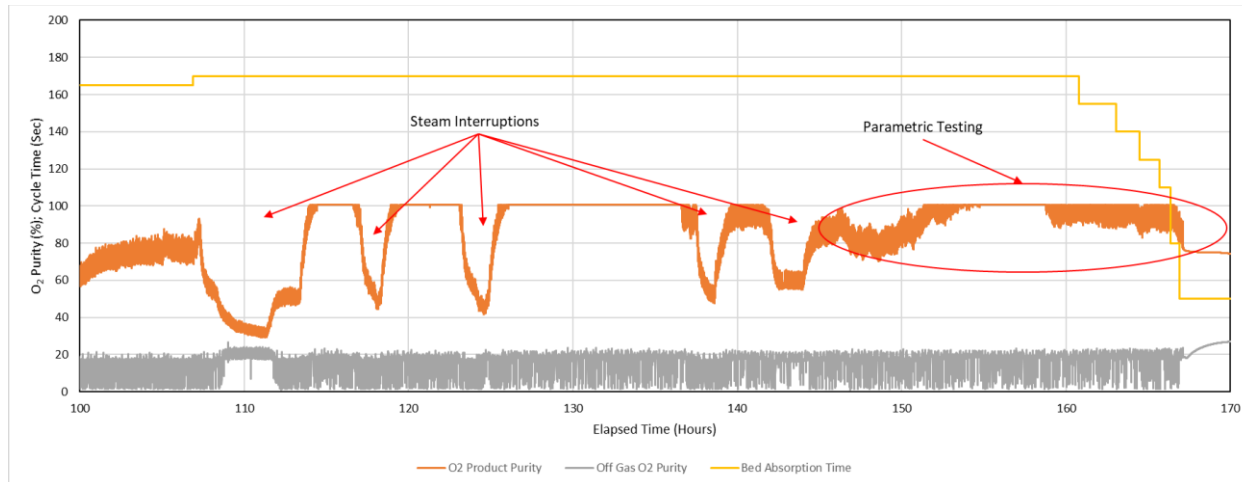


Figure 5. Stable operation with the improved steam generation and temperature. Several interruptions are indicated during the roughly 70-hour test snapshot. In between steam interruptions, the oxygen product purity is at or above 98%.

Table 1. Comparison of TDA's ASU unit against cryogenic ASU for IGCC power plants.

Case	Base Case	Case 1A	Case 2A	Base Case	Case 1B	Case 2B
IGCC Plant Type	IGCC – Cold Gas Cleanup - Selexol™			IGCC – Warm Gas Cleanup – TDA's CO ₂ Capture System		
Gasifier Type	GE	E-Gas™		GE	E-Gas™	
ASU Technology	Cryogenic	TDA Sorbent		Cryogenic	TDA Sorbent	
CO ₂ Capture, %	90	90	90	90	90	90
Gross Power Generated, MWe	727.4	731.3	701.9	674.3	739.1	725.8
Gas Turbine Power	464.0	464.0	464.0	417.5	464.0	464.0
Steam Turbine Power	257.4	258.4	237.9	246.7	264.6	261.8
Syngas/Air Expander	6.0	8.8	-	10.0	10.5	-
Auxiliary Load, kWe	192.9	162.5	167.8	120.7	141.8	142.3
Net Power, kWe	534.4	568.7	534.1	553.7	597.4	583.5
Net Plant Efficiency, % HHV	32.00	34.05	32.23	34.46	35.33	35.20
Coal Feed Rate, tonne/h	221.6	221.4	219.7	213.0	224.2	219.8
Raw Water Usage, GPM/MWe	10.92	9.32	11.46	10.55	10.42	10.31
Total Plant Cost, \$/kWe	3,359	2,926	3,092	3,212	2,840	2,775
COE without CO ₂ TS&M, \$/MWh	133	119.1	126.1	126	114.1	112.4
COE with CO ₂ TS&M, \$MWH	142	127.1	134.5	134	121.9	120.1
Cost of CO ₂ Capture, \$/tonne (including TS&M)	47	37	43	41	30	32

We observed that TDA's ASU unit provides significant improvement in overall plant performance increasing the net plant efficiency from 32% to 34.05% for the cold gas cleanup Case for GE gasifier while the improvement is lower for the warm gas cleanup case at 35.33% vs 34.46%. The 1st year Cost of Electricity (COE) and the Cost of CO₂ Capture are also lower for the TDA ASU than that for the cryogenic ASU. For an IGCC power plant integrated with a cold gas cleanup system that uses GE gasifiers, the use of our system instead of a cryogenic unit reduces the COE per MWh from \$142 to \$127.1 while the cost of CO₂ capture including TS&M goes from \$47 to \$37 per tonne. However for an IGCC power plant integrated with a warm gas cleanup system the reduction is much smaller, the COE per MWh is \$134 vs \$121.9 while the cost of CO₂ capture including TS&M is \$41 vs \$30 per tonne. The results for both GE gasifier and E-Gas gasifier based IGCC power plants equipped with TDA's Air separation and warm gas CO₂ capture systems are summarized in Table 1

1. Introduction

Oxygen generation is one of the most expensive components of any gasification system. The Air Separation Unit (ASU) and the associated compressors costs account for ~15% of the overall plant cost and the compressors consume the 5-7% of gross power plant output of the IGCC plant (Higman, 2003). The situation is even worse for an oxy-fired pulverized coal power plant where the ASU consumes 18% of the plant's output (Nskala et al., 2008).

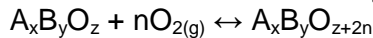
Commercial cryogenic air separation plants are inherently inefficient. In these plants, the air is cooled to ~80K where it becomes a liquid; nitrogen and oxygen are then separated via distillation. Cryo-separation requires about 10 times the minimum theoretical power (250–300 kWh per ton of O₂ instead of 30 kWh per ton) due to the large energy penalty associated with the unavoidable temperature difference between the separation process and the surroundings. This parasitic loss can be greatly reduced and the operating efficiency can be substantially improved if cryogenic temperatures are avoided.

The non-cryogenic pressure swing adsorption (PSA)-based air separation technologies are widely used for oxygen production. These are based on the selective reversible adsorption of nitrogen (but not oxygen) onto molecular sieve sorbents at high pressures (Sircar, 1988). Although operated at near ambient temperature, oxygen produced with the PSA process is slightly more expensive than that of the cryogenic units at large-scales, mainly due to the inefficiencies involved in the adsorption of the major component (nitrogen) from a high pressure stream (air) and its subsequent discharge at ambient pressure (the most of the work input provided during compression is lost). Hence, PSA suffers from a high energy penalty and a relatively high capital cost.

1.1 TDA's Air Separation Process

In this project, TDA has developed a novel air separation system based on a unique oxidation-reduction (redox) process, which will be applicable to the oxidation of both coal and natural gas.

The basic sorbent was initially invented on in previous DOE sponsored projects (DE-FG02-05ER84216 and FG02-07ER84677). In this project we improved the sorbent's operation and built and tested and analyzed a process based on it. The process uses a regenerable mixed metal oxide spinel (A_xB_yO_z) sorbent in a fixed bed cycling process; during absorption step fresh A_xB_yO_z selectively absorbs O₂ from air at pressure and forms a metal stable phase (A_xB_yO_{z+2n}) while during the regeneration step the sorbent releases the oxygen. The overall reaction is:



Unlike conventional chemical looping combustion sorbents that also work via a redox process, a key feature of the new sorbent is the auto-reduction of the higher oxidation state metal stable ($A_xB_yO_{z+2n}$) phase that allows the mixed metal oxide sorbent to change oxidation state without it needing to directly contact a reducing gas (e.g., CH_4 , H_2 , CO , syngas) or fuel. The auto-reduction of the $A_xB_yO_{z+2n}$ phase releases oxygen, which can be recovered as a pure product. The overall heat of reaction is estimated to be 7.3 kcal/mol O_2 absorbed much lower than if it was a traditional redox process (more than 40 kcal/mol).

Application to Oxy-combustion of Coal:

Figure 7 shows a high level schematic in which our separation process is integrated with a coal boiler. In the absorption step, the sorbent removes oxygen from compressed air at $684^\circ C$. Air is adiabatically compressed in the compressor section of a gas turbine roughly to 7.2 bar (1.5 bar O_2 partial pressure). This compression ratio can be achieved by the state-of-the-art turbines (for instance, the 270 MW Siemens Westinghouse W501G gas turbine used in the Air Products' ITM membrane system achieves a 19:1 ratio in multiple compression stages); the compression increases the gas temperature from ambient up to $260^\circ C$, which is further increased to $684^\circ C$ in a recuperative heat exchanger with the vitiated air exiting the absorber. Without any pre-cooling, this high pressure air stream enters to the absorption reactor and the oxygen reacts with the sorbent ($A_xB_yO_z$) to form a meta stable product ($A_xB_yO_{z+2n}$).

The sorbent removes approximately 90-95% of the oxygen from air. The oxygen depleted air stream leaving the sorbent bed still contains 1-2% vol. oxygen. The oxidation of the sorbent is exothermic, which increases the air temperature to $813^\circ C$. This hot, high pressure vitiated air stream is sent to the gas turbine expander to generate electricity. TDA's reactor replaces the combustor in a gas turbine. Further fuel topping is possible to increase the gas temperature prior to expansion to ensure higher turbine efficiency (the fuel can be natural gas or coal gas generated in a small low pressure gasifier).

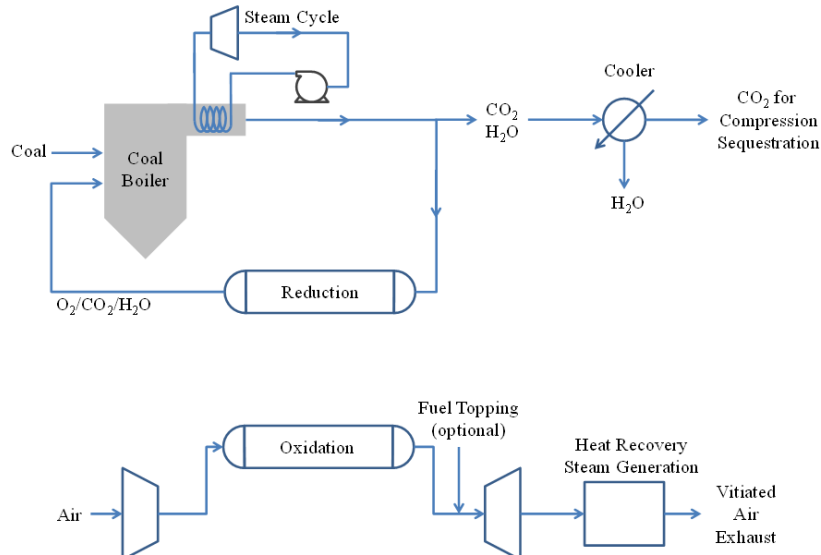


Figure 7. TDA's air separation system integrated with a coal-fired power plant.

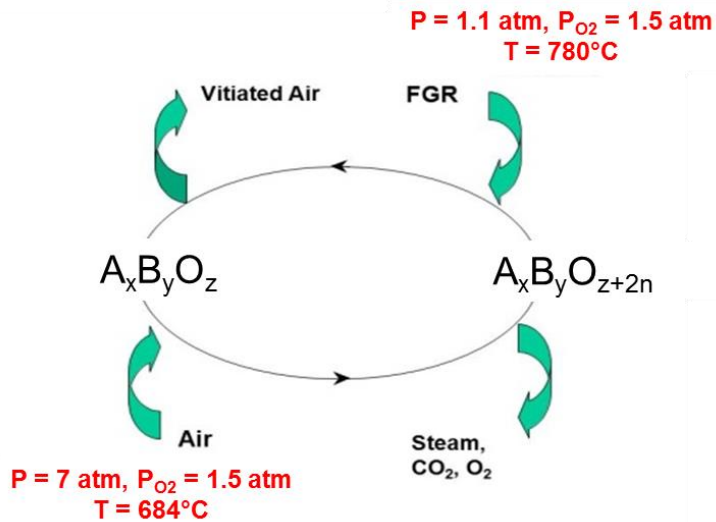


Figure 8. Oxygen transfer cycle.

The oxidation of the sorbent is exothermic, which increases the air temperature to $813^\circ C$. This hot, high pressure vitiated air stream is sent to the gas turbine expander to generate electricity. TDA's reactor replaces the combustor in a gas turbine. Further fuel topping is possible to increase the gas temperature prior to expansion to ensure higher turbine efficiency (the fuel can be natural gas or coal gas generated in a small low pressure gasifier).

The sorbent saturated with oxygen (the $A_xB_yO_{z+2n}$ metastable phase) is then regenerated by depressurizing and switching to counter current flow in steam. The sorbent is regenerated with the warm (680°C) circulation gases from the boiler. These gases (primarily consisting of steam and CO_2) reduce the O_2 partial pressure and causes the metastable phase to decompose back to $A_xB_yO_z$, liberating the absorbed oxygen. The key to our process is that because the mixed oxide sorbent on oxygen absorption is metastable, the regeneration is very fast even though we apply only a small chemical potential swing (the only swing is that of the O_2 partial pressure, as oxygen is removed from air at high pressure and released to the flue gas re-circulation loop of the main coal plant at low pressure) to return the sorbent to its original $A_xB_yO_z$ spinel structure.

Application to IGCC Plant:

In the IGCC process, air is also adiabatically compressed in the compressor section of a gas turbine (Figure 9). The hot high pressure air enters the absorption bed. The sorbent again removes approximately 90 to 95% of the oxygen from air stream. The oxygen depleted air stream along with air from a makeup compressor is burned with the synthesis gas from the gasification process to generate electricity (a desulfurized synthesis gas stream is used to prevent contamination of the sorbent). The sorbent saturated with oxygen is then regenerated by applying a pressure swing and a small purge of steam. A small high pressure superheated steam sweep ensures full sorbent regeneration (i.e., providing the O_2 partial pressure difference to facilitate sorbent auto-reduction and consequent O_2 generation).

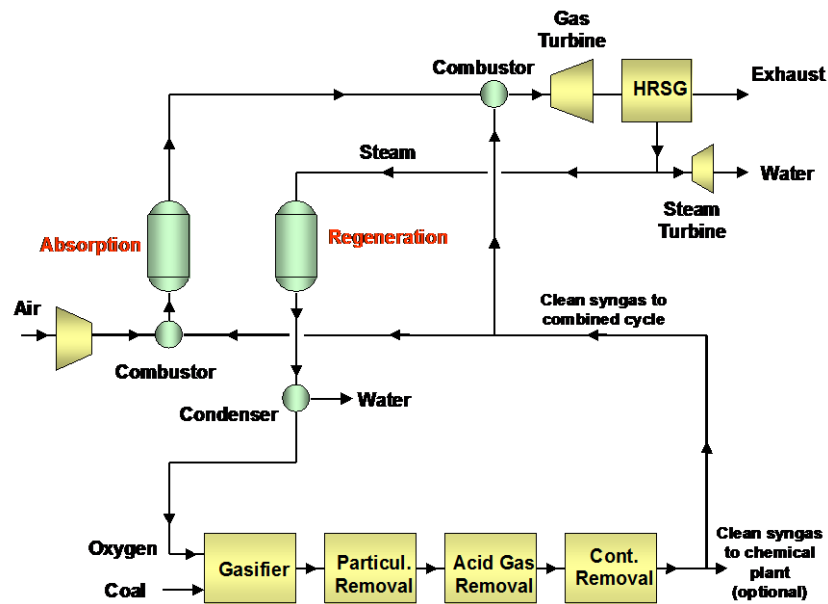


Figure 9. Integration of the air separation system to the IGCC plant.

2. Project Objectives

The objective of this work is to develop a new chemical absorbent-based air separation process which can deliver low-cost oxygen to Integrated Gasification Combined Cycle (IGCC) power plants. The new sorbent operates at high temperature, hence eliminating the thermodynamic inefficiencies inherent in the conventional cryogenic air separation units (ASU). Unlike the sorbents used in commercial Pressure Swing Adsorption (PSA) systems, our sorbent selectively removes oxygen (not nitrogen); which allows the effective utilization of the large amounts of energy in the high pressure oxygen-depleted stream. As a result, the new air separation system is highly efficient and delivers a low cost oxygen product.

In two DOE Small Business Innovative Research (SBIR) projects (DE-FG02-05ER84216; FG02-07ER84677), TDA Research Inc. (TDA) demonstrated the efficacy of the new air separation concept integrated with an IGCC plant and an oxy-combustion process. In a just completed

DOE/NETL project (DE-FE-0024060) we further advanced the technological maturity via higher fidelity testing and process design. In these projects, we showed that the sorbent can maintain a high oxygen capacity over multiple absorption/regeneration cycles. We evaluated various reactor design options (e.g., fixed-bed, fluidized-bed and moving-bed configurations) and developed a process around a fixed-bed system that removes O₂ via a combination of pressure and concentration swing (i.e., purging the regenerating bed with low pressure steam). Using the DOE evaluation methodology for a 622 MW IGCC plant with no carbon capture (DOE/NETL-2010/1397), we calculated that the new air separation system can increase the plant efficiency to 40.5%, in comparison to 39% for the same plant equipped with cryogenic separation, reducing the cost of electricity (COE) on a \$ 2011 basis to less than \$93.2 per MWh (versus \$101.2 per MWh with a cryogenic ASU). In an IGCC plant with carbon capture capability, the new ASU could reduce the cost of CO₂ captured to \$38.8/tonne and \$29.3/tonne for the conventional Selexol-based and TDA's warm gas (developed under DE-FE-0023684) CO₂ capture technologies, respectively. The cost of CO₂ capture for the same IGCC plant with a cryogenic ASU and Selexol based CO₂ removal is \$47.9/tonne. When operated as a stand-alone oxygen generator, our system can produce oxygen at \$29.5 per ton, well below the \$32/ton oxygen cost of the large-scale cryogenic separation units.

The specific objectives of this project are to increase the technical maturity and commercial viability of the new technology by: 1) demonstrating continuous oxygen generation in a prototype test system, and 2) carrying out a high fidelity process design and economic analysis. We will collaborate with the University of California, Irvine (UCI), the University of Alberta (UOA) and the Gas Technology Institute (GTI) to meet these objectives.

2.1 Work Plan

In our work, we will scale-up sorbent production and prepare quantities sufficient to support large-scale evaluation using high throughput production equipment. We will complete Manufacturing and Quality Assurance Plans that will provide a basis for commercial production. We will carry out 12,500 test cycles to demonstrate sorbent life and mechanical integrity. We will work with UOA and GTI to optimize the cycle sequence and carry out a detailed design of the sorbent reactors. UOA will develop a multi-component absorption model to predict the oxygen concentration over the bed at different stages of the cycle and assist us in optimizing the cycle sequence so that it will provide high oxygen product purity while minimizing the consumption of steam, fuel gas and power. GTI will carry out Computational Fluid Dynamics (CFD) simulations to predict concentration and temperature profiles across the bed as a function of different reactor geometries. Based on the simulation results we will design the sorbent reactors, both for the prototype test unit and a full scale plant. The prototype unit will consist of 3 fixed-bed reactors which allow us to generate a minimum of 1 kg/hr O₂ on a continuous basis. The system will be capable of stand-alone operation, treating up to 12 Nm³/hr air at different inlet pressures. In a series of tests, we will validate the results from the absorption model and CFD simulations and conduct multiple-cycle tests under optimum operating conditions, delivering a high purity oxygen product. We will work with UCI to revise the process simulation model, integrating the new technology with the GE and E-Gas gasification systems integrated with the state-of-the-art and emerging carbon capture technologies (i.e., Selexol and TDA's Warm Gas). For all cases, we will estimate the process efficiency, COE and cost of CO₂ capture, following the DOE/NETL Cost Guidelines. With the successful completion of the R&D effort, the technology will be ready for a larger pilot-scale demonstration and the technology readiness will be raised from TRL 4 to TRL 6.

3. Results

3.1 Task 1. Project Management and Planning (PMP)

PMP: The project commenced on October 1, 2015 and we updated the PMP based on inputs from the DOE project monitor and submitted it to DOE on October 27, 2015 (Milestone 1-1). We had a kick-off meeting with DOE project manager via web conference on December 7, 2015 (Milestone 1-2). A project outline, including company overview and project approach, was presented to the DOE technical staff and other interested parties, including other research groups within the overall project scope. We successfully completed all the project tasks on May 31, 2019. After submission of the final report we will co-ordinate with DOE to provide a final (Milestone 1-11). The project Milestone log is summarized in Table 2.

Sorbent and Prototype Tasks: We successfully completed 6,000 cycle life tests with the sorbent (Milestone 1-3) on June 30, 2017. We completed the design of the prototype unit (Milestone 1-4) on July 31, 2016. We completed the fabrication of the prototype test unit (Milestone 1-6) on September 28, 2018. We completed extended life tests completing more than 12,500 cycles (Milestone 1-8) on May 31, 2019. We completed the testing with our prototype unit on May 31, 2019, completing over 2,000 hours of testing in total (Milestone 1-9).

Process and System Tasks: We completed the preliminary techno-economic analysis (TEA) (Milestone 1-5) on September 30, 2017. We completed the optimization of the adsorption cycles (Milestone 1-7) on September 30, 2017. We completed the system design and cost analysis for the high temperature PSA unit and completed the final TEA (Milestone 1-10) on May 31, 2019.

Table 2. Project Milestone Log.

BP	ID	Task No.	Title	Planned Completion	Actual Completion	Verification Method
			Project Start Date	10/1/15		
1	1-1	1	Update (PMP)	11/1/15	10/27/15	PMP file
1	1-2	1	Kickoff Meeting	12/1/15	12/7/15	Presentation file
1	1-3	3	Complete 6,000 Cycle Life Test	6/30/17	6/30/17	Results update
1	1-4	6	Complete Prototype Unit Design	6/30/16	7/31/16	Design Package
1	1-5	9	Complete Preliminary TEA	9/30/17	9/30/17	Topical Report #1
			Go/No-go Decision Point	9/30/17		
1	1-6	7	Complete Fabrication of the Prototype Unit	7/31/18	9/28/18	Results update
1	1-7	5	Complete Cycle Sequence Optimization	9/30/17	9/30/17	Results update
1	1-8	3	Complete 12,500 Cycles in Sorbent Life Test	5/31/19	5/31/19	Results update
1	1-9	8	Complete 500 hrs of Testing with the Prototype Unit	5/31/19	5/31/19	Topical Report #2
1	1-10	9	Complete Final TEA	5/31/19	5/31/19	Topical Report #3
1	1-11	1	Final Review Meeting	5/31/19		Presentation file

3.2 Task 2. Sorbent Production Scale-up

As part of this task, we identified the high throughput production equipment in our production facility in Golden, CO that could be used for the scale-up production. In order to transition to the high throughput equipment for sorbent production, we first simplified the sorbent preparation methods used to introduce active phase onto support and also the amount of binders used. Next, we prepared the sorbent using these simplified preparation methods at lab-scale to confirm the sorbent performance before making a large batch in our high throughput production equipment.

The sorbent's performance relies on the intimate mixture of the metals during the synthesis process. The metal salt precursors are mixed thoroughly at room temperature in a low-intensity plow mixer, then mixed with carboxylic acids to act as a reaction promoter. The resulting solids are then transferred to a batch-based rotary calciner, Figure 10. The rotary calciner uses an atmosphere control system to vary gas flows and monitor the reaction progress. Upon heating in the calciner, the salt mixture melts into its own water of hydration, completing the intimate mixing of the components. Further heating causes the metal salts to transform into a metal-oxalate mixture – necessary to produce the final active phase. Additional heating triggers a self-propagating decomposition of the oxalate – the exotherm of metal oxidation and carbon dioxide release causes a wave of reaction moving through the bed. Since the complete reaction requires additional oxygen, the calciner uses the CO₂ concentration of the exhaust to adjust the oxygen content of the chamber to control the rate of reaction, which subsequently controls the reaction temperature. This all takes place during rotation to provide mixing and uniform gas-solid contact.

After calcination is complete, the mixed metal oxide material is ball-milled to a uniform size of -200M. This powder is used to produce the final pelletized product, suitable for use in a gas stream with minimal pressure drop. Once mixed with water, water-based rheology modifiers, and binders, the material is formed into pellets using a 2" extruder, Figure 11, with the die and cutter set up for the appropriate sizing. Moisture and binders are removed thermally in a convection oven to finalize the product.



Figure 10. Stainless steel calciner.

Further heating causes the metal salts to transform into a metal-oxalate mixture – necessary to produce the final active phase. Additional heating triggers a self-propagating decomposition of the oxalate – the exotherm of metal oxidation and carbon dioxide release causes a wave of reaction moving through the bed. Since the complete reaction requires additional oxygen, the calciner uses the CO₂ concentration of the exhaust to adjust the oxygen content of the chamber to control the rate of reaction, which subsequently controls the reaction temperature. This all takes place during rotation to provide mixing and uniform gas-solid contact.



Figure 11. 2" Extruder

Sorbent Production for Prototype Unit

60 kg of preferred sorbent powder was produced and stored as 8 batches labeled 1227-17A, 1227-17B, and 1227-35A through F. For quality control, each batch was sampled and screened for the oxygen capacity of the sorbent at 750°C using a thermogravimetric analyzer (TGA). Initially, each sample was heated to 750°C at 40°C/min under 200 mL/min N₂ flow. Then samples were exposed to cycles of: 1) Air, and 2) N₂ at 200 mL/min. The performance of all the samples was very stable (see Figure 12) and the standard deviation for each sample was always <0.05% (see Figure 13). The average capacity of all the batches was 5.69±0.28 wt%.

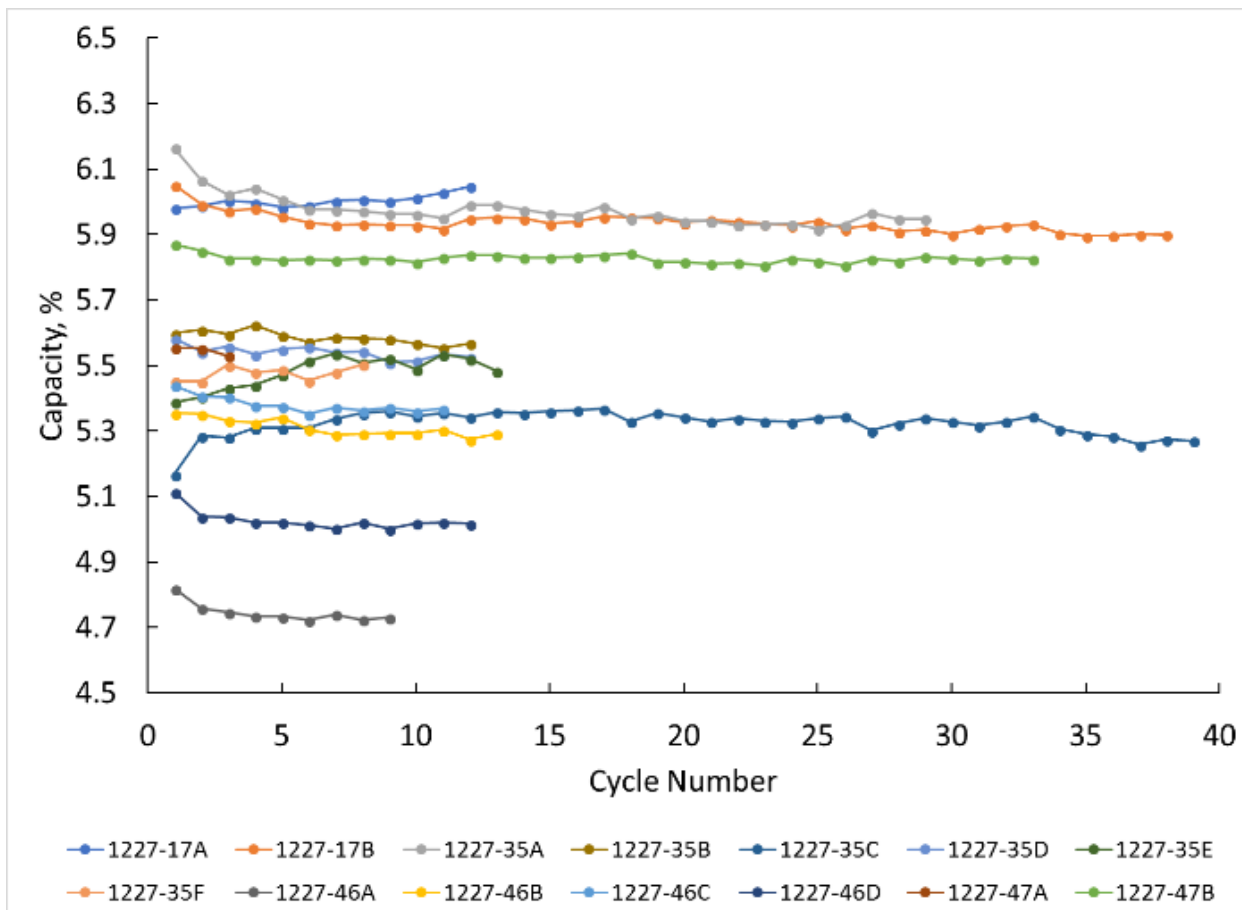


Figure 12. Results of TGA screening cycles showing stable oxygen capacity of the sorbents.

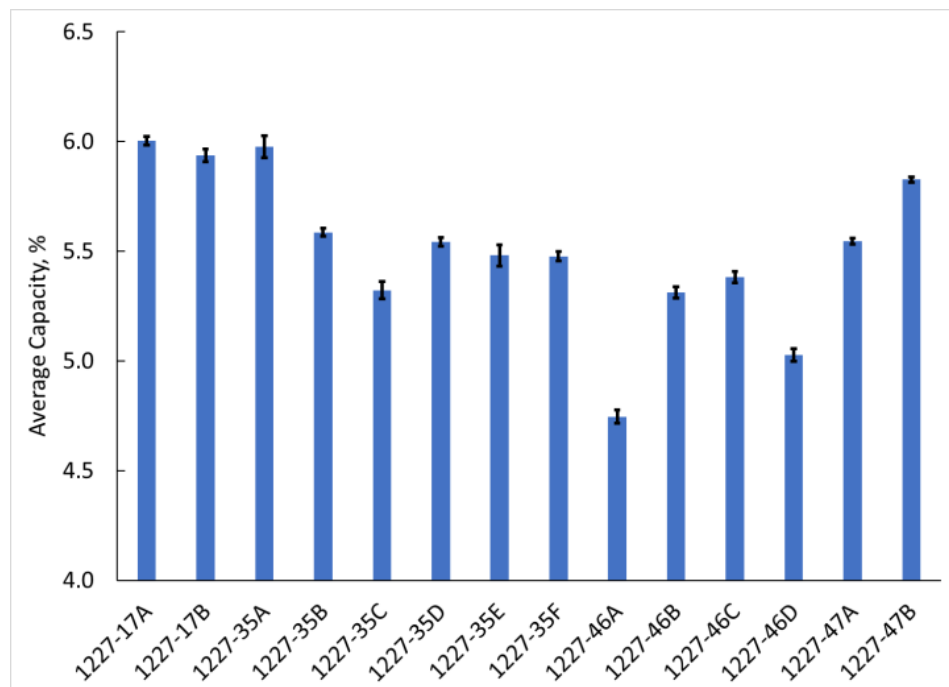


Figure 13. Average oxygen capacity of each sorbent batch from TGA data.

We formed extrudates of the sorbent powder by combining the active phase with 2 additives and labeled the batches 1227-46A through D and 1227-47A and B. Additive 1 acted as a binder to increase the crush resistance of the extrudates. Additive 2 increased the porosity and acted as an extrusion aid. The composition of each batch is shown in Table 3.

The extrudates with Additive 2 only (1227-47A and B) had much lower crush strength than those with both additives but the average capacity was unchanged compared to the active phase powder alone (within the batch to batch variability). The addition of Additive 1 (combined with Additive 2) created very strong extrudates but samples with higher levels of Additive 2 showed the greatest reduction in performance (12-17% reduction in oxygen capacity). Samples with ~24 wt% Additive 1 and ~6 wt% Additive 2 (1227-46B and C) showed the best performance while maintaining excellent crush strength with only a 5-7% reduction in oxygen capacity performance compared to the active sorbent batch average.

3.3 Task 3. Sorbent Life Tests

In this task we used the previously modified existing system from DOE contract No. DE-FE0024060 to carry out sorbent life tests with our scaled-up sorbent formulations. Figure 14 shows the modified system used for the life tests. The system uses fixed sorbent beds and is capable of pressure swing operation so that we can carry out the air separation in a high temperature pressure swing absorption process with counter current absorption and desorption. Figure 15 shows the updated P&ID for the fixed bed system with valves included for counter current operation and a bypass line to measure the feed concentration.

2,000 Cycles for IGCC Applications

We completed over 1,920 cycles under IGCC conditions, high pressure (300 psig) and high temperature (800°C) operation and the sorbent has retained a stable oxygen working capacity of 5.0% wt. at 800°C. Figure 16 shows the results from these multiple cycle tests.

Table 3. Extrudate Compositions.

Batch	Active Phase, wt%	Additive 1, wt%	Additive 2, wt%
1227-46A	63.6	8.1	28.3
1227-46B	65.2	5.8	29.0
1227-46C	69.2	6.2	24.6
1227-46D	67.5	8.5	24.0
1227-47A	73.8	0.0	26.2
1227-47B	78.9	0.0	21.1

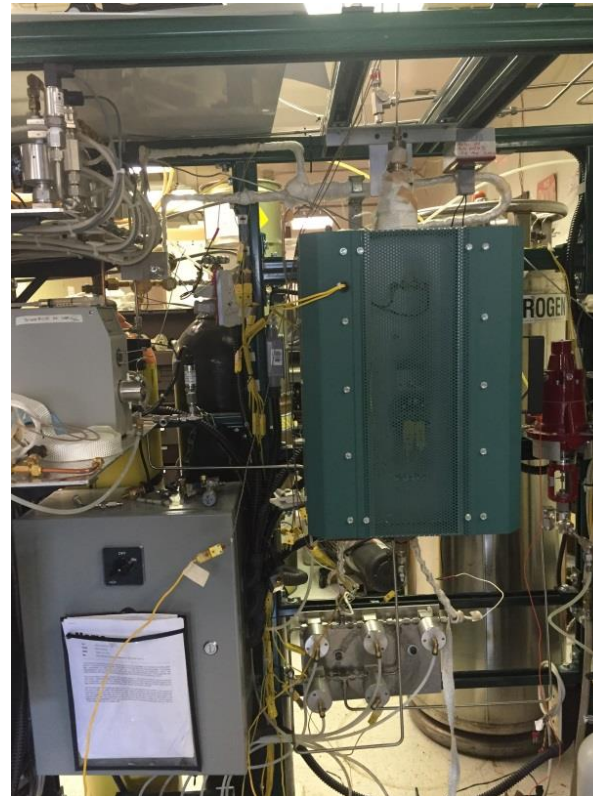


Figure 14. Modified fixed bed reactor system that allows counter current operation used for 6,000 cycle life tests.

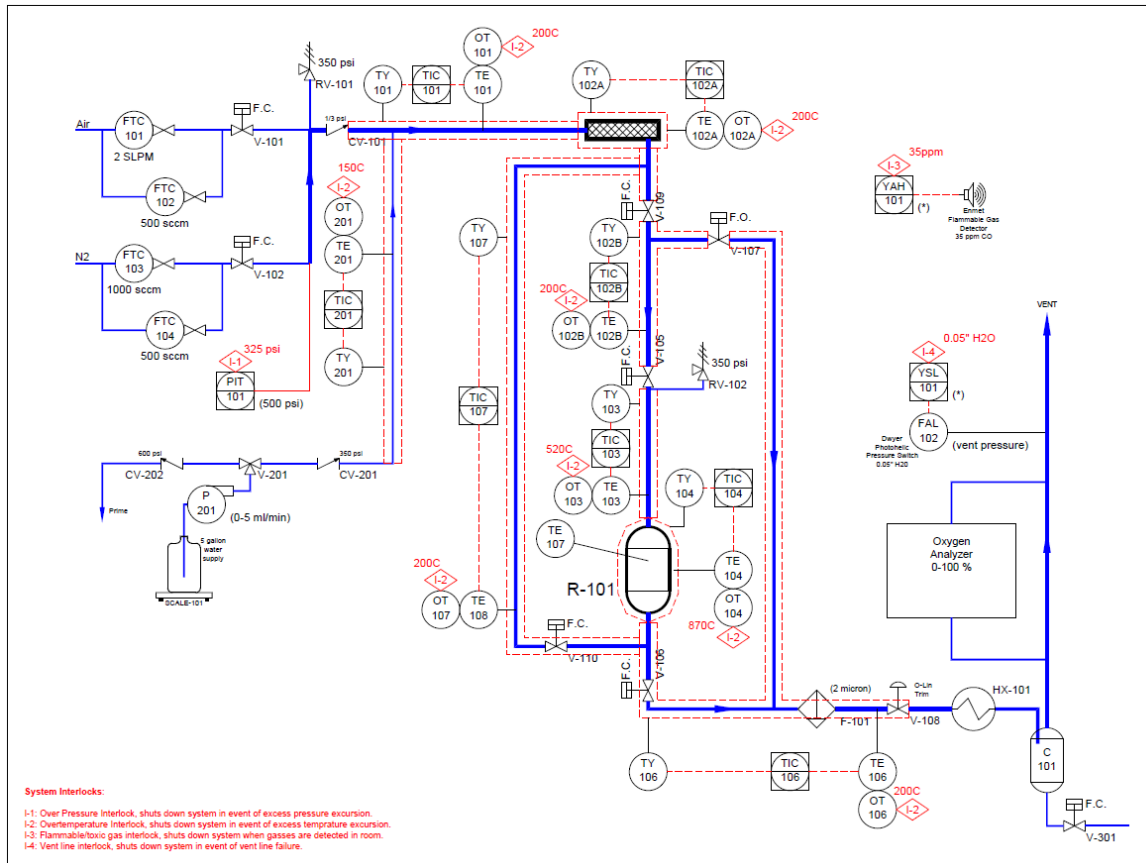


Figure 15. P&ID of the fixed bed system with capability for counter current operation.

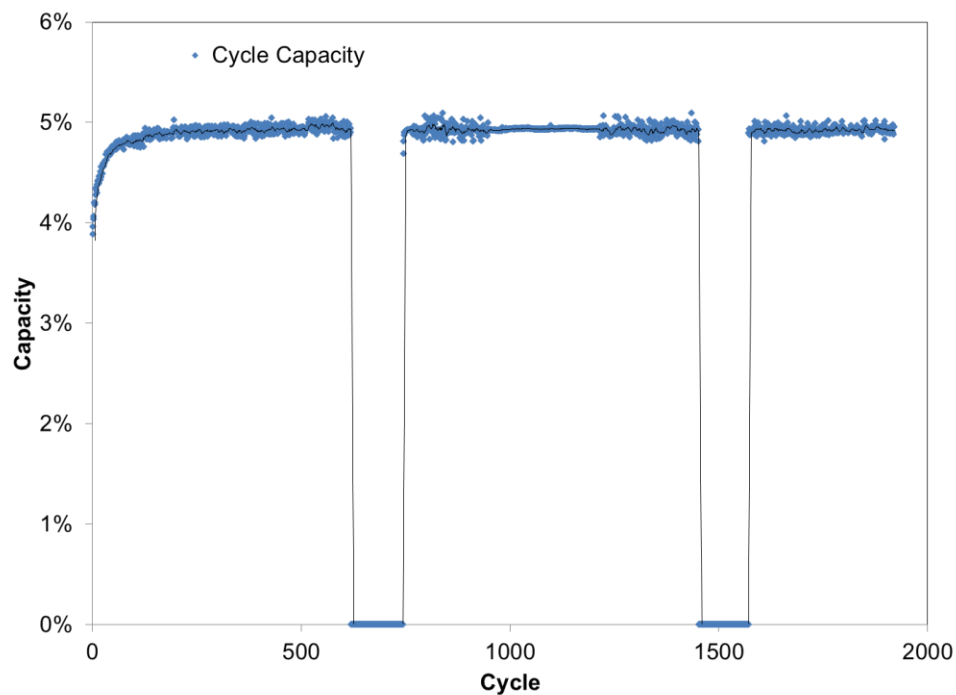


Figure 16. Results from multiple cycle life tests.

6,000 Cycles for Oxy-combustion Applications

We carried out life tests at 750°C and 100 psia adsorption pressure and 12 psig regeneration pressure (simulating the oxy-combustion operating condition). We successfully completed over 6,000 cycles at three different cycle times. At shorter cycle times, the regenerations were not complete and the sorbent's working capacity reduced as we kept cycling. However, as we increased both the adsorption and regeneration times, the working capacity (per cycle capacity) and the sorbent utilization (per h capacity) both increased. The results from the first 2,000 cycles are included in Figure 17, which shows the sorbent capacity has recovered and is on upward trend at 2,200 cycles. The graph shows both the sorbent capacity per cycle and per hour, respectively.

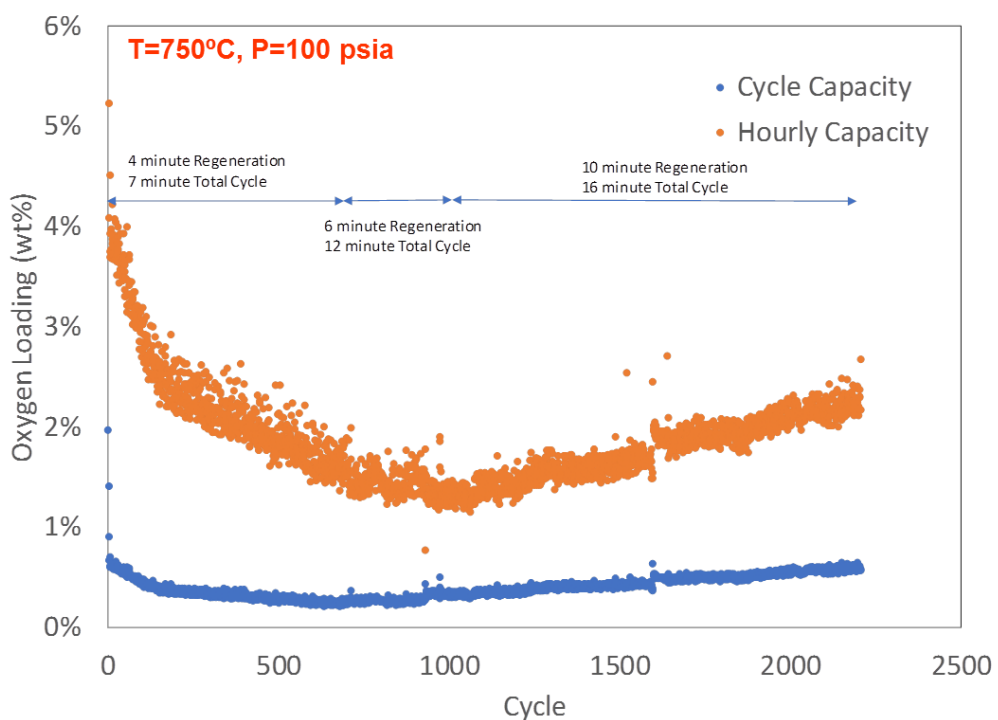


Figure 17. Sorbent life test with the proof-of-concept reactor system. Oxy-combustion plant operating condition: $P_{ads}=100$ psia.

The results from the entire 6,000 cycle tests are included in Figure 17, which shows the sorbent capacity has recovered, with capacity now similar to that at the beginning of the life test.

12,000 Cycle Life Tests

In this task we carried out long-term durability tests in a TGA to assess the impact of cycling at moderate temperature (650°C) between absorption and desorption on the sorbent life. We completed over 12,500 cycles and the sorbent still retained a good oxygen working capacity of 1.0% wt. at 650°C. Figure 19 shows the results from the multiple cycle tests. We increased the desorption time to 5 mins, which increased the working capacity and also allowed the sorbent to have a stable performance maintaining over 2% wt. O₂ working capacity.

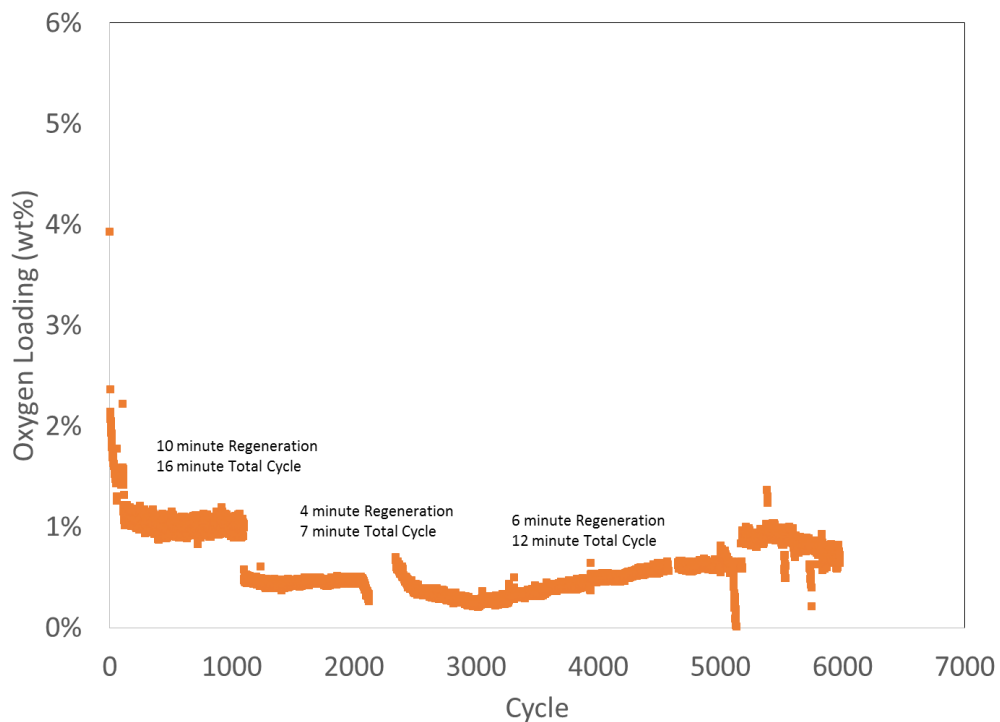


Figure 18. Sorbent life test with the proof-of-concept reactor system. Oxy-combustion plant operating condition: $P_{ads}=100\text{psia}$.

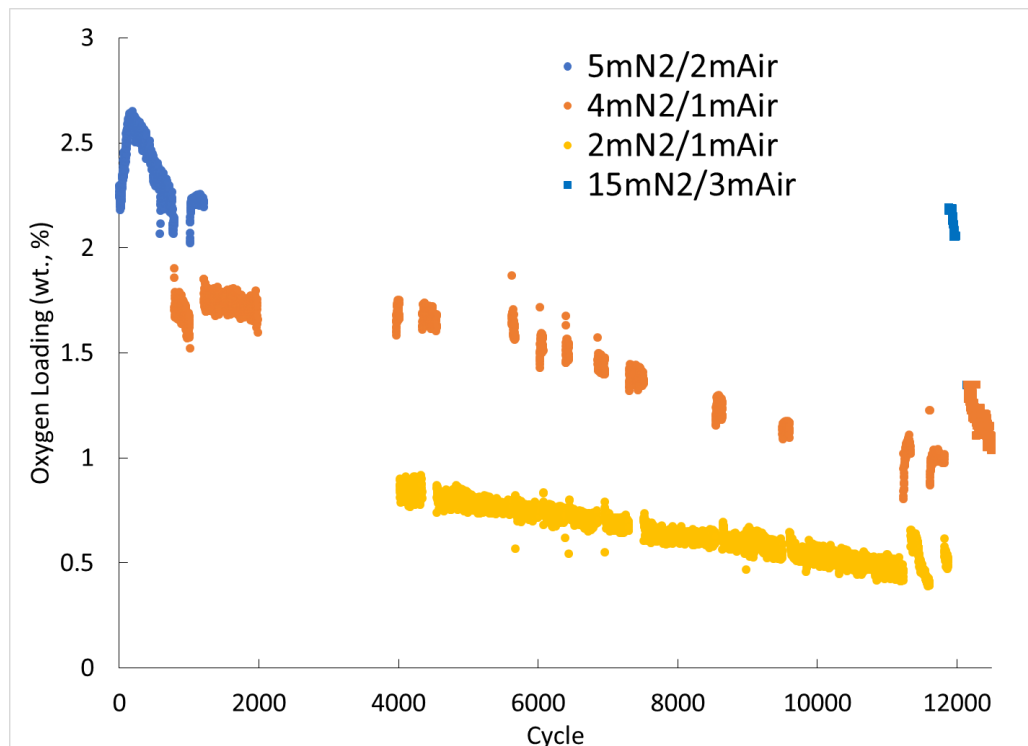


Figure 19. Extended sorbent life test under rapid cycle conditions.

3.4 Task 4. Adsorption, CFD Modeling and Reactor Design

TDA shared the breakthrough test data from our earlier work under DOE contract No. DE-FE0024060 with our partners University of Alberta (Edmonton, Canada) and Gas Technology Institute (Des Plaines, IL). With the test data, particularly those datasets with breakthrough observed, GTI has developed baseline assumptions and boundary conditions for the initial computational fluid dynamics (CFD) model. This includes thermo-physical characteristics of the packed bed material, reaction dynamics and rate parameters, and operating conditions external to the vessel during normal cycling. Similarly UOA developed adsorption models based on the breakthrough data shared by TDA.

3.4.1 CFD Modeling and Reactor Design

GTI first simplified the absorption dynamics and modeled the uptake process. The results from the models for the sorbent-only section of the reactor were fitted to TDA provided experimental data to extract isotherm and kinetics rate parameters for the primary sorption/desorption process. For all of the breakthrough datasets with the modified sorbent arrangement (24 g of sorbent) there are three datasets at 750°C, four at 800°C, and four at 850°C. Using an approximate Langmuir rate model to fit O₂ adsorption versus time, the rate constant *k* is estimated with an exponential fit for each bed temperature. As shown in the example dataset in Figure 20, the data are generally linear for the initial uptake of O₂, then shift to a better exponential decay fit as the sorbent approaches saturation, which could be a feature of the sorbent, the test conditions, and the instrumentation (sampling delay to O₂ analyzer, for example). To apply the best fit for all cases, the rate parameter *k* is determined as having an ending normalized sorption of 95% of the saturated value and if feasible, an R² to the dataset of 0.975 or greater. Figure 21 shows these values for all cases, which are generally good, except for the 850°C tests, which were carried out at lower space velocity. The complete details of the CFD model developed and the initial results obtained are provided in Appendix A.

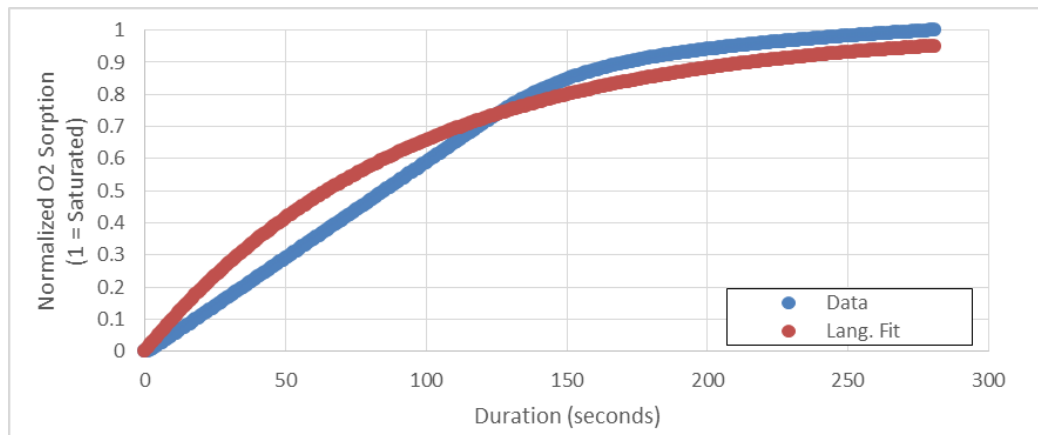


Figure 20. Example of Fit to Sorption Data.

Upon review of the first set of CFD results (included in Appendix A), TDA noted that they had a better estimate of the heat of sorption than what was used in this study. As noted previously, GTI used a heat of reaction, approximating the adsorption process as this reaction: M_xO_y + O₂ ⇌ M_xO_{y+2}, which when taking into account the assumed sorbent porosity was modeled as 75.6 kJ/mol O₂ adsorbed (or 18.1 kcal/mol O₂ adsorbed). By using previous test data and performing a quasi-steady state energy balance (Figure 22), TDA estimated the heat of sorption directly as a range from 7.3 to 10.2 kcal/mol O₂ adsorbed (30.5 to 42.7 kJ/mol O₂ adsorbed). While the previous value used for simulation, 75.6 kJ/mol O₂ adsorbed, is within the same order of

magnitude of these heat of sorption estimates, certainly the heat of reaction approach results will tend to overestimate heat release during the adsorption stage which will lead to incorrect conclusions regarding the need for heat management.

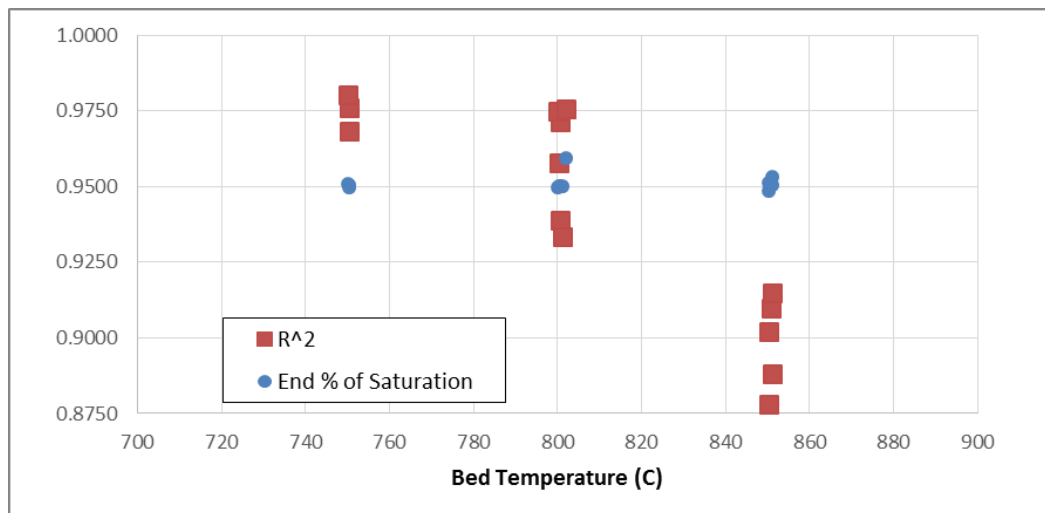


Figure 21. Values for R^2 and % of saturation at end of fit for all datasets.

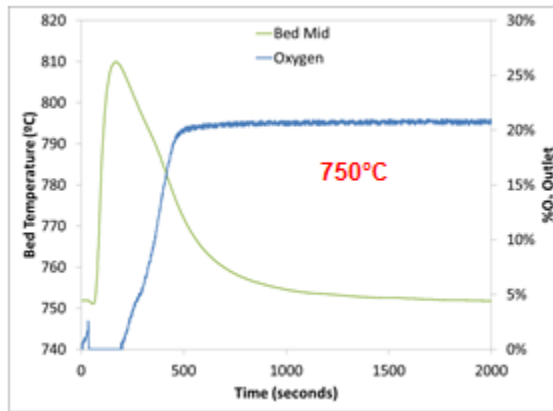


Figure 22. TDA Bed Temperature Plot

As a result, GTI revised the simulation *user-defined function* (UDF) and programmed a piecewise linear heat of sorption ranging from 30.5 to 42.7 kJ/mol O₂ adsorbed for sorbent temperatures from 750°C to 800°C, with constant values above/below this temperature range. All simulations were re-ran prior to exploring thermal management strategies further. While only select data and outputs are shown in this section for brevity, the remainder of data/figures from re-run simulations are contained within an Appendix in Appendix A.

Calibration runs with revised heat of sorption

For the validation simulations, using the TDA experimental sorbent testing by TDA with the small sorbent section (24 g sorbent), the adjusted heat of sorption does reduce the peak sorbent temperatures observed (Figure 22). Generally, each case of modeling assumptions shows a reduction in 40-80°C overall. For those model assumptions that are later used in parametric analysis, Cases 4-C, 4-F, and 4-H, these represent peak temperature rises of 104°C, 92°C, and 54°C, this is slightly above but in line with the 60°C rise observed in testing (Figure 23). Note that in comparison to the TDA-observed 60°C rise (Figure 22), this is not directly

comparable as simulations are for the 800°C inlet case while this figure represents a 750°C case and for a fixed measurement point while the simulation results concern a peak sorbent temperature throughout the bed.

With a modeled heat of sorption, lower than the previous heat of reaction assumption, the sorbent capacity is also affected as shown in Figure 24. With cooler sorbent temperatures overall for all cases, the sorbent capacity is similarly reduced and all simulation cases slightly better agreement with sorbent capacity data. Breakthrough timing results are not significantly affected by the shift to heat of sorption.

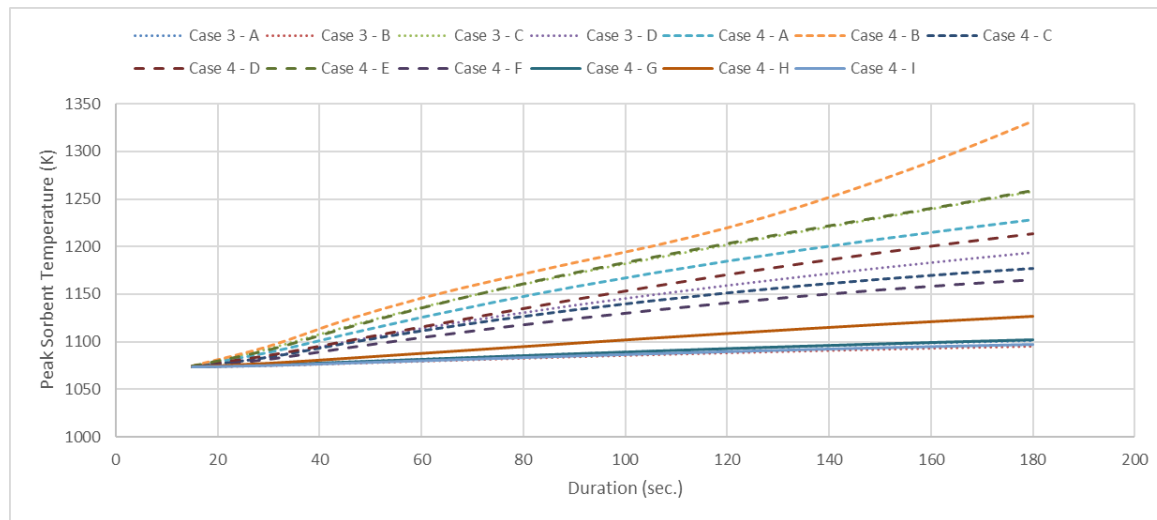


Figure 23. Peak Sorbent Temperatures for Calibration Simulation – Various Cases

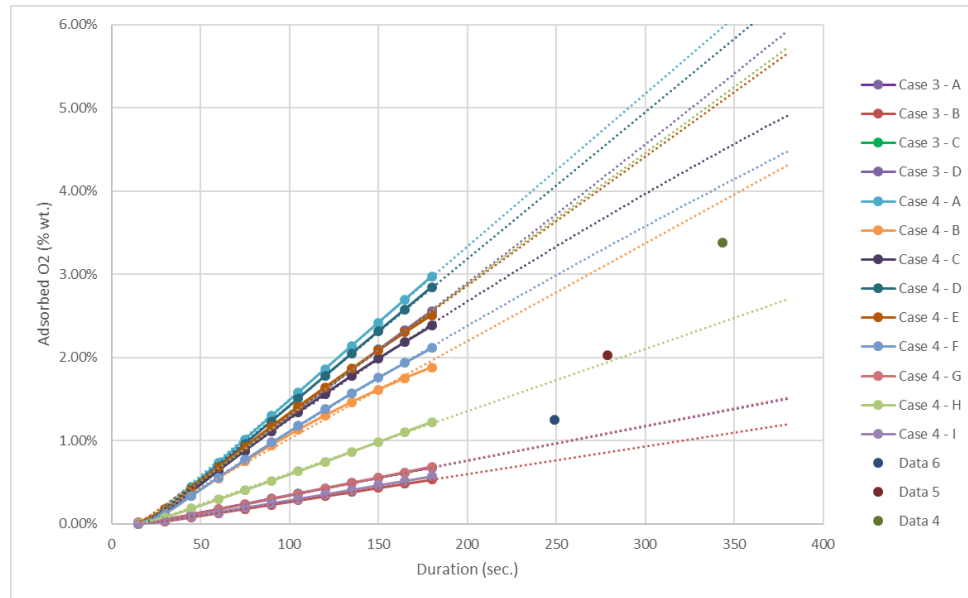


Figure 24. Sorbent Capacity with Time for Validation Modeling vs. Test Data

Simulation of 1 kg/hr O₂ system

Building on calibration of the two-dimensional baseline model validation of the ASU, using updated and expanded experimental datasets from TDA, a scaled up 1 kg O₂/hr system was simulated for optimization. While the calibration results were suggestive that some modeling

assumptions captured baseline test data better than others, the full suite of test conditions in were evaluated initially for this simulation.

A new CFD model was built using the dimensions of a larger vessel provided by TDA (Figure 25). This has a production target of 1 kg O₂/h, contains approximately 32 kg of sorbent, and an expected cycle time of 30 minutes. To evaluate expected breakthrough timing other dynamics (e.g. heat release), began with the adsorption step modeling. The model was setup such that the vessel still has short sections with open vessel and with inert support media, as with prior testing, for sake of continuity with prior modeling. These were later removed to accelerated model convergence as they were found to be unnecessary.

Initial estimates for the 1 kg/h vessel, used to establish model boundary conditions and frame results, are:

- Using the same sorbent density/porosity as baseline simulations and assuming a target O₂ capacity of 1.57% by wt., the sorbent needed is approximately 32 kg, occupying 40.2 L.
- For a four-bed system and applying a 20% safety factor, TDA increases this to 12 L per vessel. Within each vessel is approximately 9.5 kg of sorbent.
- To yield 1 kg O₂/hr of operation for a four bed system, that necessitates each vessel produces 0.25 kg O₂/hr. Assuming that the cycle time is 30 minutes, a good estimate based on baseline testing by TDA, this is further broken down to 0.125 kg O₂/cycle/vessel or about 3.9 mol O₂ per cycle per vessel.
- Qualitatively, from baseline data, the cycle segment durations are expected to be, roughly:
 - Adsorption Step: About 15-20% of the cycle, or up to 6 minutes.
 - Depressurization Step: About 5-7% of the cycle, or up to 2 minutes.
 - Purge/Regeneration Step: About 60-70% of the cycle, or up to 21 minutes.
 - Pressurization Step: About 6-10% of the cycle, or up to 3 minutes.

With CFD simulations four primary cases are explored for a 1 kg/hr O₂ system, which are: 1) the baseline system as proposed with insulated walls including variation of insulation levels and gas flow rates, 2) a system using a combined syngas/steam purge versus a 100% steam purge, 3) active thermal management using a water jacket, and 4) active thermal insulation using an internal tube down the vessel centerline.

Beginning with the adsorption step, shifting to a heat of sorption approach reduces observed sorbent temperatures at the “middle thermocouple” within the larger system. Figure 26 shows this TC measurement after 6 minutes into the adsorption step with the low and high flow cases simulated previously. For all modeled assumptions (Case 3 A/B and Case 4 A – I) and simulating two external heat transfer boundary conditions, the temperature rise is generally modest. For low flow cases (top figure) the rise is less than 20°C, in most cases negligible. For

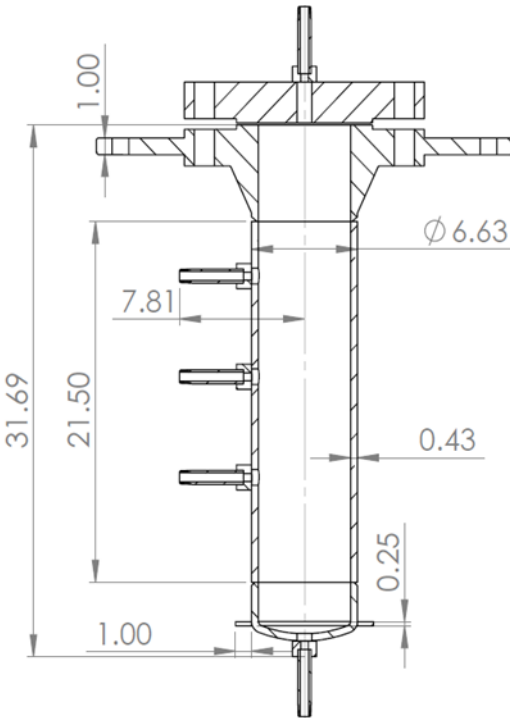


Figure 25. 1kg/h Vessel Geometry.

the higher flow cases (lower figure), temperature rise observed at this thermocouple (TC) is similarly low with the exception of Case 4-D which was previously shown to grossly overestimate sorbent capacity. For this portion of the analysis, the major conclusions still hold, with the following added detail. As noted previously, matching superficial velocities of baseline experimental data does not yield an adsorption step that yields the desired loading of 3.9 mol O₂ adsorbed per cycle in six minutes – where slightly over 20 minutes is expected to be necessary. To match this target, the “moderate” flow rate (increasing this superficial velocity matched-flow by three times) could reach this target within 8-9 minutes based using the calibrated modeling assumptions. This may be acceptable for operation and, with a small increase in flow, the 6 minute target could be reached readily. As shown below and with the balance of adsorption data are shown in an appendix to the CFD Results Appendix A, this higher flow rate case does yield a larger sorbent bed temperature rise and will necessitate thermal management.

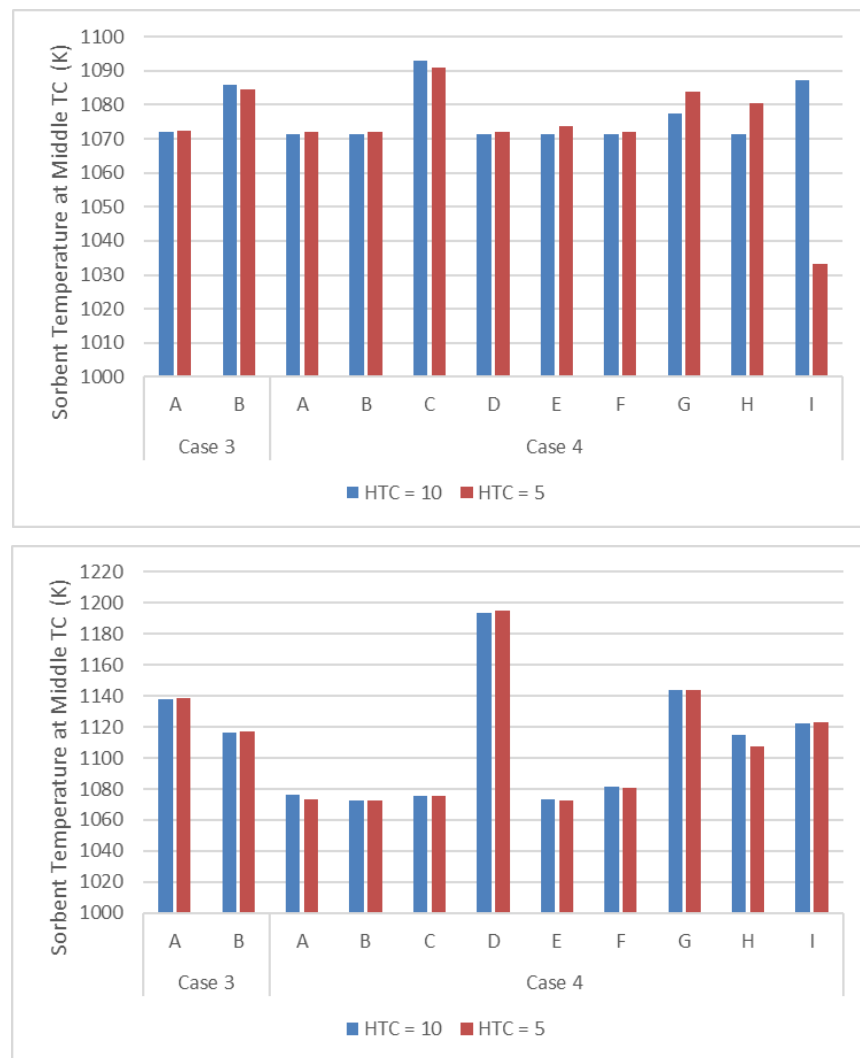


Figure 26: Middle TC Temperature After 6 Minutes (K) for Low Flow (Top) and Moderate Flow (Bottom) Cases

Concerning the regeneration step, the shift to a heat of sorption approach has a very minor impact on results. The conclusions still hold from the prior analysis, which suggest that: a) the regeneration target may be readily reached within the 20 minute target step, with this duration

possibly too long, b) steam purge yields greater regeneration rates over syngas/steam purge, and c) on the impact of regeneration flow rate, lower flow rates are more ideal. A complete set of revised data are in Appendix B to the CFD Report (Appendix A).

As noted in prior analysis with modeling the heat of reaction and extended to revised modeling with the heat of sorption, thermal management may be necessary for two major reasons:

- 1) An increased gas flow rate may be necessary for the geometry selected to accommodate the 1 kg/hr O₂ output target rate. Simulation suggests that a flow rate of greater than three times a flow rate matching the superficial gas velocity of prior TDA experimental data is necessary for the adsorption step not to be excessively long. While simulation data also suggest that the regeneration step may be shorter than expected, a higher flow rate in the adsorption step is still required for the full 30 minute cycle target. With increased loading, the observed temperature rise in the sorbent will also be larger and will likely exceed the 30-40°C upper limit.

As an example, returning to the adsorption modeling and examining the impact of higher gas flow rates and higher external heat transfer coefficient (HTC), that represent greater rates of external cooling, select calibrated cases in Figure 27 indicate a need for thermal management.

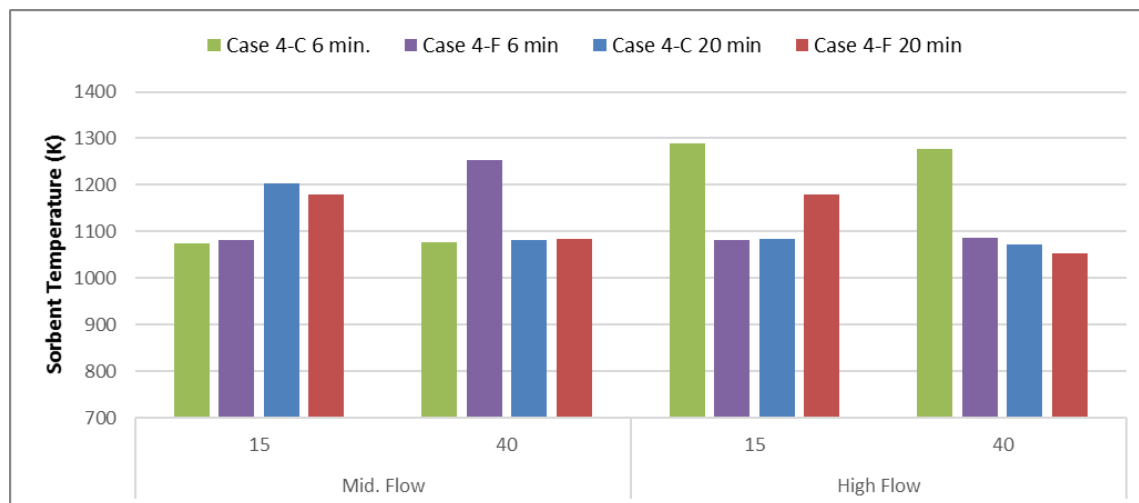


Figure 27. Sorbent Temperature at Middle TC for Select Cases with Higher Flow Rate and External HTC after 6 and 20 minutes

- 2) Prior analysis with the heat of sorption suggest that the peak sorbent temperature can be much higher than the observed temperatures at stationary thermocouple locations. For example, the sorbent loading dynamics for the adsorption step with Case 4-C (Figure 28) are such that the front of the sorbent heats up quickly and the peak sorbent temperature and middle TC show a large temperature difference at 6 minutes. After 20 minutes of sorbent loading, the hot zone spreads out and downstream. In this scenario, a short adsorption step could potentially have excessively hot sorbent temperature. This is influenced by gas flow rates (sorbent loading) and the assumptions of this model.

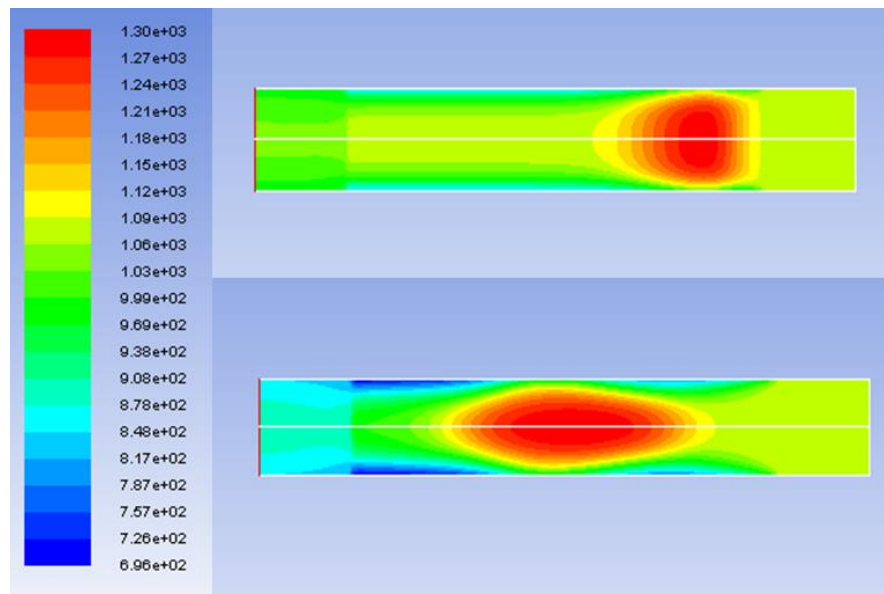


Figure 28. Sorbent Bed Temperatures (K) for Case 4-C at 6 minutes (top) and 20 minutes (bottom) for Moderate Gas Flow Rates

U

sing assumptions for Case 4-C and Case 4-F, the 2-D axi-symmetric model was modified to add two forms of axi-symmetric cooling, jacket cooling in an annulus and a cooling water tube running down the vessel centerline (see Figure 29). Five levels of cooling water flow were simulated for each case during an extended adsorption step with the previously noted “moderate” gas flow. Sorbent temperatures for Case 4-C, with similar results for Case 4-F, are shown in Figure 30. Generally, the peak temperature is minimally affected by cooling method or cooling water flow rate, while the jacket cooling method results in a lower mass-weighted average sorbent temperature which decreases with increasing cooling water flow rate. These temperatures are directly proportional to the sorbent loading (Figure 31) in which the jacket cooling case overcools a larger portion of the sorbent and as a result the sorbent loading is lower. From the standpoint of system design, it is likely that internal cooling tubes are better for system capacity, however they must be more distributed throughout the vessel to limit the peak sorbent temperatures.

Thus, in summary, the conclusions are:

- Jacket and inner tube cooling are viable thermal management options in that the average sorbent temperature is reduced, however optimization is needed.
- Jacket cooling may overcool, or “quench” the sorption process and result in an unacceptable loss of sorbent capacity.
- Peak sorbent temperatures are largely unaffected by each cooling method, regardless of cooling water flow rate, thus more distributed thermal management is needed.

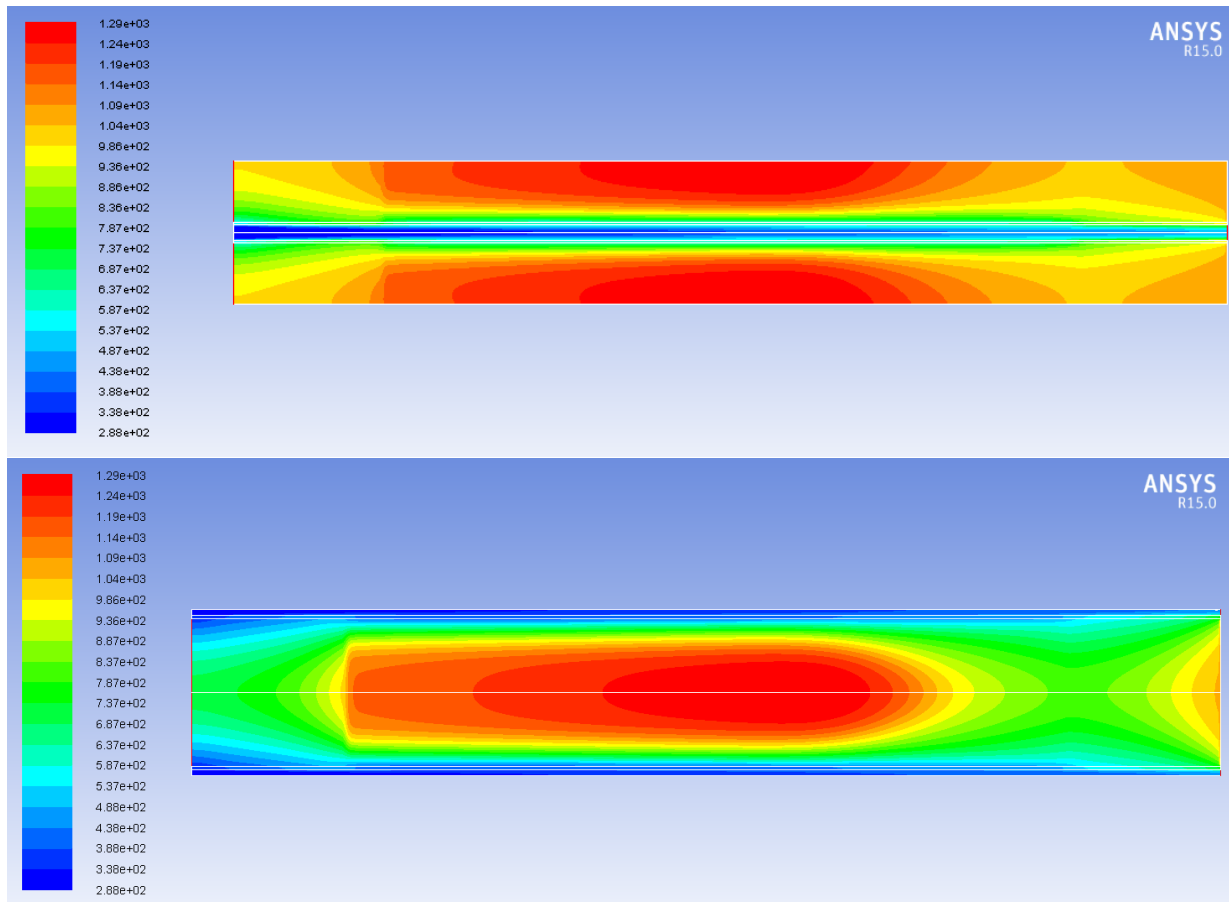


Figure 29. Example Simulation Results (Temperature Contours) for Cooling with Inner Tube (Top) and Jacket Cooling (Bottom)

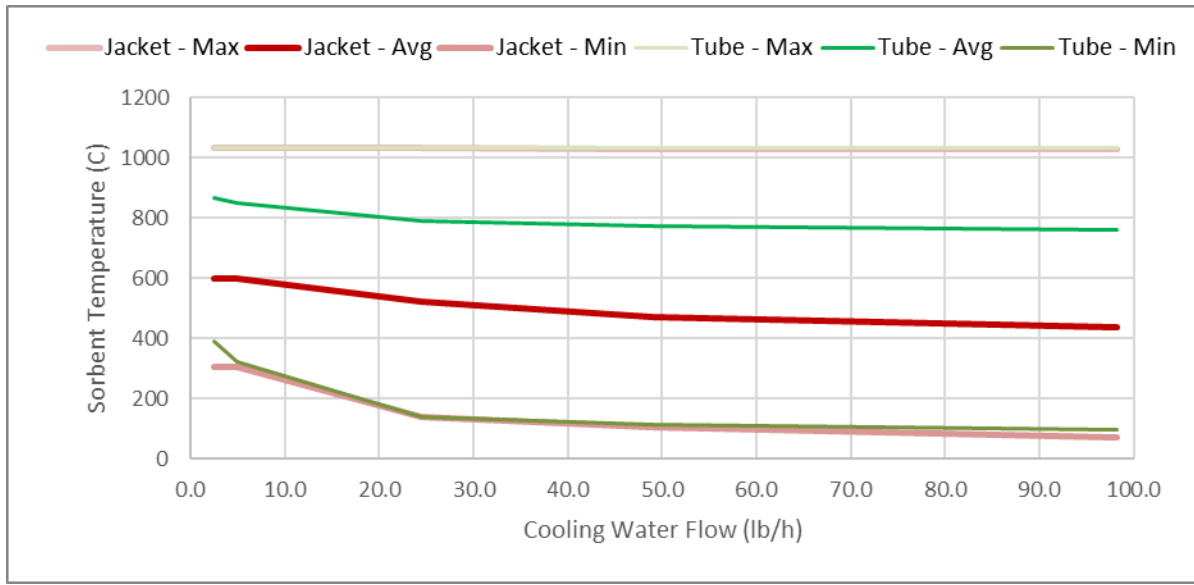


Figure 30. Sorbent Temperature for Active Cooling Simulations with Max/Average/Min Temperatures for Jacket Cooling (Red) and Inner Tube Cooling (Green).

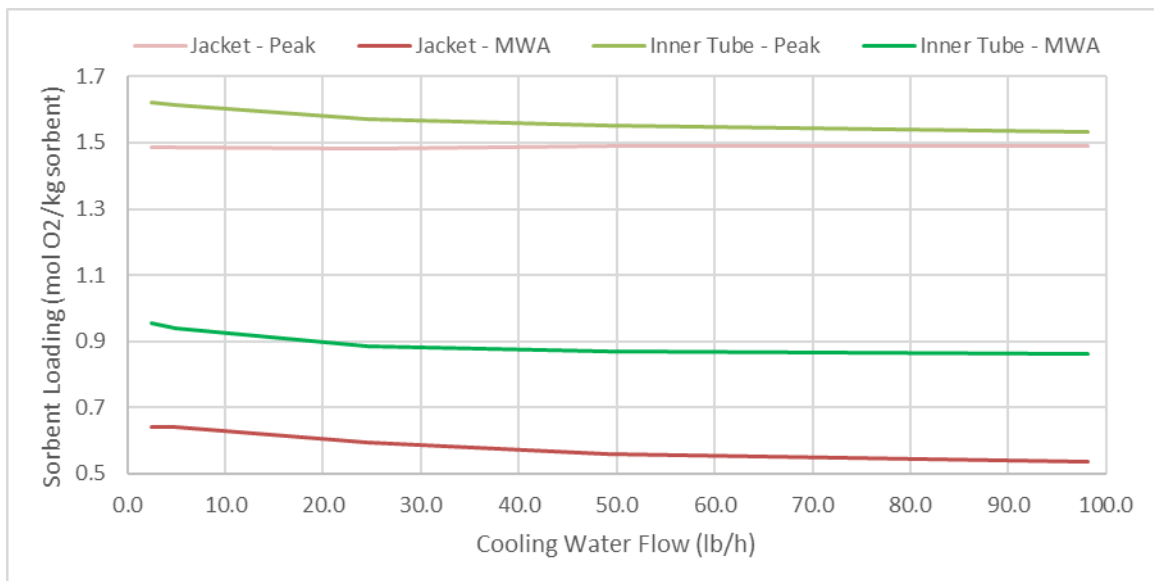


Figure 31. Peak and Mass-Weighted Average (MWA) Sorbent Loading for Jacket and Inner Tube Cooling Methods

Overall Conclusions

Concerning simulation calibration, an extensive series of calibration runs were performed including an adjustment to how the heat of sorption is treated as reported in this addendum. The framework outlined in this report can be applied to a more expansive dataset to adjust how the Arrhenius Rate and Langmuir-Freundlich model parameters are defined. In addition to this, further modeling improvement could be made concerning the physical definition of the sorbent itself, including incorporation of more detailed data that capture, among other things, a) the sorbent pressure effective thermal conductivity, accounting for porosity, to minimize what may be an overestimation of the internal sorbent thermal gradients and b) the overall sorbent pressure drop.

A review of conclusions from these simulations are as follows:

Case 1 – Baseline Simulation

- An increased gas flow rate may be necessary for the geometry selected to accommodate the 1 kg/hr O₂ output target rate. Simulation suggests that a flow rate of greater than three times a flow rate matching the superficial gas velocity of prior TDA experimental data is necessary for the adsorption step not to be excessively long. However, for this step to be 8-9 minutes or shorter, this higher flow rate will yield greater sorbent loading, temperature rise, and will likely necessitate thermal management.
- Simulation data suggest that the regeneration step may be shorter than expected, when matching superficial velocities of the baseline experimental data and extrapolating based upon UCI process modeling, the regeneration step can reach the desired output of 3.9 mol O₂ released per cycle and may be able to do so readily within 20 minutes. Simulation data suggest this may be too long.
- Data are inconclusive regarding the benefit of increasing the regeneration inlet flow rate, however based on prior model validation, these models suggest a lower flow rate is more ideal.

Case 2 – Syngas/Steam Purge

- Generally, the steam purge (UCI Case 2) versus the combined syngas/steam purge (Case 1A) has greater regeneration rates and may be preferable.
- All other findings of the baseline simulation extend to this case.

Case 3/4 – Jacket and Internal Tube Cooling

- Jacket and inner tube cooling are viable thermal management options in that the average sorbent temperature is reduced, however optimization is needed.
- Jacket cooling may overcool, or “quench” the sorption process and result in an unacceptable loss of sorbent capacity.

Peak sorbent temperatures are largely unaffected by each cooling method, regardless of cooling water flow rate, thus more distributed thermal management.

3.4.2 Adsorption Modeling

TDA's process uses a unique sorbent to support an oxidation-reduction (redox) process:



The metal oxide phase auto-reduces by changing T, P, oxygen partial pressure. The auto-reduction releases oxygen, which can be recovered as a pure product. The sorbent removes some (~30%) but not all the O₂ from high pressure air drawn into the gas turbine. The regeneration step is carried out using warm sweep gas (superheated steam) ideally under isobaric/isothermal conditions.

TDA's experimental setup

An experimental dynamic column breakthrough apparatus was design and built in TDA's facilities. The Breakthrough experiments allow understanding the dynamics of the separation system and determined mass and heat transfer parameters, which subsequently are implemented in the simulation and optimization part of the project. Since this separation system is expected to operate at temperatures around 800°C, the breakthrough experiment will help to determine the equilibrium adsorption isotherms that unfortunately cannot be obtained using a standard gravimetric or volumetric system. A simple schematic of the experiment can be seen in Figure 32. A column filled with a non-porous material, i.e., denstone, is used to dissipate the heat effects of the exothermic chemisorption reaction and the high temperature of the process. Mass flow controllers, temperature and pressure transducers along with an Oxygen detector are used to keep track of the process and the gas composition.

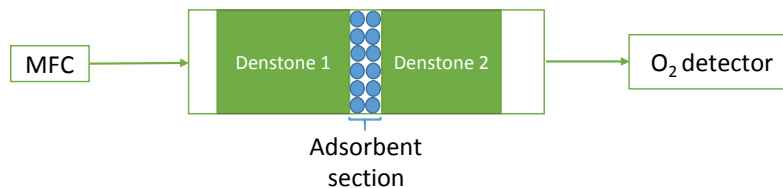


Figure 32. Schematic of the Breakthrough apparatus.

A detailed description of the dimension of the apparatus and some of the adsorbent properties is shown in Table 4

Table 4. System dimensions

<i>Dimensions</i>	
Column length	55.88 cm
Inner diameter (cm)	3.20
Column volume (cm ³)	449.5
Adsorbent section volume (cm ³)	30.64
Piping length (cm)	647.70
Piping volume (cm ³)	47.26
Bed voidage (-)	0.35
Adsorbent mass (g)	24.3
Particle Porosity	0.64

Breakthrough Modeling

Model Equations: Adsorption column dynamics are described using a one-dimensional mathematical model (Hagpannah et al. 2013). The following assumptions are made:

- The gas flow is described by an axially dispersed plug flow model
- The gas phase is ideal
- Mass transfer resistance is controlled by the particle macropores, described by the linear driving force model
- There is no concentration, pressure or temperature gradient in the radial direction
- The system is adiabatic
- Adsorbent properties are uniform in the column
- Darcy's law describes the column's pressure drop

University of Alberta's in-house code written in MATLAB was used to simulate breakthrough. This code accounts for mass, momentum and energy transfer equations. Finite volume methods were implemented to discretize partial differential equations listed in Table 5. The one-dimensional column was discretized into 30 finite volume elements in the axial direction (Hagpannah et al. 2013). The model equations were solved, with necessary boundary conditions, using an in-built ODE solver in MATLAB. For adsorption, the feed gas was introduced at the column inlet, $z=0$, at the feed pressure, P_{feed} , and temperature, T_{feed} . O_2 was adsorbed over N_2 , which was assumed inert. The end of the column, $z=L$, remains open for O_2 breakthrough after the column becomes saturated. Note that these models have been verified at pilot-plant scales units (using 80 kg of adsorbent) and have been published in multiple papers and presented at multiple international conferences (Krishnamurthy et al. 2014).

Table 5. Model equations used for breakthrough simulation.

Gas phase component and total mass balances:

$$\begin{aligned} \frac{\partial y_i}{\partial t} + \frac{y_i}{P} \frac{\partial P}{\partial t} - \frac{y_i}{T} \frac{\partial T}{\partial t} &= \frac{T}{P} D_L \frac{\partial}{\partial z} \left(\frac{P}{T} \frac{\partial y_i}{\partial z} \right) - \frac{T}{P} \frac{\partial}{\partial z} \left(\frac{y_i P}{T} v \right) - \frac{RT}{P} \frac{1-\varepsilon}{\varepsilon} \frac{\partial q_i}{\partial t} \\ \frac{1}{P} \frac{\partial P}{\partial t} - \frac{1}{T} \frac{\partial T}{\partial t} &= -\frac{T}{P} \frac{\partial}{\partial z} \left(\frac{P}{T} v \right) - \frac{RT}{P} \frac{1-\varepsilon}{\varepsilon} \sum_{i=1}^{n_{\text{comp}}} \frac{\partial q_i}{\partial t} \end{aligned} \quad (2)$$

Solid phase mass balance, linear driving force model:

$$\frac{\partial q_i}{\partial t} = \alpha_i (q_i^* - q_i) \quad (3)$$

Column Energy balance:

$$\begin{aligned} \left[\frac{1-\varepsilon}{\varepsilon} \left(\rho_s C_{p,s} + C_{p,a} \sum_{i=1}^{n_{\text{comp}}} q_i \right) \right] \frac{\partial T}{\partial t} \\ = \frac{K_z}{\varepsilon} \frac{\partial^2 T}{\partial z^2} - \frac{C_{p,g}}{R} \frac{\partial (vP)}{\partial z} - \frac{C_{p,g}}{R} \frac{\partial P}{\partial t} - \frac{1-\varepsilon}{\varepsilon} C_{p,a} T \sum_{i=1}^{n_{\text{comp}}} \frac{\partial q_i}{\partial t} \end{aligned} \quad (4)$$

$$+ \frac{1-\varepsilon}{\varepsilon} \sum_{i=1}^{ncomp} (-\Delta H_i) \frac{\partial q_i}{\partial t} - \frac{2h_{in}(T - T_w)}{\varepsilon r_{in}}$$

Darcy's Law for pressure drop:

$$v = \frac{4}{150\mu} \left(\frac{\varepsilon}{1-\varepsilon} \right)^2 r_p^2 \left(-\frac{\partial P}{\partial z} \right) \quad (5)$$

True Breakthrough Response and blank experiments

Prior of performing dynamic column breakthrough experiments, it is necessary to quantify the dead volume of the total system. Accounting for the contributions of the dead volume allow determining the sorbent capacity with accuracy since the amount of gas that is neither adsorbed nor inside the column is taking into account in the mass balance of the system as shown in Equation (6).

$$\frac{P_{ref} F_{in} Y_{in}}{RT_{ref}} \int_0^{\infty} \left(1 - \frac{F_{out} Y_{out}}{F_{in} Y_{in}} \right) dt = \overbrace{V_{col} \varepsilon C_{avg}}^{voids} + \overbrace{V_{dead} C_{avg}}^{dead volume} \quad (6)$$

Dead volume experiments were performed using the same column as the actual breakthrough experiment but without sorbent. In this way, the dead volume will include the piping plus the volume of the denstone and adsorbent section of the column. The sorbent volume at the end should be deducted from the dead volume in order to obtain the real value. The calculation of the dead volume, V_{dead} , from equation (6) gives a value of 518 cm³ after subtracting the sorbent section volume.

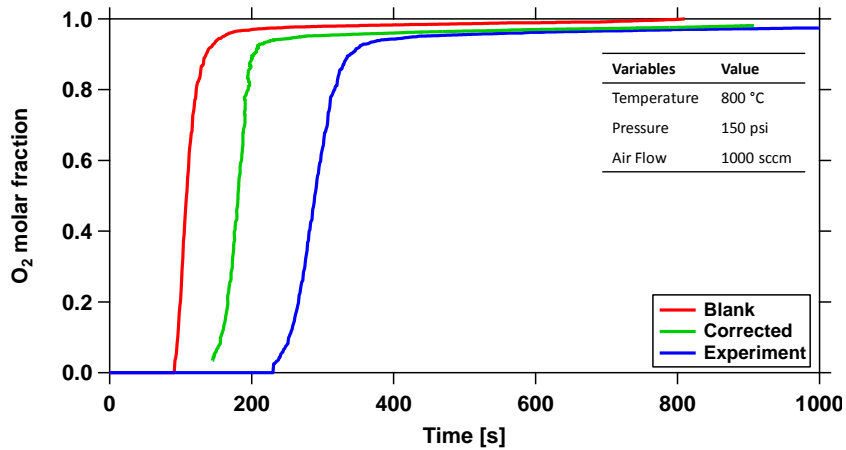


Figure 33. Dead volume experiment

After collecting actual breakthrough experimental data, also known as the composite response, extra-column effects must be subtracted. This is to ensure that the data collected represents only what happens within the column's packed length. The composite response is corrected by the point by point, PBP, method, Equation (7). This was a different approach than how extra-column effects were corrected in the isotherm.

$$t_{blank_{resp}} = t_{blank} + t_{denst1} + t_{denst2} + t_{empty} - t_{pipe} \quad (7)$$

$$t_{ads} = t_{expt} - t_{blank_resp} \quad (8)$$

Point by point correction creates a true response, t_{ads} , based of a difference between the composite, t_{exp} , and blank, $t_{blank_response}$, responses via an interpolation. The blank response was performed in the same as the dead volume experiments. Figure 33 shows the difference between blank, breakthrough and corrected breakthrough composition profile for a certain experiment. Corrected breakthrough profile is calculated using equations (7) and (8). Figure 34 shows the corrected curve for one of the experiments performed at 800°C and 300 psia. From the experiment, it was possible to determine that the dead time of the system for a feed flow of 1000 sccm is around 141 seconds.

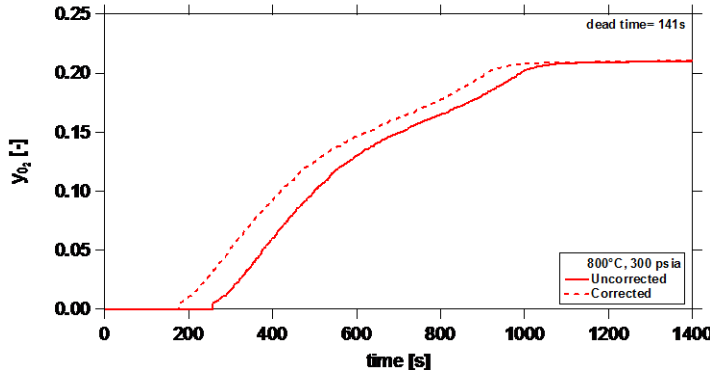


Figure 34. Point by point correction

3.4.2.1 Determination of adsorption isotherms from breakthrough experiments:

Oxygen loadings were determined using dynamic column breakthrough. A mixture of 21.5% oxygen balanced Nitrogen was fed to the column. The total pressure was varied between 12 to 300 psi as shown in Figure 35 in order to have different oxygen partial pressures while temperature in the system was kept at 800°C. Temperature profiles are also shown in Figure 35

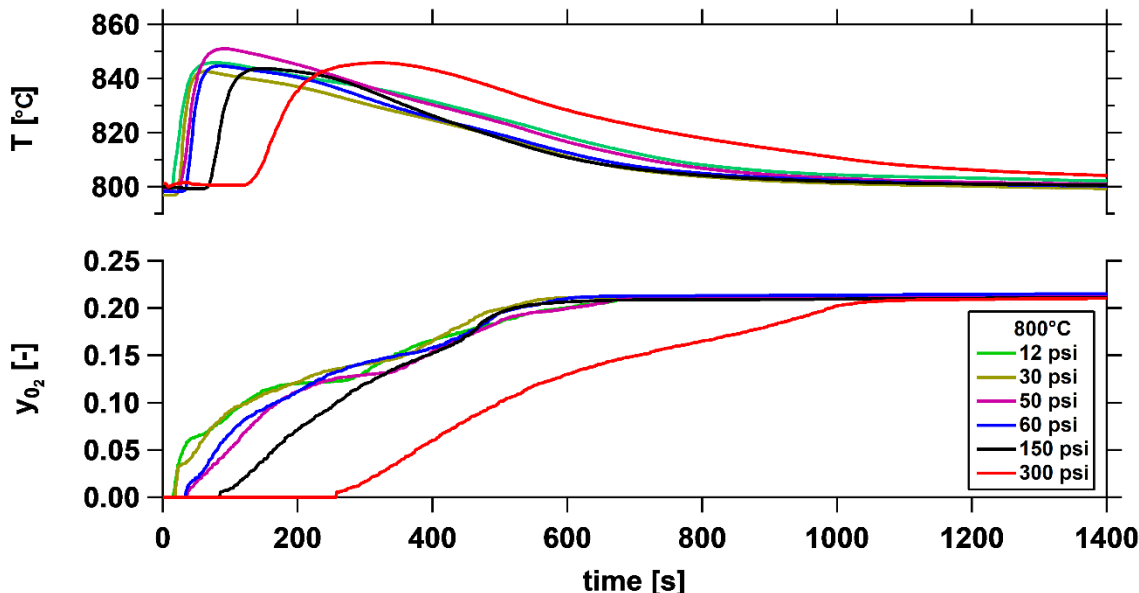


Figure 35. Experimental breakthrough composition and temperature profiles

Accumulation can be determined through integration of the breakthrough curve or through the accumulation of material in each phase of the column plus the dead volume contributions. After a given breakthrough, the accumulation was determined via mass balance, i.e., Equations (9) to

(13). The calculated loadings are repeatable; all experiments were confirmed with at least one other experiment at the same conditions. Experimental oxygen loadings were used to fit the Langmuir isotherm parameters. A comparison between the experimental and the calculated oxygen loadings along with the Langmuir isotherm parameters is shown in Figure 36.

$$in - out = Accumulation \quad (9)$$

$$F_{in}\rho_{in} - F_{out}\rho_{out} = \overbrace{V_{col}\epsilon C_{avg}}^{\text{voids}} + \overbrace{V_{col}(1-\epsilon)q^*}^{\text{solid}} + \overbrace{V_{dead}C_{avg}}^{\text{dead volume}} \quad (10)$$

$$\int_0^{\infty} \left(\frac{F_{in}P_{ref}T_{col}}{P_{in}T_{ref}} \frac{P_{in}y_{in}}{RT_{col}} \right) dt - \int_0^{\infty} \left(\frac{F_{out}P_{ref}T_{col}}{P_{out}T_{ref}} \frac{P_{out}y_{out}}{RT_{col}} \right) dt = Accumulation \quad (11)$$

$$\frac{P_{ref}F_{in}y_{in}}{RT_{ref}} \int_0^{\infty} \left(1 - \frac{F_{out}y_{out}}{F_{in}y_{in}} \right) dt = \overbrace{V_{col}\epsilon C_{avg}}^{\text{voids}} + \overbrace{V_{col}(1-\epsilon)q^*}^{\text{solid}} + \overbrace{V_{dead}C_{avg}}^{\text{dead volume}} \quad (12)$$

$$\frac{\frac{P_{ref}F_{in}y_{in}}{RT_{ref}} \int_0^{\infty} \left(1 - \frac{F_{out}y_{out}}{F_{in}y_{in}} \right) dt - V_{col}\epsilon C_{avg} - V_{dead}C_{avg}}{V_{col}(1-\epsilon)} = q^* [=] \frac{\text{mol of } O_2}{\text{cm}^3 \text{ of adsorbent}} \quad (13)$$

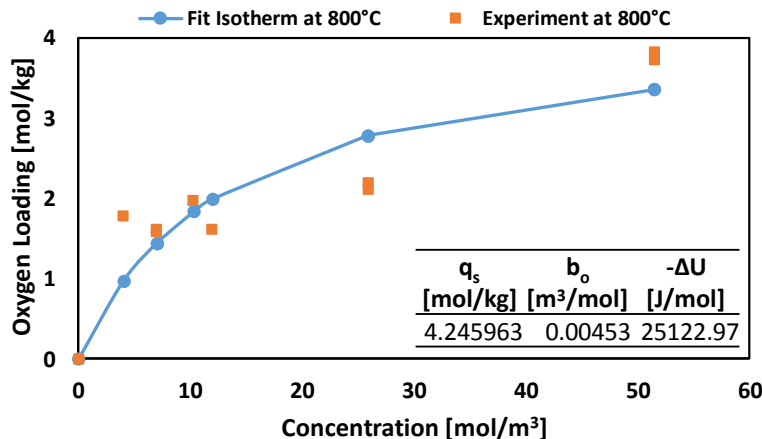


Figure 36. Experimental Oxygen loading and isotherm fit

Simulating Experimental Results

The first step in the simulations was to validate the experimental results obtained from the breakthrough experiments. Figure 37 shows the comparison between the experimental breakthrough profile and the simulated profile using the model described above. The simulation is able to match the O_2 elution time but the shape of the curve follows a sharper path in the simulation case. The temperature profile depicted in Figure 38 shows the same elution time for the thermal front but in this case, the experimental temperature profile has a higher temperature rate compared to the simulated profile. *This difference in the simulation is due to the absence of data about the thermal properties of the material such as heat capacity and heat transfer coefficients.* The determination of the thermal properties of the material will be carried out in a future stage of this project.

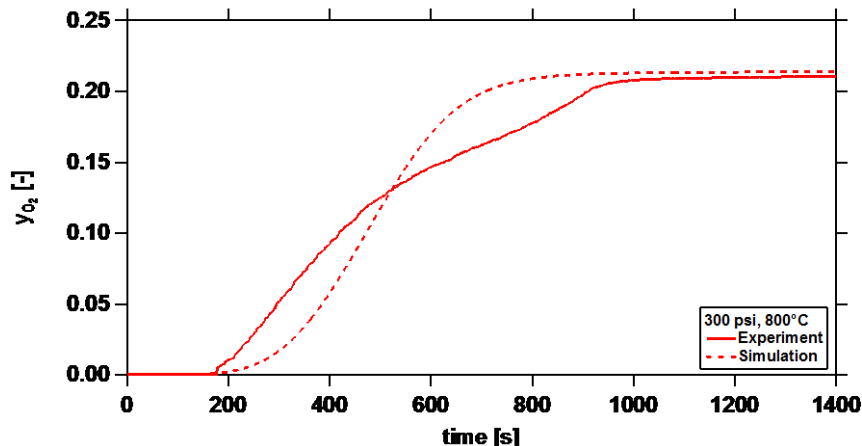


Figure 37. Experimental and simulated breakthrough composition profile

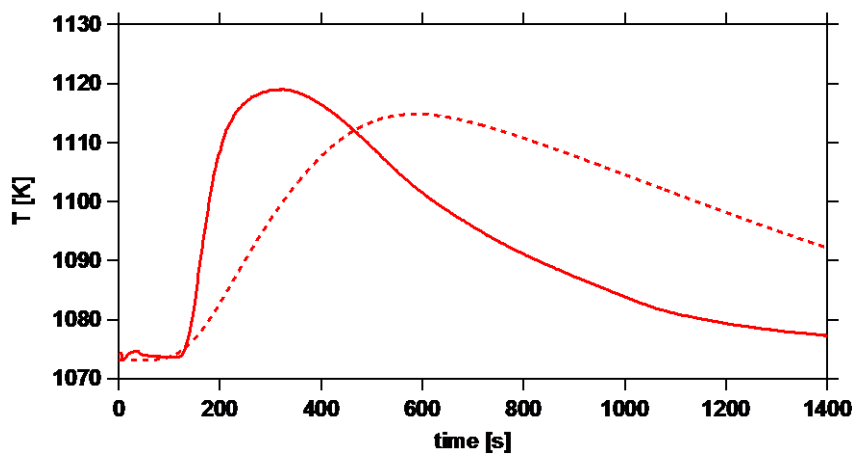


Figure 38. Experimental and simulated breakthrough temperature profile

3.4.2.2 Simulation of pressure swing adsorption (PSA) processes

After the breakthrough profiles for O₂ were predicted well by the simulation, a 4-step pressure swing adsorption (PSA) cycle was configured to run a pilot scaled simulation of the material for performance evaluation. The PSA cycle used in this work, consists of a light product pressurization, adsorption, co-current blowdown and a counter-current evacuation step. The key features of these steps are explained below:

- I. **Adsorption:** Feed gas (21.5% O₂ and 78.5% N₂) is introduced at z=0 at feed pressure (P_H), in this case 310 psia and temperature (T_{feed}) equal to 800 °C. The strongly adsorbed component (O₂) is adsorbed preferentially over the weakly adsorbing component (N₂) in this step. The end, z=L is kept open and N₂ being the weakly adsorbed component is collected at this end, while the bed is saturated with the feed.
- II. **Co-current blowdown:** The feed end of the column (z=0) is closed and the column is depressurized from high pressure (P_H) to an intermediate pressure (P_{INT}) from the z=L end. This step removes the weakly adsorbed component from the solid and the gas phase and is primarily a light product step, thereby increasing the concentration of the strongly adsorbed component (O₂) in the column. Due to depressurization, a small amount of the strongly adsorbed component could be lost from the N₂ product end.

- III. **Counter-current evacuation:** The end, $z=0$ is concentrated with the strongly adsorbed component (O_2) and in order to remove the O_2 from the bed, the column is closed at the end, $z=L$ and is depressurized from an intermediate pressure (P_{INT}) to a low pressure (P_L). This is typically the O_2 product step and depending on the low pressures attained during this step, the bed can be regenerated completely or a significant amount of O_2 could remain in the solid phase.
- IV. **Light Product Pressurization:** The column at the end of counter-current evacuation step is at a low pressure (P_L). The column is pressurized from $z=L$ end using N_2 product gas while the other end ($z=0$) is closed. The product is introduced into the column at a high pressure (P_H) is predominantly N_2 . The pressurization and depressurization in the column follows a pre-defined exponential pressure profile.

The performance of the PSA cycles discussed in this section is determined using key performance metrics, purity and recovery:

$$\text{Purity, } P_u(O_2) = \frac{\text{Total moles of } O_2 \text{ in extract product in one cycle}}{\text{Total moles of gas in extract product in one cycle}} \quad (14)$$

$$\text{Recovery, } R_e(O_2) = \frac{\text{Total moles of } O_2 \text{ in extract product in one cycle}}{\text{Total moles of } O_2 \text{ fed into the column in one cycle}} \quad (15)$$

3.5 Task 5. Optimization of Cycle Sequence

Optimization of pressure swing adsorption (PSA) processes

Pressure swing processes are complex chemical operations as they involve discrete non-continuous steps and they are inherently operated at non-steady states. These processes involve the transfer of both heat and mass between the gas and the solid phase. Finally, from Table 6, it is clear that there are many operating variables that can be chosen over a wide range of operating conditions. The key question from the perspective of operating a large-scale process is **“What combination of these variables gives the best performance?”** This is a very complex problem to solve. Over the years, our group has developed state-of-the art optimization. In this, we combine a multi-objective optimizer with detailed process models. This optimizer searches > 5000 unique set of operating conditions; performs detailed simulations; and identifies the best performance that a material can achieve. **As shown recently, performing full model optimization is the best way to select materials as simple metrics such as selectivity and working capacity are not reliable (Rajagopalan et al. 2016).**

	t adsorption [s]	t blowdown [s]	t evacuation [s]	P blowdown [psi]	P evacuation [psi]	Feed velocity [m/s]
Lower bound	5	20	20	102	72	0.01
Upper bound	100	200	200	310	101	2

Table 6. Process variables used in the full-model optimization

To perform the optimization, a non-dominated sorting genetic algorithm II (NSGA-II) available in Matlab was used. An initial population was chosen from within the bound of operating conditions

shown in Table 6. The optimization of the performance indicators of purity and recovery was done simultaneously and the resulting points are shown in Figure 8.

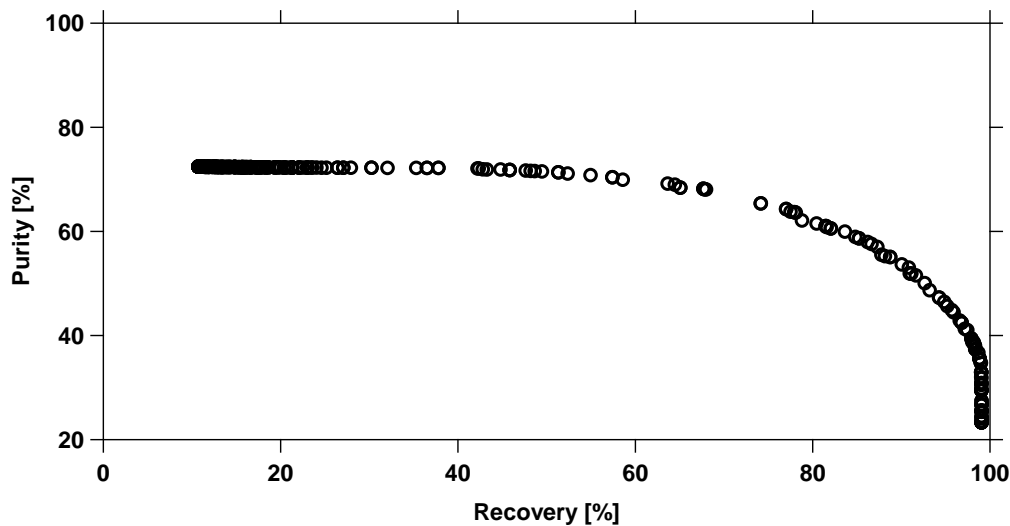


Figure 39. Pareto front Purity vs Recovery for TDA material using a LPP cycle

The curve shown in Figure 39 is called as a the “Pareto front” which provides the best combination of purity and recovery that the material can achieve **As can be seen the TDA sorbent is able to purify oxygen up to 70% using an evacuation step of 72 psi (~5 bar).** Higher O₂ purities were achieved with the evacuation pressure decreased to atmospheric conditions; however, by doing so, the cost of compression will also increase and therefore, affecting the economics of the process.

4-bed Scheme - 2

Total Cycle time (a min) Idle time (0 min)

Time (min)	Stage 1			Stage 2			Stage 3			Stage 4		
	a	b	c	d	b	c	d	b	c	d	b	c
Bed 1	ADS	EQ1D	CoBD	CnBD		PURGE		EQ1R		PRESS		
Bed 2	EQ1R	PRESS			ADS		EQ1D	CoBD	CnBD		PURGE	
Bed 3	PURGE	EQ1R	PRESS			ADS		EQ1D	CoBD	CnBD		
Bed 4	EQ1D	CoBD	CnBD		PURGE		EQ1R	PRESS			ADS	

4-bed Scheme - 5

Total Cycle time (a min) Idle time (0 min)

Time (min)	Stage 1		Stage 2		Stage 3			Stage 4	
	a	b	b	d	e			d	
Bed 1	ADS	BD			PURGE				PRESS
Bed 2	PURGE	PRESS	ADS	BD		PURGE			
Bed 3		PURGE		PRESS	ADS		BD	PURGE	
Bed 4	BD		PURGE		PRESS		ADS		

Figure 40. Optimized PSA cycle sequence and steps.

A detailed evaluation of the TDA material for air separation was performed. Experiments revealed that the material has high O₂ affinity. The biggest strength of this material is its negligible N₂ capacity. Detailed process optimization shows that the material can produce superior O₂ purity at modest recoveries. We further optimized the PSA cycle sequence we use for the high temperature air separation. Figure 40 shows the optimized PSA sequences based on the adsorption and CFD models developed in Task 4. The 4-bed scheme- 2 maximizes recovery by including pressure equalization with both co and countercurrent depressurization while 4-bed scheme -5 maximizes the purge time to provide a higher working capacity.

3.6 Task 6. Design of 1 kg/hr Prototype Unit

We completed the engineering and design of the 1-kg/hr prototype unit and finalized the build of materials for fabrication. The prototype unit contains 4-beds to provide continuous oxygen production, while each of the beds undergoes a set of transitions between the various steps in the adsorption cycle, namely adsorption, pressure equalization, blowdown, desorption/purge and pressurization. Typical steps in our adsorption cycle sequence are provided in Figure 41. The reactor will be fabricated using Incoloy 800HT. Incoloy was selected as a lower-cost alternative to Inconel 625 in order to reduce material cost without adversely impacting the vessel strength or lifetime. Pressure vessel calculations have been completed in order to determine the shell thickness, and creep calculations have been performed in order to verify that the service life will meet or exceed the 2000 hours required by the lifetime testing in this research plan. As detailed below, in the final material specs for the system we decided to use Incoloy pipe, tubing, and fittings in the high-temperature region and type 316 stainless steel tubing and fittings in the intermediate-temperature regions.

Total Cycle time (a min)		Idle time (2*c min)			Stage 1			Stage 2			Stage 3			Stage 4		
Time (min)		a		b	c	d	b	c	d	b	c	d	b	c	d	
Bed 1		ADS		EQ1D	HOLD	EQ2D	BD	PURGE	EQ2R	EQ1R	HOLD	PRESS				
Bed 2		EQ1R	HOLD	PRESS		ADS	EQ1D	HOLD	EQ2D	BD	PURGE	EQ2R				
Bed 3		BD	PURGE	EQ2R	EQ1R	HOLD	PRESS		ADS	EQ1D	HOLD	EQ2D				
Bed 4		EQ1D	HOLD	EQ2D	BD	PURGE	EQ2R	EQ1R	HOLD	PRESS		ADS				

Figure 41. Typical cycle sequence for the 1-kg/hr prototype unit.

Although a suitable high-temperature valve has been identified for use at the full process temperature of 850°C, the cost, size, weight, and lead time were deemed excessive for the prototype system's scale. Therefore, an alternative U-series high-temp bellow valves from Swagelok with service to 632°C at our maximum operating pressure of 350 psig was selected. This modification required that the prototype system be divided into high-temperature and intermediate-temperature regions with appropriate overtemperature and overpressure protection for each region. In addition to the temperature and pressure protection, a series of adjustments were required to perform the final gas heating in the transition between the intermediate-temperature region (600°C operating temperature) where the process control instrumentation and flow control valves are located and the high-temperature (800°C operating temperature) region that houses the high-temperature heat exchangers and sorbent vessels. The detailed process and instrumentation diagram (P&ID) and the drawings for the reactor are provided in Figure 42 and Figure 43. The 3-D layout for the entire skid is provided in Figure 44.

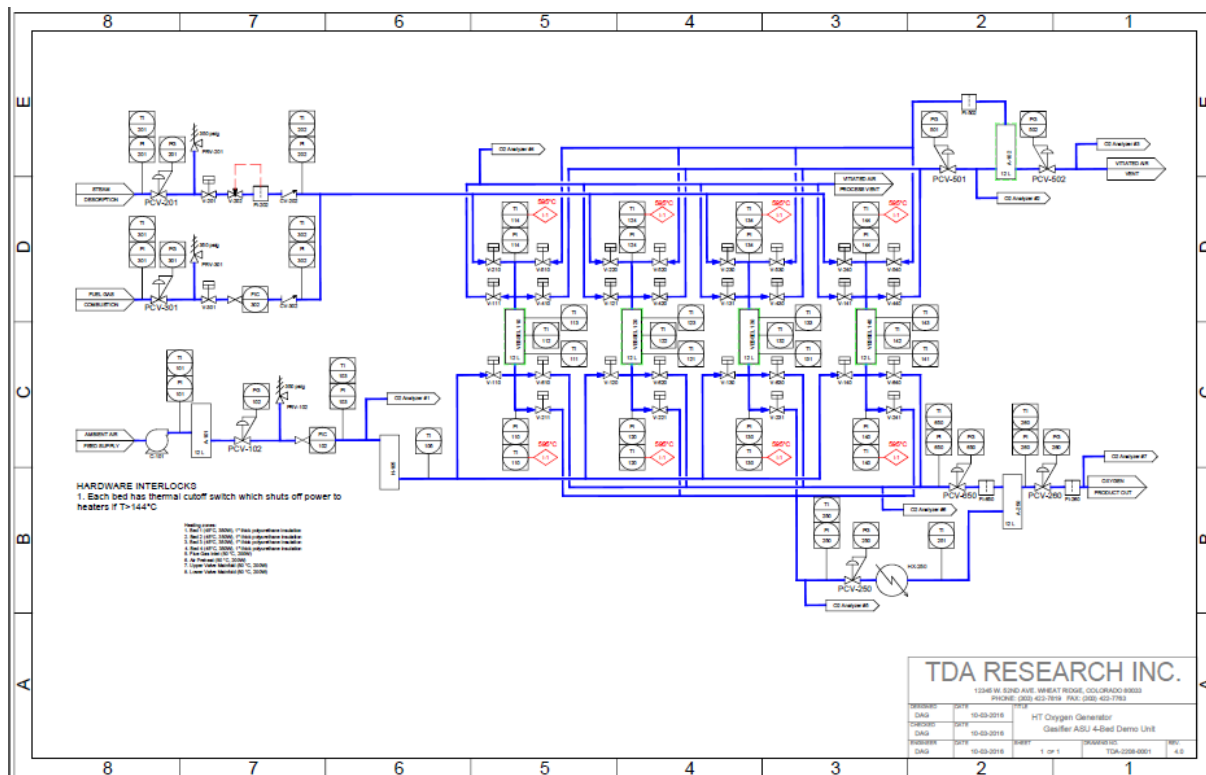


Figure 42. P&ID of the 1-kg/hr prototype unit.

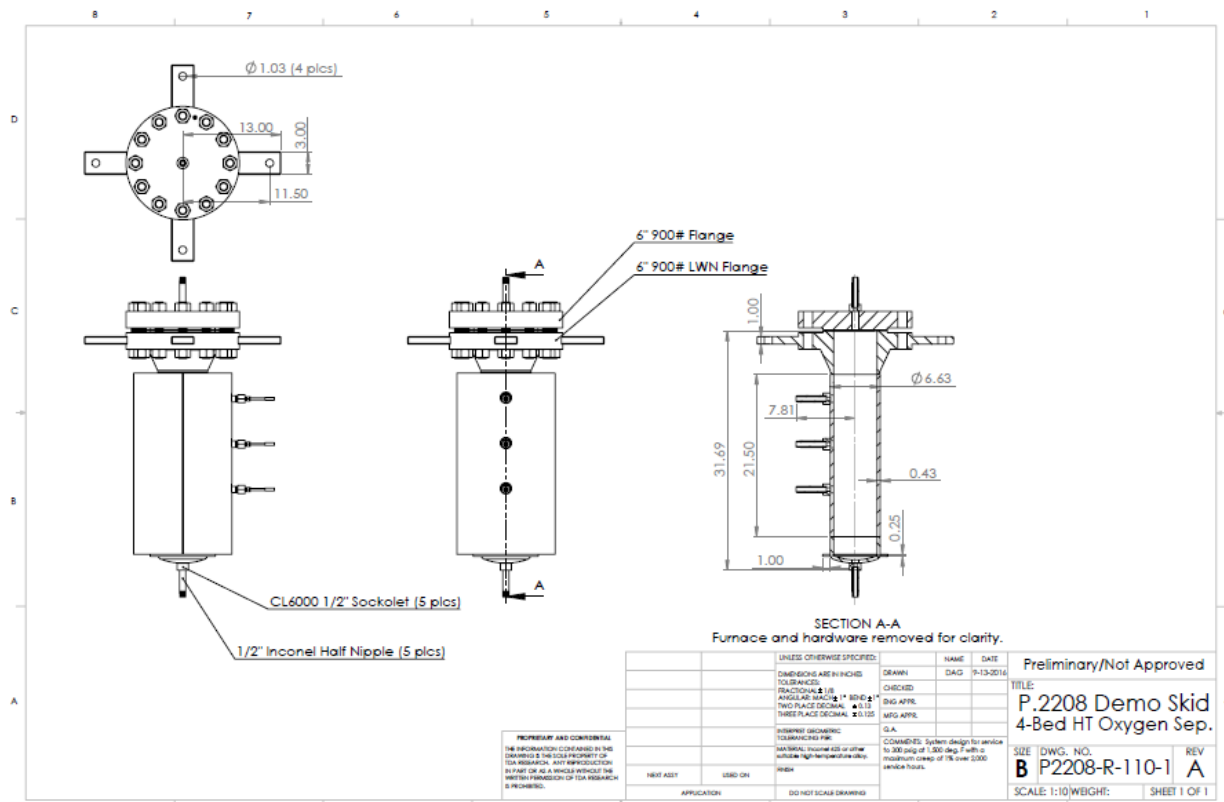


Figure 43. Drawing of the sorbent bed for the 1-kg/hr prototype unit.

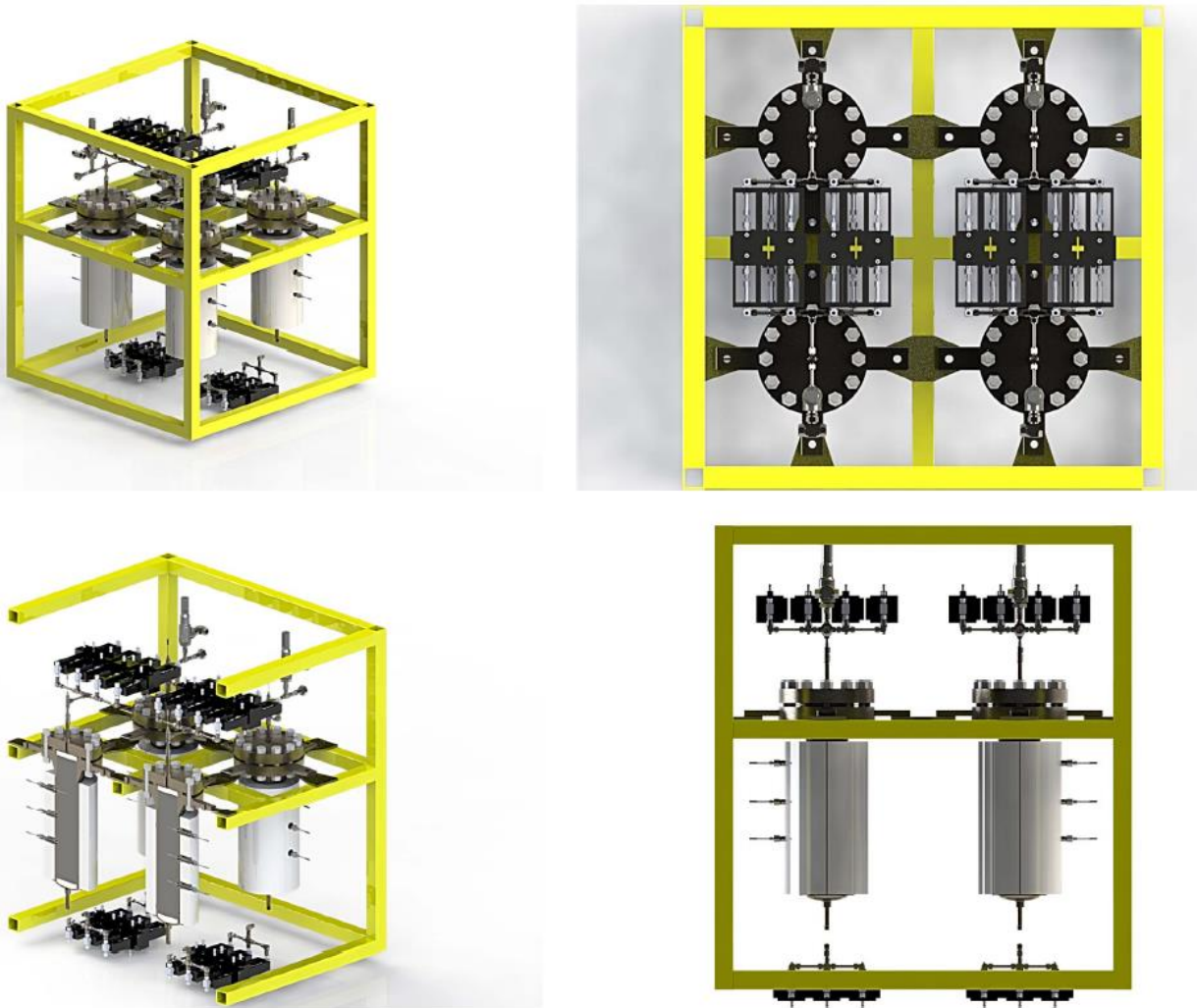


Figure 44. 3-D layout of the 1-kg/hr oxygen production prototype unit.

3.7 Task 7. Fabrication of 1 kg/hr Prototype Unit

Next, we finalized the computer control specification for the system and secured final approval drawings from vendors for several components including the large electric furnaces (Mellen, Inc.) that are required for heating the reactor vessels. In addition to acquiring the off-the-shelf components necessary for construction, we prepared the final build-to drawings for the various reactor vessels, accumulator vessels, heat exchangers, and structural framing necessary for the demo system. These drawings were finalized, received final internal approval and released to fabrication. The structural steel framework for the 4-bed system was



Figure 45. The completed structural frame assembly for the demo-scale tests system with mounted electronics enclosure and high-temperature tube furnaces.

cut, welded, and painted. The electronics enclosure that contains all of the controls for the system (including the onboard PC to run the LabView control system) was populated with all of the major components and affixed to the side of the structural frame. The clamshell-style electric furnaces (Mellen) was received and mounted on the skid frame. Figure 45 shows the complete frame in the TDA shop with the Mellen tube furnaces and the electronics enclosure mounted. One furnace has been opened to show a completed vessel in position for reference. Figure 46 shows the populated electronics enclosure before final wiring and Figure 47 shows a close up of a complete reactor vessel positioned within the furnace. A custom reactor support has been designed and attached to the structural frame and cast high-temperature structural insulators have been ordered to position the reactors during high-temperature operation. A prototype of the cast insulator can be seen for size reference in Figure 47.

Final Vessel Design and Fabrication

Having previously sourced and ordered the Inconel 800H pipe and plate required for the reactor vessel, TDA has finalized the pressure vessel calculations based on the available material in order to complete a design that meets all the requirements of Section VIII, Division I of the ASME Boiler & Pressure Vessel (B&PV) code (2012 edition). The final design and review has resulted in a vessel rated for a maximum allowable operating temperature (MAWT) of 805°C (1481°F) and a maximum allowable operating pressure (MAWP) of 295 psi. The minimum design metal temperature (MDMT) is set at -20°C (-4°F) and the minimum time to creep-rupture has been determined via the Larson-Miller relationship to be 13,760 hours or roughly 1.57 years. For this calculation the creep-rupture data provided in section III of the B&PVC was used to calculate the Larson Miller Parameter from a maximum stress intensity value of 3 ksi. The later was determined by doubling the stress intensity calculated for the main cylindrical vessel shell and confirmed via finite element analysis performed using SolidWorks Simulation Professional (2016 version) on a simplified 3D model assembled within the software environment. Based on the MAWP and the ratio of the allowable stress value at MAWT to the allowable stress value at room temperature the hydrostatic test pressure was determined to be 3064.33 psi.

We then completed fabrication of the 4 reactor vessels and hydrostatic tested them to 1.5x the operating pressure. We then mounted the accumulator vessels, assembling the main system valves and plumbing, obtaining and mounting the regeneration steam generator and inlet air preheater, and completing the field wiring of the components. Upon completion of those tasks, the final heat traces for the heated lines were installed and the lines were insulated. Finally, TDA installed a custom LabView control program based on a general program currently in use on a number of similar test systems and a complete system shakedown was completed. Upon



Figure 46. The electronics enclosure with the main components populated and awaiting field wiring to the instrumentation.



Figure 47. A complete Incoloy 800H vessel positioned within one of the Mellen tube furnaces.

completion of the system shakedown, the system was loaded with the large-batch sorbent material from the scale-up production runs.

Figure 48 shows the picture of the complete prototype unit after fabrication with all four high temperature high pressure reactors. Figure 49 illustrates the fabrication and assembly of the ceramic insulation/support to the bottom end of the reactor.

We designed and incorporated passive cooling loops to cool the Steam/O₂ mixtures from 800°C to \leq 600°C to safeguard the system valves. We also employed additional passive cooling to protect the instrumentation. Figure 50 (left) shows the picture of the passive cooling loop installed on the end of the reactor. Figure 50 (right) shows the solidworks flow simulation of the passive cooling loop illustrating the degree of cooling that can be accomplished.

After completion of the final construction and assembly of the 4-bed, 10 scfm demonstration system. The system was shipped from TDA's fabrication shop in our Wheat Ridge, CO facility to our lab in Golden, CO (Figure 51) and was positioned in the lab space designated for testing. All of the system I/Os were installed and the final electrical integration was completed.



Figure 48. The completed structural frame assembly with the high temperature reactors and tube furnaces installed.

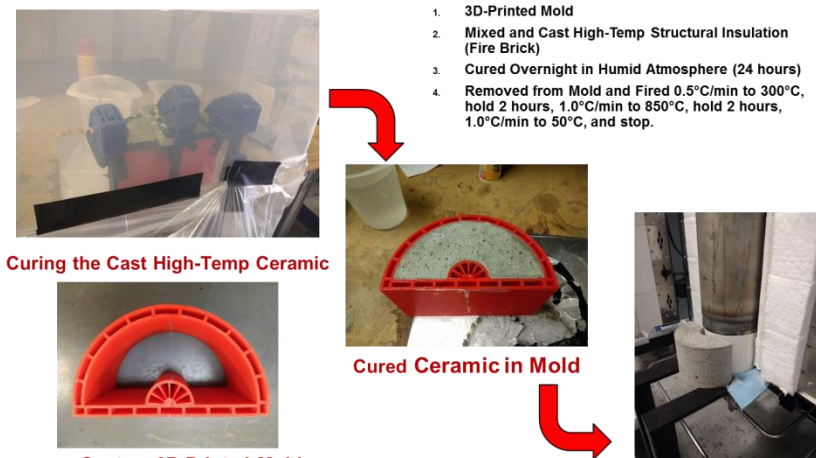


Figure 49. Fabrication of the Ceramic insulation/support.

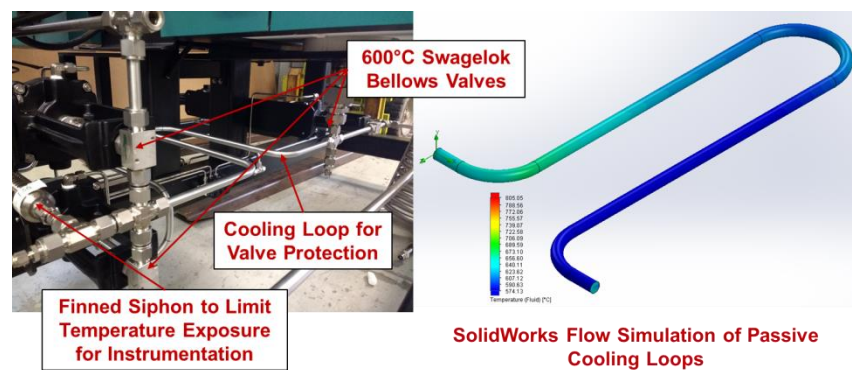


Figure 50. High-temperature passive cooling loops.

The electronics enclosure containing all of the controls for the system (including the onboard PC to run the LabView control system) with all of the major components was completed (Figure 53) and affixed to the side of the structural frame.

System Integration and Shakedown

The final system integration was then completed with the system being powered directly from a 3-phase 480 V (wye) main electrical supply (see Figure 52). Interconnects to/from TDA's municipal water supply and house compressed air service were established. Connections for the various gas services (process air inlet, methane inlet, oxygen-depleted air outlet, and oxygen product outlet) were made, and the connection for the relief manifold outlet was plumbed. In the case of the various outlets (including the relief header (see Figure 54), all are permanently plumbed to a dilution duct running through the ceiling of the test facility and exhausting outside of the building. A pitot tube affixed to the dilution duct provides control system feedback ensuring that the blower remains operational throughout all testing. In the event of a failure of the blower, the pitot signal arriving at the test unit's control system initiates a safety shutdown—requiring manual interaction and blower re-start before testing can resume. Additional hand-operated emergency stops (latching E-Stop buttons) are also integrated into the system and situated on either side of the rig. The e-stop buttons trigger an emergency interruption of power that will open the main high voltage contactor, de-energizing all of the heater control zones and terminating all pumps while leaving the low-voltage equipment powered in order to facilitate system monitoring and controlled shutdown/restart. The E-Stop activation also registers on the control system as an input variable—triggering additional software-generated shutdown procedures that close off the inlet valves and safely depressurizes the system in accordance with the approved SOP (Standard/Safe Operating Procedure).



Figure 51. Prototype unit being moved from TDA's Fabrication shop to the test lab.



Figure 53. The electronics enclosure with the main components populated and showing field wiring to the instrumentation.



Figure 52. The prototype unit as installed at TDA's Golden, CO test facility with power delivered from the 3-phase 480V (wye) connection and the on-board control PC energized.



Figure 54-Relief header assembly, relief indicating sensor, and outlet plumbing that integrates to dilution duct above drop ceiling.

3.8 Task 8. Testing of the Prototype Unit

After completing the fabrication of the prototype unit, we generated an as-built P&ID. We then completed the final engineering review and documented the final P&ID for the system and secured final approval from TDA's Safety officer for testing. Figure 55 shows the picture of the prototype unit installed at TDA's TM facility in Golden, CO.

For this deployment, a custom control sequence was developed for the 4-bed, high-temperature oxygen sorbent testing. The sequence includes a master calling sequence that steps through the complete sequence cycle along with a series of subroutines to handle individual tasks. In this manner, it is possible to quickly bring any/all beds online/offline using simple state (logic) variables assigned to the various beds. Moreover, it is also possible to selectively activate and deactivate various aspects of the "complete" cycle sequence. This includes turning on/off steps like the co-current and/or counter-current blowdown steps,



Figure 55. Prototype unit installed at TDA's TM facility

selecting to repressurize beds using hot, oxygen-depleted off-gas from the O₂ absorption phase or with feed air (or a combination thereof), and the ability to determine the number of beds in regeneration at any point in time (single, sequential bed regeneration is the default; however, tests were also conducted with a dual-bed and 3-bed staggered, concurrent regeneration scheme.

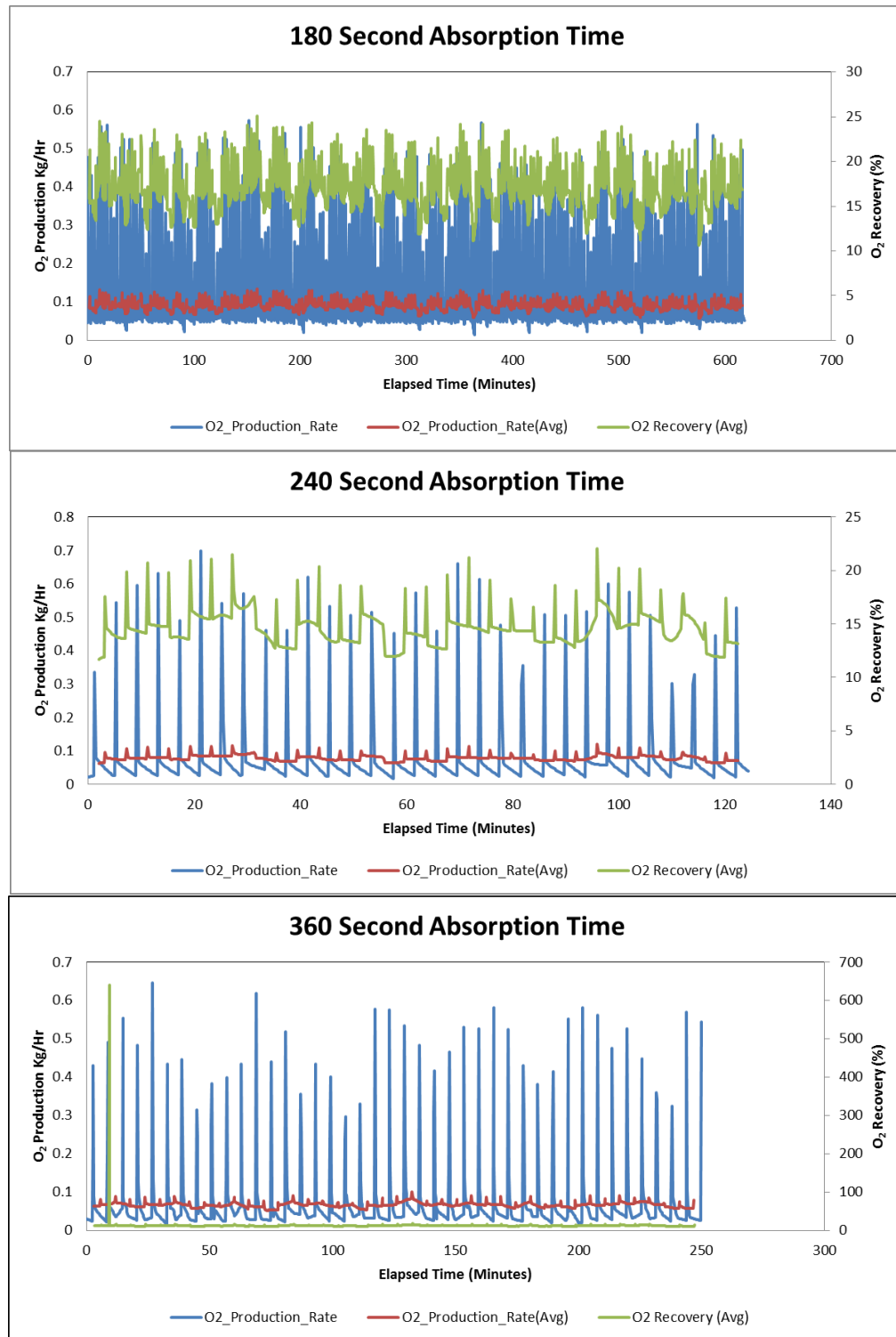


Figure 56. Impact of absorption time.

Data generated throughout the shake-down and testing period was collected in TDA's custom process historian and stored as a series of individual text files with each data series being stored in a separate file. This approach allows for each data point to be logged independently using an adjustable deadband to set the required amount of data drift between adjacent datapoints. Although a slight oversimplification, the data recording is limited to points that surround a change in slope in the raw data stream. If the data does not change slope for a specified period in time, a data point is recoded regardless in order to maintain a positive record of the point. Using this data, it is possible to recreate the raw data while minimizing the required storage and bandwidth. The latter is especially important for remote testing where data is transmitted via the Internet from a remote testing site back to TDA's offices.

Single Bed Tests

In the initial testing, we carried out single bed tests, reproducing the bench-scale test conditions in order to provide a basis for comparing the performance of the prototype unit against our earlier bench-scale tests. After the initial performance characterization is complete, we carried out multibed cycling tests to assess the impact of long-term testing and provide additional data useful in determining the expected sorbent lifetime under realistic operating conditions.

In the initial single bed tests, we completed over 200 hours of testing with our prototype unit. The impact of the absorption time is presented in Figure 56. Figure 57 shows that the bed middle temperatures are maintained at 800°C in these tests. We observed that the sorbent utilization was higher with shorter cycles, resulting in 0.2 kg of oxygen production per hour. In these single cycle tests we observed oxygen purity of 70%. The instantaneous oxygen production peaked at 0.7 kg/hr at a absorption time of 240 sec.

Overall System Performance

The system was initially brought online for commissioning and shakedown on October 29, 2018 and data collection concluded on May 31, 2019. During that period, the system was operational (defined as having at least 1 bed online and operating in either absorption or regeneration/desorption mode at any given time) for a total of 1,814 hours and the individual

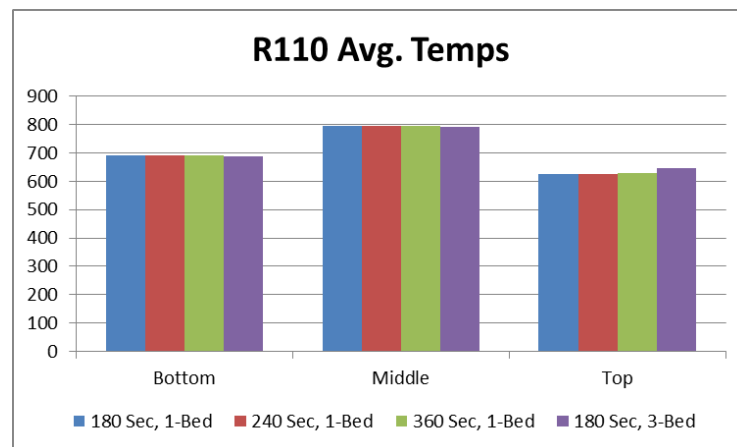


Figure 57. Bed temperatures in single bed tests.

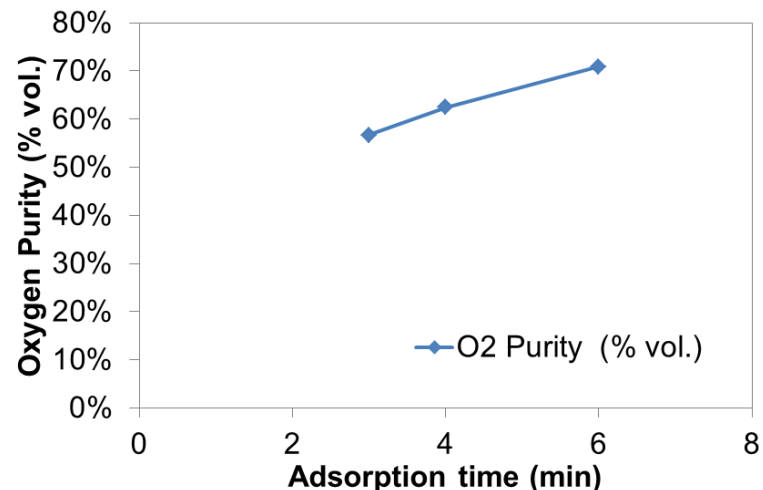


Figure 58. Oxygen purity at different absorption time.

beds cycled (a complete process cycle for a given bed consisting of a discrete oxygen absorption step followed by an oxygen desorption step) 8,192 times on average for a total of 32,769 combined cycles. From the process historian, it is also possible to accurately integrate the time at temperature for the individual beds. Since all 4 beds were online for roughly the same amount of time, reactor 140 is used as an example. Table 7 integrates the time at or above each temperature threshold for each of the 3 internal bed TCs present in reactor 140. In this reactor (as with the other 3 reactors) the internal temps are arranged sequentially from top to bottom with TE-1422 being at the top and TE-1444 being at the bottom. Each bed was packed with 4.5 kg of material with inert alumina packing (spherical; diameter approximately 1/8") above and below the active oxygen sorbent. The TCs were arranged such that the upper and lower measurement points were situated in the upper and lower inert packings while the central TCs were positioned at the center of the sorbent packing. From the estimates of the time at temperature, each of the sorbent bed was at process temperature (650°C or higher) for a total of 2300 hours.

Table 7. Time at (or above) temperature for reactor R-140 by internal TC location

R-140 Time at Temp (hours)			
	TE-1422	TE-1433	TE-1444
500°C	2352	2363	1946
550°C	2337	2351	1521
600°C	2317	2339	861
650°C	2299	2317	207
700°C	1299	2227	0
750°C	392	1637	0
800°C	0	170	0
850°C	0	0	0

Improved Steam Delivery

The initial system performance suffered from poor steam temperature and availability. Because the oxygen desorption process is inherently endothermic, poor steam temperature is especially problematic in that it tends to depress oxygen desorption which reduces overall system performance. In the prototype tests at the intermediate bench scale, temperature management was expected to be a significant engineering challenge. The main issue encountered was the availability of lab-scale equipment capable of extended operation at the combined temperature and pressure (up to 20 bar and temperatures from 650–850°C) required for the chemical phase change material to operate effectively. In order to combat these challenges, TDA designed a steam system that incorporates an on-demand steam generator fed by an HPLC-style positive-displacement piston pump. The piston pump is directly fed from municipal water that has been additionally purified through a reverse osmosis water conditioner. The pump rate is set automatically by the desired steam-to-oxygen ratio (controlled by the oxygen feed rate) and the initial steam boiler is operated at a constant temperature using a PID control loop. A back-pressure controller located downstream of the steam generator maintains a constant supply pressure for the steam which then passes into an on-line superheater. For proper operation, the initial steam generator is set to provide a small amount of superheat in order to maintain a "dry" steam feed going into the superheater.

Despite the apparent simplicity of the system, difficulties were experienced with both the HPLC feed pump and with the back-pressure control on the steam. On the feed side, the piston pump initially struggled to maintain adequate head and reduce pulsing. This lead to significant breaks in the delivery of water to the steam generator and subsequent steam supply interruptions. As a result of the process design, interruptions in steam supply result in immediate performance interruptions as the driving force for oxygen desorption (oxidation state change on the sorbent material) is removed—effectively placing the system into an unintended hold state. Interruptions in water delivery (or delivery state instability) had further impacts on the PID-controlled steam superheater, which struggled to maintain a constant output steam temperature when water delivery was interrupted and the resulting steam pressure and flow fluctuated at the superheater

inlet. This resulted in an overall temperature drop on the sorbent beds during the desorption/regeneration phase that had the effect of pausing the O₂ production. Due to the short cycle times (necessary to maximize production while minimizing sorbent inventory and capex costs), the amount of time required for steam recovery was much longer than an individual bed absorption/desorption cycle thereby causing entire ¼ cycle period to be essentially missed.

In order to improve the system, the water delivery was modified to incorporate a pressure control on the water (liquid phase side) of the inlet stream to the stage-1 steam generator. The outlet pressure control on the dry steam was further increased to allow for a constant pressure gradient throughout the equipment, and a manual control valve was added downstream of the steam superheater in order to maintain some control on the pressure within the superheater. Although these changes did not completely eliminate all of the lab-scale system steam issues, they were sufficient to allow for stable operation with a superheated steam temperature of roughly 550 deg. C (lower than our preferred operating temperature of 650°C and above). This was sufficient to allow for the final steam heating to take place in the upper inert packing within the reactor and allowed for operation with a steam regeneration temperature between 650–750°C. The resulting data is shown in Figure 59. Here it can be seen that when the steam is properly delivered to the system, the oxygen product purity can achieve 98+%. For the testing shown, additional purity improvements were also obtained by incorporating a co-current depressurization (blow-down) step to allow for the oxygen-depleted gas in the sorbent bed voids to be expelled prior to product collection. Parametric testing performed at the end of the testing period indicated shows the impact of decreasing the cycle time (without changing the amount of co-current blow-down). The overall impact is to increase the number of cycles in a given time (with a corresponding increase in O₂ production rate) while resulting in a slight decrease in the resulting O₂ purity (a drop from roughly 100% down to approximately 90% is indicated).

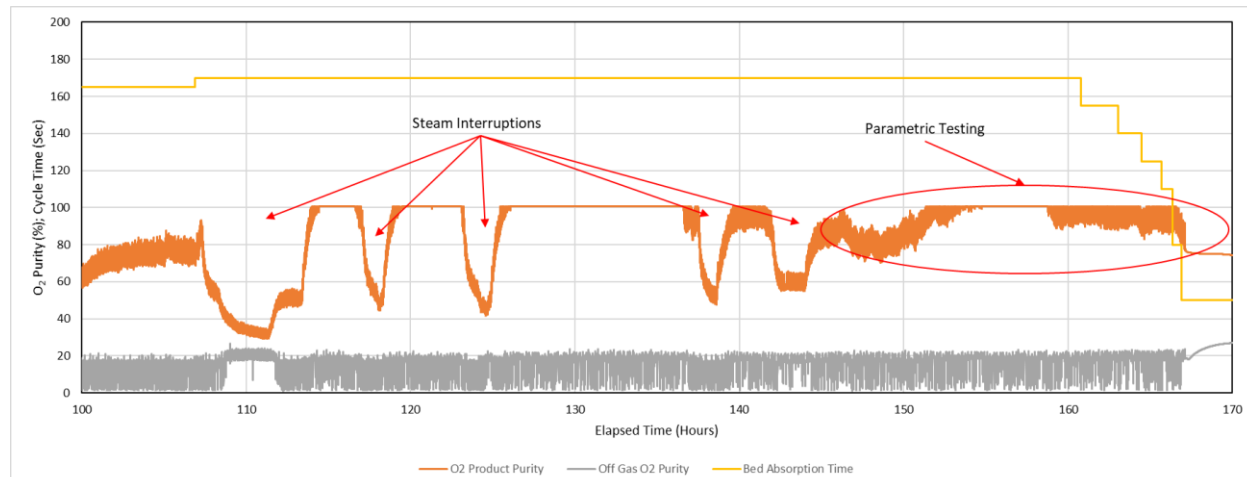


Figure 59. Stable operation with the improved steam generation and temperature. Several interruptions are indicated during the roughly 70-hour test snapshot. In between steam interruptions, the oxygen product purity is at or above 98%.

Impact of Bed Absorption Cycle Time

With the system operating at the highest possible steam temperatures, the overall oxygen product purity was observed to increase significantly. At this point, it was generally possible to operate with purities greater than 97%; however, occasional fluctuations in the steam delivery pressure (and the resulting steam delivery rate and temperature) introduced numerous short-term deviations in the otherwise steady-state O₂ product stream. Despite these interruptions,

sufficient data was collected to allow an examination of the relationship between purity and production rate. The graph in Figure 60 shows the inverse proportionality between purity and rate. Taking the data presented at the high-purity side of the graph, we can estimate the amount of sorbent material required to produce the desired 1 kg/hr while maintaining the 98% purity. For the current tests, each of the 4 sorbent beds was loaded with 4.5 kg of material yielding a total

sorbent inventory of 18 kg. Assuming larger beds could be utilized, the 1 kg/hr rate would require at most 330 kg of sorbent material. This seems like a significant increase in sorbent material; however, the current beds include a significant amount of inert packing at the inlet/outlet of each bed. In this testing the inert packing is necessary to perform final temperature adjustment on the gas streams and was a necessary compromise to allow for low-cost commodity hardware to be used at the high operating temperatures. Unfortunately, a side-effect of the extra bed volume is a significant amount unused void space. A consequence of this void space is the retention of excess quantity of oxygen-depleted air (nitrogen enriched) at the end of each $\frac{1}{4}$ cycle. In order to boost the purity, the excess nitrogen must be expelled from the bed during a depressurization purge step. In this process, a fraction of the O₂ product is lost in order to increase the purity of the final product stream. Previous testing indicated that the overall O₂ purity can exceed 0.2 kg/hour and the instantaneous oxygen production peaked at 0.7 kg/h at a absorption time of 240 sec. (testing utilized the same 4.5 kg/bed sorbent inventory; see Figure 56) when none of the O₂ is sacrificed in an effort to increase purity. In addition, these earlier tests were performed prior to steam system modifications and likely were the result of incomplete oxidation state cycling on the sorbent material (suggesting the true capacity should be greater). In the earlier testing, the minimum cycle time reached was 30 seconds of absorption per bed. Assuming bed design optimization can significantly reduce the amount on inert packing required and results in a concomitant reduction in void space and depleted air retention within the bed, it should be possible to reduce the sorbent quantity required for a 1 kg/hr production rate to less than 50 kg.

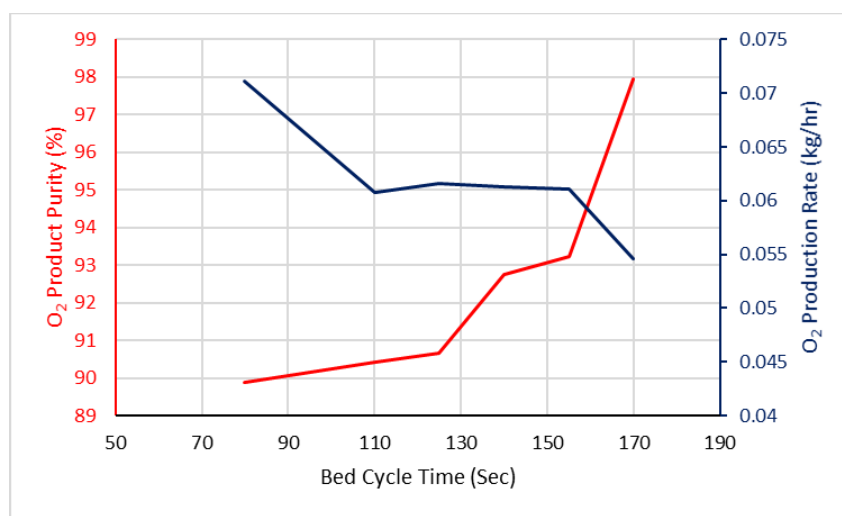


Figure 60. Relationship between O₂ product purity and production rate.

3.9 Task 9. Techno-economic analysis

As part of their subcontract work under DE-FE-0026142 project (TDA#2208), the Advanced Power and Energy Program (APEP) of the University of California, Irvine (UCI) developed simulation models to estimate the performance and cost of the TDA's Advanced air separation concept for:

1. IGCC Plants utilizing the GE type gasifier
2. IGCC Plants utilizing the E-Gas type gasifier

The following lists the cases developed:

Case 1A - IGCC power plant equipped with GE gasifier integrated with TDA's sorbent ASU with cold gas capture1

Case 1B - IGCC power plant equipped with GE gasifier integrated with TDA's sorbent ASU and warm gas capture

Case 2A - IGCC power plant equipped with E-Gas gasifier integrated with TDA's sorbent ASU with cold gas capture2

Case 2B - IGCC power plant equipped with E-Gas gasifier integrated with TDA's sorbent ASU and warm gas capture

Plant cost estimates and capital requirements were estimated with input provided by TDA for the proprietary air separation unit (ASU) equipment. APEP estimated consumables and the plant efficiency, and incorporated TDA's cost estimates for the ASU sorbent system for all cases, and trace component removal and CO₂ PSA separation systems for the warm gas capture cases, into the power plant cost estimates to estimate the overall plant cost, cost of electricity (COE), and cost of CO₂ capture.

Table 8 shows the overall plant performance for IGCCs with cold gas cleanup with TDA's ASU for GE and E-Gas gasifiers. Table 9 shows the overall plant performance for IGCCs with warm gas cleanup with TDA's ASU for GE and E-Gas gasifiers. Table 10 and Table 11 show the overall plant performance for IGCCs with cryogenic ASUs for the cold and warm gas cleanup cases for GE gasifier, respectively (results from our earlier study under a previous DOE Contract #DE-FE0024060). We observed that TDA's ASU unit provides significant improvement in overall plant performance increasing the net plant efficiency from 32% to 34.05% for the cold gas cleanup Case for GE gasifier while the improvement is lower for the warm gas cleanup case from 34.46% to 35.33%. The 1st year Cost of Electricity (COE) and the Cost of CO₂ Capture are also lower for the TDA ASU than that for the cryogenic ASU. For an IGCC power plant integrated with a cold gas cleanup system that uses GE gasifiers, the use of our system instead of a cryogenic unit reduces the COE per MWh from \$142 to \$127.1 while the cost of CO₂ capture including TS&M goes from \$47 to \$37 per tonne. However for an IGCC power plant integrated with a warm gas cleanup system the reduction is much smaller, the COE per MWh is \$134 vs \$121.9 while the cost of CO₂ capture including TS&M is \$41 vs \$30 per tonne. Table 12 and Table 13 shows the plant cost summary for the IGCC power plant with TDA ASU for the cold gas and warm gas cleanup cases, respectively for the GE and E-gas gasifiers. Table 14 and Table 15 shows the plant cost summary for the IGCC power plant with cold and warm gas cleanup cases with cryogenic ASU for GE gasifier, respectively. Table 16 shows the cost of electricity and cost of CO₂ capture for TDA ASU for the IGCC cases cold and warm gas cleanup cases with GE and E-gas gasifiers while Table 17 shows the results with GE-gasifier for the cryogenic ASU for the cold and warm gas cleanup cases from our earlier DOE study for comparison.

Cold Gas Cleanup. The TDA's sorbent ASU in a GE type gasifier based IGCC showed a substantial improvement in the thermal performance of an IGCC with cold gas cleanup, a 7% decrease in overall plant heat rate over the corresponding IGCC designed with a cryogenic ASU (heat rate decreased from 11,297 kJ/kWh to 10,574 kJ/kWh). The TDA ASU in an E-Gas type gasifier based IGCC with cold gas cleanup showed a less substantial improvement in the thermal performance, about 4% decrease in overall plant heat rate over the corresponding IGCC designed with a cryogenic ASU (heat rate decreased from 11,645 kJ/kWh to 11,169 kJ/kWh).

Warm Gas Cleanup. The advantage in overall plant thermal efficiency of using the TDA ASU was lower with warm gas cleanup in IGCC using GE type gasifiers. The TDA ASU in a GE type gasifier based IGCC with warm gas cleanup, showed a 3% decrease in overall plant heat rate over the corresponding IGCC designed with a cryogenic ASU (heat rate decreased from 10,492 kJ/kWh to 10,189 kJ/kWh). Further optimization of this case may possibly improve its heat rate. The TDA ASU in an E-Gas type gasifier based IGCC with warm gas cleanup showed a similar improvement in the thermal performance as seen with cold gas cleanup, a 4% decrease in overall plant heat rate over the corresponding IGCC designed with a cryogenic ASU (heat rate decreased from 10,667 kJ/kWh to 10,228 kJ/kWh).

The advantage seen for the TDA ASU based cases is primarily due to the replacement of the nitrogen injected (typically supplied by a cryogenic ASU) into the gas turbine for NOx control with depleted air from TDA's ASU, thereby saving power associated with the nitrogen compression as well as air compression. Note that the amount of air supplied to the elevated pressure train (in our simulation) of a cryogenic ASU being a larger fraction of the total air supplied to this cryogenic ASU (i.e., air supplied to elevated pressure and low pressure trains combined), the nitrogen being supplied by the elevated pressure train.

The TDA ASU shows a greater improvement in the specific plant cost (\$/kW basis) of an IGCC with cold gas cleanup, as much as 13% and 11% decrease in this cost for cases 1A and 2A over the corresponding cryogenic ASU based IGCC also with cold gas cleanup. Its advantage in the specific plant cost was a bit lower for an IGCC with warm gas cleanup, a 10% and 9% decrease for cases 1B and 2B over the corresponding cryogenic ASU based IGCC also with warm gas cleanup.

The TDA ASU also shows a greater improvement in the 1st year cost of electricity (COE) of an IGCC with cold gas cleanup, as much as 11% and 8% decrease in this cost for cases 1A and 2A over the corresponding cryogenic ASU based IGCC also with cold gas cleanup, this decrease in this cost attributable to the heat rate and specific plant cost advantages. Its advantage in the COE was also significant for the IGCCs with warm gas cleanup; the 1st year COE decreased by as much as 8% and 7% for cases 1B and 2B over the corresponding cryogenic ASU based IGCC also with warm gas cleanup, again this decrease being attributable to the heat rate and specific plant cost advantages.

It should be noted that the performance of some of the process units or equipment such as the cryogenic ASU (reference cases used for comparison), the Selexol™(used in the cold gas cleanup cases) and the gas turbine (all cases) were estimated by us and it is recommended that vendors be contacted for both performance and cost data in a more detailed study in the future. It should be also mentioned that the costs of the TDA sorption based ASUs on a total plant basis were estimated by TDA. These ASU cost estimates are substantially lower than those appearing in the referenced NETL/DoE report for the cryogenic ASUs which were used as the basis for the reference cases (used in the comparisons). This reduced cost of the TDA sorption

based ASU over the cryogenic ASU is a major reason for the substantial improvement in the economics presented in this report.

In the simulations carried out by UCI, the TDA ASU shows a substantial improvement in the thermal performance for an IGCC with cold gas cleanup. The advantage seen for the cold gas cleanup case is due to the replacement of the nitrogen injected into the gas turbine for NOx control with depleted air from the ASU, thereby saving the nitrogen compression power as well as air compression power (amount of air supplied to the elevated pressure train in our simulation).

Table 8. Overall Plant Performance – IGCCs with TDA ASU - Cold Gas Cleanup.

CASE	1A	2A
GROSS POWER GENERATED (AT GENERATOR TERMINALS), kWe		
GAS TURBINE POWER	464,000	464,000
STEAM TURBINE POWER	258,428	237,948
SYNGAS EXPANDER POWER	8,779	-
TOTAL POWER, kWe	731,207	701,948
AUXILIARY LOAD SUMMARY, kWe		
COAL HANDLING	450	446
COAL MILLING	2,278	2,261
COAL SLURRY PUMPS	792	629
SLAG HANDLING & DEWATERING	1,130	1,114
AIR SEPARATION UNIT MAIN AIR COMPRESSOR	61,024	60,640
GAS TURBINE EXTRACTION AIR COMPRESSOR	1,702	1,560
OXYGEN COMPRESSOR	22,827	20,688
SYNGAS RECYCLE COMPRESSOR	-	1,269
TAIL GAS RECYCLE COMPRESSOR	1,718	5,915
CO2 COMPRESSOR	31,237	31,660
BOILER FEEDWATER & DEMIN PUMPS	4,616	5,746
VACUUM CONDENSATE PUMP	321	425
PROCESS CONDENSATE & SWS SYSTEMS	717	49
HUMIDIFIER & BFW CIRCULATING PUMPS	222	302
COOLING WATER CIRCULATING PUMPS	4,882	4,283
COOLING TOWER FANS	2,465	2,162
SCRUBBER PUMPS	72	396
SELEXOL UNIT	19,125	21,314
GAS TURBINE AUXILIARIES	1,000	1,000
STEAM TURBINE AUXILIARIES	112	104
CLAUS & TAIL GAS TREATING AUXILIARIES	205	203
MISCELLANEOUS BALANCE OF PLANT	2,922	3,042
TRANSFORMER LOSSES	2,708	2,600
TOTAL AUXILIARIES, kWe	162,523	167,807
NET POWER, kWe	568,684	534,141
% NET PLANT EFFICIENCY, % HHV	34.05	32.23
NET HEAT RATE		
KJ/KWH	10,574	11,169
BTU/KWH	10,022	10,587
CONDENSER COOLING DUTY		
10^6 KJ/H	1,455	1,223
10^6 BTU/H	1,379	1,159
CONSUMABLES		
AS-RECEIVED COAL FEED		
KG/H	221,412	219,679
LB/H	488,213	484,392
THERMAL INPUT, KWT HHV	1,669,897	1,656,828
RAW WATER USAGE		
M^3/MIN	20.05	23.16
GPM	5,298	6,120
CARBON CAPTURED, %	90	90

Table 9. Overall Plant Performance – IGCCs with TDA ASU - Warm Gas Cleanup.

CASE	1B	2B
GROSS POWER GENERATED (AT GENERATOR TERMINALS), kWe		
GAS TURBINE POWER	464,000	464,000
STEAM TURBINE POWER	264,588	261,787
SYNGAS EXPANDER POWER	10,545	-
TOTAL POWER, kWe	739,133	725,787
AUXILIARY LOAD SUMMARY, kWe		
COAL HANDLING	455	446
COAL MILLING	2,307	2,262
COAL SLURRY PUMPS	756	662
SLAG HANDLING & DEWATERING	1,144	1,123
AIR SEPARATION UNIT MAIN AIR COMPRESSOR	60,532	64,957
OXYGEN & DEPLETED AIR COMPRESSORS	23,731	22,208
GT EXTRACTION AIR COMPRESSOR	1,793	1,243
SYNGAS RECYCLE COMPRESSOR	-	1,234
CO2 PURIFICATION & COMPRESSION	30,011	26,944
BOILER FEEDWATER & DEMIN PUMPS	4,932	5,422
VACUUM CONDENSATE PUMP	372	412
PROCESS CONDENSATE & SWS SYSTEMS	554	84
BFW CIRCULATING PUMPS	86	98
COOLING WATER CIRCULATING PUMPS	4,780	4,531
COOLING TOWER FANS	2,413	2,287
SCRUBBER PUMPS	72	395
DESULFURIZER UNIT	4,978	4,885
GAS TURBINE AUXILIARIES	1,000	1,000
STEAM TURBINE AUXILIARIES	115	114
H2SO4 UNIT	(3,968)	(3,736)
MISCELLANEOUS BALANCE OF PLANT	2,958	3,043
TRANSFORMER LOSSES	2,738	2,688
TOTAL AUXILIARIES, kWe	141,759	142,303
NET POWER, kWe	597,373	583,484
% NET PLANT EFFICIENCY, % HHV	35.33	35.20
NET HEAT RATE,		
KJ/KWH	10,189	10,228
BTU/KWH	9,657	9,694
CONDENSER COOLING DUTY		
10^6 KJ/H	1,589	1,498
10^6 BTU/H	1,506	1,420
CONSUMABLES		
AS-RECEIVED COAL FEED		
KG/H	224,171	219,805
LB/H	494,297	484,670
THERMAL INPUT, KWT HHV	1,690,706	1,657,778
RAW WATER USAGE		
M^3/MIN	23.55	22.78
GPM	6,223	6,018
CARBON CAPTURED, %	90	90

Table 10. Overall Plant Performance – IGCCs with Cryogenic ASU - Cold Gas Cleanup.

ASU		Cryogenic
GROSS POWER GENERATED (AT GENERATOR TERMINALS) kW		
GAS TURBINE POWER		464,000
STEAM TURBINE POWER		257,403
SYNGAS EXPANDER POWER		5,968
TOTAL POWER, kW		727,370
AUXILIARY LOAD SUMMARY	kW	
COAL HANDLING		450
COAL MILLING		2,280
COAL SLURRY PUMPS		757
SLAG HANDLING & DEWATERING		1,133
AIR SEPARATION UNIT AUXILIARIES		1,094
AIR SEPARATION UNIT MAIN AIR COMPRESSOR		67,717
GAS TURBINE EXTRACTION AIR COMPRESSOR		-
OXYGEN COMPRESSOR		10,707
NITROGEN COMPRESSOR		35,860
TAIL GAS RECYCLE COMPRESSOR		1,692
CO2 COMPRESSOR		30,959
BOILER FEEDWATER & DEMIN PUMPS		4,702
VACUUM CONDENSATE PUMP		337
PROCESS CONDENSATE & SWS SYSTEMS		770
HUMIDIFIER & BFW CIRCULATING PUMPS		25
COOLING WATER CIRCULATING PUMPS		5,406
COOLING TOWER FANS		2,729
SCRUBBER PUMPS		72
SELEXOL UNIT		19,159
GAS TURBINE AUXILIARIES		1,000
STEAM TURBINE AUXILIARIES		112
CLAUS & TAIL GAS TREATING AUXILIARIES		205
MISCELLANEOUS BALANCE OF PLANT		3,068
TRANSFORMER LOSSES		2,694
TOTAL AUXILIARIES, kW		192,927
NET POWER	kW	534,443
NET PLANT EFFICIENCY	% HHV	32.00
NET HEAT RATE		
	kJ/kW·h	11,249
	BTU/kW·h	10,662
CONDENSER COOLING DUTY		
	10^6 kJ/H	1,580
	10^6 BTU/H	1,498
CONSUMABLES		
AS-RECEIVED COAL FEED		
	kg/H	221,584
	LB/H	488,592
THERMAL INPUT, kW HHV		1,670,059
RAW WATER USAGE		
	M^3/MIN	22.09
	GPM	5,836
CARBON CAPTURED	%	90

Table 11. Overall Plant Performance – IGCCs with Cryogenic ASU - Warm Gas Cleanup.

ASU TECHNOLOGY	Cryogenic
GROSS POWER GENERATED (AT GENERATOR TERMINALS) kW	
GAS TURBINE	417,554
STEAM TURBINE	246,746
SYNGAS EXPANDER	10,031
ASU DEPLETED AIR EXPANDER	-
TOTAL POWER kW	674,331
AUXILIARY LOAD SUMMARY kW	
COAL HANDLING	432
COAL MILLING	2,192
COAL SLURRY PUMPS	723
SLAG HANDLING & DEWATERING	1,088
AIR SEPARATION UNIT AUXILIARIES	212
AIR SEPARATION UNIT MAIN AIR COMPRESSOR	41,424
OXYGEN & DEPLETED AIR COMPRESSORS	20,373
GT EXTRACTION AIR COMPRESSOR	
NITROGEN COMPRESSOR	7,550
CO2 PURIFICATION & COMPRESSION	26,673
BOILER FEEDWATER & DEMIN PUMPS	4,735
VACUUM CONDENSATE PUMP	328
PROCESS CONDENSATE & SWS SYSTEMS	504
BFW CIRCULATING PUMPS	86
COOLING WATER CIRCULATING PUMPS	4,512
COOLING TOWER FANS	2,278
SCRUBBER PUMPS	69
DESULFURIZER UNIT	4,812
GAS TURBINE AUXILIARIES	900
STEAM TURBINE AUXILIARIES	107
H2SO4 UNIT	(3,782)
MISCELLANEOUS BALANCE OF PLANT	2,949
TRANSFORMER LOSSES	2,498
TOTAL AUXILIARIES kW	120,661
NET POWER kW	553,671
NET PLANT EFFICIENCY % HHV	34.46
NET HEAT RATE	
	kJ/kWh
	10,446
	BTU/kWh
	9,901
CONDENSER COOLING DUTYNET POWER	
	10^6 kJ/H
	1,385
	10^6 BTU/H
	1,313
CONSUMABLES	
AS-RECEIVED COAL FEED	
	kg/H
	213,013
	LB/H
	469,694
THERMAL INPUT, kW HHV	1,606,553
RAW WATER USAGE	
	M^3/MIN
	22.10
	GPM
	5,839
CARBON CAPTURED	%
	90

Table 12. Plant Cost Summary (2011 \$1000) – IGCCs with TDA ASU - Cold Gas Cleanup.

CASE	1A	2A
ASU	148,622	141,460
Fuel receiving, preparation & feeding	114,692	111,764
Gasifier, syngas cooler & aux (Case 2 A includes syngas scrubber)	308,866	310,217
Gasification foundations	19,027	21,363
Ash handling	55,324	45,055
Soot Recovery + SARU	7,035	
Flare stack system (for Case 1 A, included in gasifier aux above)		3,700
Shift reactor	22,019	16,055
LTGC (Case 1A includes syngas scrubber, Case 2A includes syngas humidifier)	26,304	51,701
Blowback gas systems		1,636
Fuel gas piping	1,741	1,931
Gas cleanup foundations	1,811	1,964
Hg Removal	4,140	3,729
Selexol	256,553	255,802
Claus + TG Recycle	40,641	40,428
CO2 compression, dehydration + pumping	66,545	67,228
Syngas Expander	11,797	
Gas turbine + generator + auxiliaries	159,299	159,009
HRSG, ducting + stack	56,225	56,633
Steam turbine + generator + auxiliaries	83,886	79,887
Surface condenser	5,858	5,273
Feedwater system	19,143	27,648
Water makeup + pretreating	2,220	2,470
Other feedwater subsystems	3,997	4,030
Service water systems	7,191	7,094
Other boiler plant systems	8,154	8,128
Fuel oil system & nat gas	2,315	2,297
Waste water treatment	2,733	2,697
Misc. power plant equipment	3,119	3,043
Cooling water system	39,396	36,007
Accessory electric plant	106,706	105,993
Instrumentation & controls	32,989	32,444
Improvement to site	23,622	23,151
Buildings & structures	22,343	21,683
Total	1,664,315	1,651,517

Table 13. Plant Cost Summary (2011 \$1000) – IGCCs with TDA ASU - Warm Gas Cleanup.

CASE	1B	2B
ASU	177,683	177,112
Fuel receiving, preparation & feeding	115,633	111,806
Gasifier, syngas cooler & aux (Case 2B includes syngas scrubber)	311,825	310,355
Gasification foundations	19,145	21,369
Ash handling systems	55,702	45,069
Soot Recovery + SARU	7,079	0
Flare stack system (for Case 1 B, included in gasifier aux above)	0	3,701
Warm gas desulfurization	34,858	34,418
H ₂ SO ₄ unit	76,355	75,537
Shift reactor	22,429	15,335
Syngas scrubber (for Case 2B, included in gasifier aux)	13,387	
Blowback gas systems	0	1,636
Fuel gas piping	2,539	2,694
Gas cleanup foundations	1,844	1,877
Trace contaminant removal	4,418	4,436
CO ₂ separation / recycle	156,969	141,082
CO ₂ purification / heat recovery	27,459	29,867
CO ₂ compression / drying / pumping	66,971	60,911
Syngas Expander	13,413	0
Gas turbine + generator + auxiliaries	159,299	159,009
HRSG, ducting + stack	56,667	56,862
Steam turbine + generator + auxiliaries	85,281	85,406
Surface condenser	6,234	6,091
Feedwater system	25,840	21,697
Water makeup + pretreating	2,489	2,441
Other feedwater subsystems	4,065	4,312
Service water systems	7,254	7,096
Other boiler plant systems	8,296	8,714
Fuel oil system & nat gas	2,315	2,297
Waste water treatment	2,758	2,698
Misc. power plant equipment	3,127	3,068
Cooling water system	38,802	37,493
Accessory electric plant	107,225	107,598
Instrumentation & controls	33,042	32,446
Improvement to site	23,646	23,152
Buildings & structures	22,371	21,685
Total	1,696,417	1,619,271

Table 14. Plant Cost Summary (2011 \$1000) – IGCC with Cryogenic ASU - Cold Gas Cleanup.

ASU TECHNOLOGY	Cryogenic
ASU	283,246
Fuel receiving, preparation & feeding	114,864
Gasifier, syngas cooler & aux	309,409
Gasification foundations	19,049
Ash handling	55,393
Soot Recovery + SARU	7,043
Shift reactor	22,072
Syngas scrubber + LTGC	26,365
Fuel gas piping	1,748
Gas cleanup foundations	1,815
Hg Removal	4,149
Selexol	256,722
Claus + TG Recycle	40,705
CO2 compression, dehydration + pumping	66,124
Syngas Expander	9,014
Gas turbine + generator + auxiliaries	159,299
HRSG, ducting + stack	53,929
Steam turbine + generator + auxiliaries	83,711
Surface condenser	6,109
Feedwater system	19,266
Water makeup + pretreating	2,348
Other feedwater subsystems	3,989
Service water systems	7,202
Other boiler plant systems	8,137
Fuel oil system & nat gas	2,315
Waste water treatment	2,738
Misc. power plant equipment	3,115
Cooling water system	41,906
Accessory electric plant	106,471
Instrumentation & controls	33,206
Improvement to site	23,627
Buildings & structures	22,348
Total	1,797,434
Total \$/kW	3,359

Table 15. Plant Cost Summary (2011 \$1000) –IGCC with Cryogenic ASU - Warm Gas Cleanup.

ASU TECHNOLOGY	Cryogenic
ASU	275,321
Fuel receiving, preparation & feeding	111,801
Gasifier, syngas cooler & aux	299,804
Gasification foundations	18,662
Ash handling systems	54,160
Soot Recovery + SARU	6,900
Warm gas desulfurization	33,567
H ₂ SO ₄ unit	73,950
Shift reactor	21,543
Syngas scrubber	12,878
Fuel gas piping	2,450
Gas cleanup foundations	1,772
Trace contaminant removal	4,504
CO ₂ separation / recycle	190,699
CO ₂ purification / heat recovery	26,245
CO ₂ compression / drying / pumping	60,371
Syngas Expander	12,952
Gas turbine + generator + auxiliaries	159,299
HRSG, ducting + stack	52,664
Steam turbine + generator + auxiliaries	81,213
Surface condenser	5,655
Feedwater system	23,755
Water makeup + pretreating	2,379
Other feedwater subsystems	3,868
Service water systems	6,996
Other boiler plant systems	7,884
Fuel oil system & nat gas	2,257
Waste water treatment	2,659
Misc. power plant equipment	3,059
Cooling water system	37,220
Accessory electric plant	102,888
Instrumentation & controls	33,030
Improvement to site	23,549
Buildings & structures	22,257
Total	1,778,212
Total \$/kW	3,212

Table 16. Process economics for IGCC plants with TDA ASU.

CASE	1A	1B	2A	2B
Net power, MW	569	597	534	583
Net efficiency, % HHV	34	35.33	32.23	35.20
Capacity factor (CF), %	80	80	80	80
Total plant cost (TPC), \$	1,664,314,918	1,696,416,960	1,651,517,116	1,619,271,109
6 month labor cost	15,663,392	15,992,802	15,621,324	15,412,414
1 month maintenance materials	2,759,060	2,840,628	2,748,643	2,696,913
1 month non-fuel consumables	822,579	1,204,070	882,800	1,154,424
1 month waste disposal	493,094	497,712	489,247	488,054
25% of 1 month fuel cost at 100% CF	3,056,093	3,094,175	3,032,174	3,033,914
2% of TPC	33,286,298	33,928,339	33,030,342	32,385,422
60 day supply of fuel & consumables at 100% CF	25,736,447	26,789,461	25,666,515	26,216,048
0.5% of TPC (spare parts)	8,321,575	8,482,085	8,257,586	8,096,356
Initial catalyst & chemicals cost, \$	23,833,053	21,163,514	23,848,019	19,863,479
Land	900,000	900,000	900,000	900,000
Other owners's costs (15% of TPC)	249,647,238	254,462,544	247,727,567	242,890,666
Financing costs	44,936,503	45,803,258	44,590,962	43,720,320
Total overnight cost (TOC), \$	2,073,770,249	2,111,575,546	2,058,312,295	2,016,129,119
Fixed operating cost for initial year of operation (OCF), \$	64,613,083	65,913,942	64,272,989	63,210,250
Annual feed cost at above CF for initial year (OCV1), \$	117,353,955	118,816,306	116,435,489	116,502,293
Other annual variable operating cost at above CF for initial year (OCV2), \$	39,117,431	43,607,132	39,558,625	41,658,151
Annual CO2 transporting, storing, and monitoring cost at above CF for initial year (OCV3), \$	32,109,618	32,363,737	31,668,370	31,735,198
Annual byproduct revenues at above CF for initial year (OCV4), \$	4,245,347	12,952,498	4,212,050	12,411,871
1st year cost of electricity (COE) w/o CO2 TS&M, \$/MWh	119.1	114.1	126.1	112.4
1st year cost of electricity (COE), \$/MWh	127.1	121.9	134.5	120.1
1st year CO2 capture cost without CO2 TS&M compared to corresponding IGCC (w/o CO2 capture), \$/tonne	22	17	33	18
1st year CO2 capture cost without CO2 TS&M compared to SCPC (w/o CO2 capture), \$/tonne	47	43	43	40
1st year CO2 avoided cost with CO2 TS&M compared to corresponding IGCC (w/o CO2 capture), \$/tonne	37	30	53	32
1st year CO2 avoided cost with CO2 TS&M compared to SCPC (w/o CO2 capture), \$/tonne	64	57	76	55

Table 17. Process economics for IGCC plants with Cryogenic ASU.

Type Plant	IGCC - Cold G	IGCC - Warm
ASU Technology	Cryogenic	Cryogenic
Net power, MW	535	554
Net efficiency, % HHV	32	34
Capacity factor (CF), %	80	80
Total plant cost (TPC), \$	1,797,434,483	1,778,212,157
6 month labor cost	16,244,043	16,201,037
1 month maintenance materials	2,902,840	2,892,191
1 month non-fuel consumables	855,413	1,234,680
1 month waste disposal	494,220	501,265
25% of 1 month fuel cost at 100% CF	3,063,070	2,940,167
2% of TPC	35,948,690	35,564,243
60 day supply of fuel & consumables at 100% CF	25,856,274	25,634,658
0.5% of TPC (spare parts)	8,987,172	8,891,061
Initial catalyst & chemicals cost, \$	16,222,858	19,962,588
Land	900,000	900,000
Other owners's costs (15% of TPC)	269,615,172	266,731,824
Financing costs	48,530,731	48,011,728
Total overnight cost (TOC), \$	2,227,054,965	2,207,677,599
Fixed operating cost for initial year of operation (OCF), \$	68,436,775	67,966,318
Annual feed cost at above CF for initial year (OCV1), \$	117,621,897	112,902,405
Other annual variable operating cost at above CF for initial year (OCV2), \$	40,823,740	44,430,104
Annual CO2 TS&M cost at above CF for initial year (OCV3), \$	32,044,094	30,753,565
Annual byproduct revenues at above CF for initial year (OCV4), \$	4,255,199	12,230,306
1st year cost of electricity (COE) w/o CO2 TS&M, \$/MWh	133	126
1st year cost of electricity (COE), \$/MWh	142	134
1st year CO2 capture cost with CO2 TS&M compared to corresponding IGCC (w/o CO2 capture), \$/tonne	47	41
1st year CO2 capture cost with CO2 TS&M compared to SCPC (w/o CO2 capture), \$/tonne	71	66

3.9.1 TDA's System Design

In this task we carried out a detailed design of TDA's high temperature air separation process. This included the design of the reactor housing for the full-scale reactors, engineering drawings and 3-dimensional layouts for the reactor system. The design also included all the critical components such as the sorbent beds, inlet and exit accumulators, all valves and manifolds needed for the system to complete the cycle sequence. We also estimated the bare equipment cost for the unit, which was provided to our partner University of California Irvine (UCI), who included it in their overall cost estimate and where all the ancillary equipment such as heat exchangers, foundation and engineering and installation labor were included.

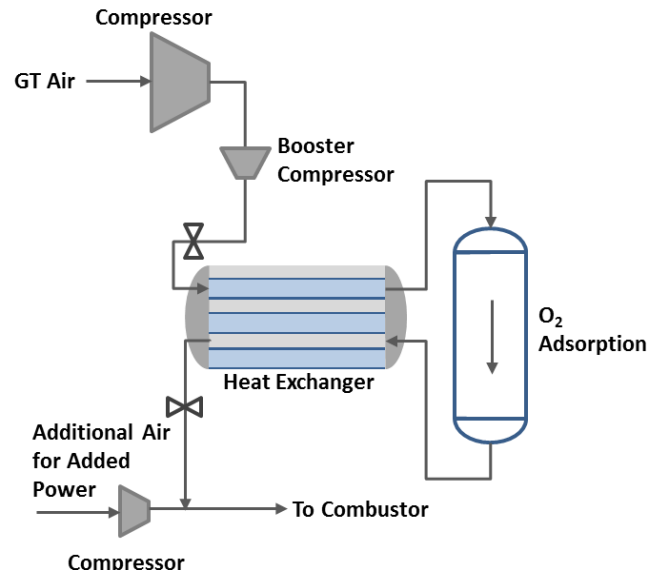


Figure 61. Absorption process.

TDA's Air Separation System

TDA's novel air separation system uses a unique oxygen absorption/desorption process. The process uses a metal oxide spinel (M_xO_y) sorbent in several fixed-bed reactors (at least two); one reactor contains the fresh M_xO_y that selectively absorbs O_2 from air at pressure and forms metal stable phase, while the second reactor regenerates the sorbent, releasing the oxygen. We use a pressure swing process as described below:

In the absorption step (Figure 61), the sorbent removes oxygen from a compressed air stream at $750^\circ C$ (in our application this will be the compressed air from the gas turbine used in the IGCC plant). Air is adiabatically compressed in the compressor section roughly to 20 bar. This high pressure air stream enters the absorption reactor and most of the oxygen reacts with the sorbent to form a metal stable phase.

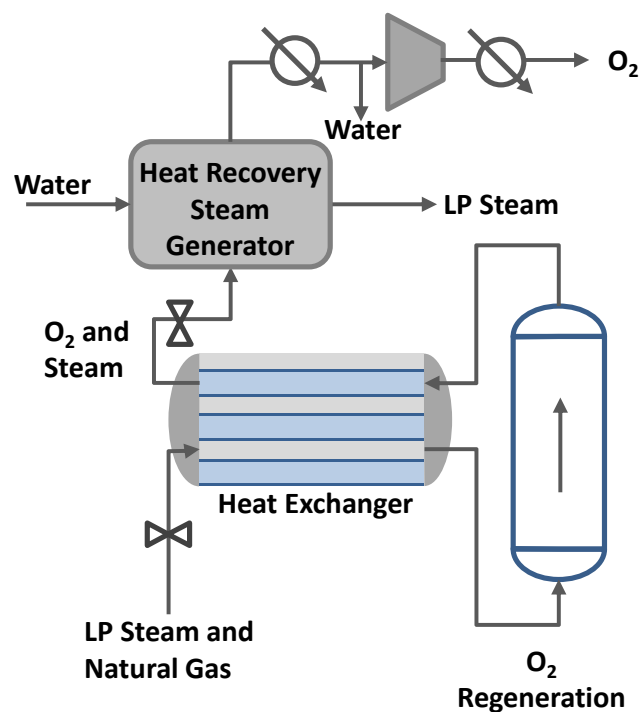


Figure 62. Regeneration process.

The sorbent removes approximately 90-95% of the oxygen from air. The absorption of oxygen is exothermic and increases the air temperature to $815^\circ C$ (leaving the system). Some of this heat is captured by heating the feed air in a recuperative heat exchanger. Additional air dilution provided by a small compressor maintains the desired turbine inlet temperature. After cooling, the gas is fed to the gas turbine combustor.

As the sorbent saturates with oxygen, the gas flow is switched to start the regeneration (Figure 62). In several steps, the bed pressure is reduced to 1 atm and steam/fuel mixture sweeps across the bed to promote the auto-reduction of the sorbent and liberation of O₂. The small amount of fuel provides the energy to drive the endothermic regeneration process and compensate for heat losses (desulfurized synthesis gas is used to eliminate sulfur contamination). Because the sorbent is metastable at the regeneration temperature in the higher oxidation state, the O₂ release is very fast even though only a small chemical potential difference is applied (we only swing the O₂ partial pressure, oxygen is removed from air at high pressure and released to the steam sweep at a low partial pressure). The regeneration off-gas consists of steam and O₂ (and some CO₂); steam is condensed, O₂ is compressed and feeds into a storage tank from which the desired flow of oxygen is metered to the gasifier.

For the system design, we used the process analysis completed by UCI to determine the bed size and the required steam purge. We produced detailed system designs for the air separation unit of the plant. The air separation sorbent relies on a multi-bed PSA scheme to make the greatest use of sorbent. The number of beds required varies based on the case analyzed.

The sorbent properties are summarized in Table 18. A schematic of a single reactor vessel is given in Figure 63. This same reactor design is used for all of the cases. A summary of the 8 bed cycle schematic is given in Figure 64. The system cost analysis for the four UCI design cases are reported in Table 19 through Table YY. The cost analysis included the estimates for the cost of the vessels, internals, valves, and insulation for the entire system.

Table 18. Summary of sorbent characteristics

Sorbent Properties	TDA OxySorb™
Bulk density	1.25 kg/L
Extrudate diameter	0.125 in
Pellet L/D	1.5
Bed external voids	0.3
Particle voids	0.3
Capacity per cycle	1.57% wt.



Figure 63. Overview of reactor design

	Stage 1	Stage 2	Stage 3		Stage 4		Stage 5	Stage 6	Stage 7		Stage 8	
Time (min)	0.75	0.75	0.37	0.38	0.37	0.38	0.75	0.75	0.37	0.38	0.37	0.38
Bed 1	ADS		EQ1D	EQ2D	EQ3D	BD	PURGE		EQ3R	EQ2R	EQ1R	PRESS
Bed 2	EQ1R	PRESS	ADS		EQ1D	EQ2D	EQ3D	BD	PURGE		EQ3R	EQ2R
Bed 3	EQ3R	EQ2R	EQ1R	PRESS	ADS		EQ1D	EQ2D	EQ3D	BD	PURGE	
Bed 4	PURGE	EQ3R	EQ2R	EQ1R	PRESS	ADS		EQ1D	EQ2D	EQ3D	BD	PURGE
Bed 5	PURGE		EQ3R	EQ2R	EQ1R	PRESS	ADS		EQ1D	EQ2D	EQ3D	BD
Bed 6	EQ3D	BD	PURGE		EQ3R	EQ2R	EQ1R	PRESS	ADS		EQ1D	EQ2D
Bed 7	EQ1D	EQ2D	EQ3D	BD	PURGE		EQ3R	EQ2R	EQ1R	PRESS	ADS	
Bed 8	ADS		EQ1D	EQ2D	EQ3D	BD	PURGE		EQ3R	EQ2R	EQ1R	PRESS
												ADS

Figure 64. Overview of 8 bed cycle scheme. Total Cycle time = 8 min.

Table 19. Summary of TDA ASU Plant Costs – Case 1A (\$ 2011 basis) integrated with IGCC plant with GE gasifier and cold gas cleanup.

Item/Description	Scale	\$ 1,000	Total Pant Cost - TDA ASU (including Initial Sorbent Load)						\$ 158,351	
	Equipment Cost	Material Cost	Labor		Erected Cost	Eng Fee	Contingencies		Total Plant Cost	
			Direct	Indirect			Process	Project	\$	\$/kW
Vessels										
O2 Adsorption Vessels	\$ 11,801	\$ 12,119	\$ 11,470		\$ 35,391	\$ 3,539	\$ 7,078	\$ 8,848	\$ 54,856	
					\$ -	\$ -	\$ -	\$ -	\$ -	
Vessel Valves										
Vessel Valves	\$ 941		\$ 188		\$ 1,130	\$ 113	\$ 226	\$ 282	\$ 941	
Train Isolation Valves	\$ 118				\$ 118	\$ 12	\$ 24	\$ 29	\$ 118	
Spares	\$ 196				\$ 196	\$ 20	\$ 39	\$ 49	\$ 196	
Pressure Relief	\$ 417		\$ 83		\$ 500	\$ 50	\$ 100	\$ 125	\$ 417	
Compressor System										
Compressors	\$ 36,110	\$ 9,750	\$ 10,590		\$ 56,449	\$ 5,645	\$ 11,290	\$ 14,112	\$ 87,496	
Heat Exchangers										
Shell and Tube	\$ 1,881	\$ 1,312	\$ 1,041		\$ 4,233	\$ 423	\$ 847	\$ 1,058	\$ 6,562	
Sorbent										
Sorbent material		\$ 7,765							\$ 7,765	
Total Plant Cost - TDA ASU (excluding Initial Sorbent Load)										
									\$ 150,586	

Table 20. Summary of TDA ASU Plant Costs – Case 2A (\$ 2011 basis) integrated with IGCC plant with E-gas gasifier and cold gas cleanup.

Item/Description	Scale	\$ 1,000	Total Pant Cost - TDA ASU (including Initial Sorbent Load)						\$ 151,264	
	Equipment Cost	Material Cost	Labor		Erected Cost	Eng Fee	Contingencies		Total Plant Cost	
			Direct	Indirect			Process	Project	\$	\$/kW
Vessels										
CO2 Adsorption Vessels/Accumulators	\$ 10,118	\$ 10,392	\$ 9,835		\$ 30,345	\$ 3,035	\$ 6,069	\$ 7,586	\$ 47,035	
Vessel Valves										
Vessel Valves	\$ 1,883		\$ 377		\$ 2,259	\$ 226	\$ 452	\$ 565	\$ 1,883	
Train Isolation Valves	\$ 118				\$ 118	\$ 12	\$ 24	\$ 29	\$ 118	
Spares	\$ 196				\$ 196	\$ 20	\$ 39	\$ 49	\$ 196	
Pressure Relief	\$ 411		\$ 82		\$ 493	\$ 49	\$ 99	\$ 123	\$ 411	
Compressor System										
Compressors	\$ 36,110	\$ 9,750	\$ 10,590		\$ 56,449	\$ 5,645	\$ 11,290	\$ 14,112	\$ 87,496	
Heat Exchangers										
Shell and Tube	\$ 1,864	\$ 1,300	\$ 1,031		\$ 4,194	\$ 419	\$ 839	\$ 1,049	\$ 6,501	
Sorbent										
Sorbent material		\$ 7,624							\$ 7,624	
Total Plant Cost - TDA ASU (excluding Initial Sorbent Load)										
									\$ 143,640	

Table 21. Summary of TDA ASU Plant Costs – Case 1B (\$ 2011 basis) integrated with IGCC plant with GE gasifier and warm gas cleanup.

Item/Description	Scale	\$ 1,000	Total Pant Cost - TDA ASU (including Initial Sorbent Load)						\$ 187,520	
	Equipment Cost	Material Cost	Labor		Erected Cost	Eng Fee	Contingencies		Total Plant Cost	
			Direct	Indirect			Process	Project	\$	\$/kW
Vessels										
CO2 Adsorption Vessels/Accumulators	\$ 10,513	\$ 10,797	\$ 10,219		\$ 31,528	\$ 3,153	\$ 6,306	\$ 7,882	\$ 48,869	
Vessel Valves										
Vessel Valves	\$ 1,883		\$ 377		\$ 2,259	\$ 226	\$ 452	\$ 565	\$ 1,883	
Train Isolation Valves	\$ 118				\$ 118	\$ 12	\$ 24	\$ 29	\$ 118	
Spares	\$ 196				\$ 196	\$ 20	\$ 39	\$ 49	\$ 196	
Pressure Relief	\$ 415		\$ 83		\$ 499	\$ 50	\$ 100	\$ 125	\$ 415	
Compressor System										
Compressors	\$ 44,562	\$ 18,693	\$ 13,027		\$ 76,283	\$ 7,628	\$ 15,257	\$ 19,071	\$ 118,238	
Heat Exchangers										
Shell and Tube	\$ 2,808	\$ 1,960	\$ 1,595		\$ 6,363	\$ 636	\$ 1,273	\$ 1,591	\$ 9,863	
Sorbent										
Sorbent material		\$ 7,937							\$ 7,937	
Total Plant Cost - TDA ASU (excluding Initial Sorbent Load)										
									\$ 179,582	

Table 22. Summary of TDA ASU Plant Costs – Case 2B (\$ 2011 basis) integrated with IGCC plant with E-gas gasifier and warm gas cleanup.

Item/Description	Scale	\$ 1,000	Total Pant Cost - TDA ASU (including Initial Sorbent Load)						\$ 187,779	
	Equipment Cost	Material Cost	Labor		Erected Cost	Eng Fee	Contingencies		Total Plant Cost	
			Direct	Indirect			Process	Project	\$	\$/kW
Vessels										
CO2 Adsorption Vessels/Accumulators	\$ 9,969	\$ 10,238	\$ 9,690		\$ 29,896	\$ 2,990	\$ 5,979	\$ 7,474	\$ 46,340	
Vessel Valves										
Vessel Valves	\$ 1,956		\$ 391		\$ 2,347	\$ 235	\$ 469	\$ 587	\$ 1,956	
Train Isolation Valves	\$ 122				\$ 122	\$ 12	\$ 24	\$ 31	\$ 122	
Spares	\$ 204				\$ 204	\$ 20	\$ 41	\$ 51	\$ 204	
Pressure Relief	\$ 425		\$ 85		\$ 510	\$ 51	\$ 102	\$ 128	\$ 425	
Compressor System										
Compressors	\$ 45,822	\$ 19,136	\$ 13,515		\$ 78,473	\$ 7,847	\$ 15,695	\$ 19,618	\$ 121,633	
Heat Exchangers										
Shell and Tube	\$ 2,737	\$ 1,910	\$ 1,552		\$ 6,199	\$ 620	\$ 1,240	\$ 1,550	\$ 9,608	
Sorbent										
Sorbent material		\$ 7,491							\$ 7,491	
Total Plant Cost - TDA ASU (excluding Initial Sorbent Load)										
									\$ 180,288	

4. Conclusions and Recommendations

In this work, we scaled-up the sorbent production and prepared quantities sufficient to support large-scale evaluation using high throughput production equipment. We completed Manufacturing and Quality Assurance Plans that will provide a basis for commercial production. We carried out over 12,500 absorption/ regeneration cycles to demonstrate sorbent life. We worked with UOA and GTI to optimize the cycle sequence and carried out a detailed design of the sorbent reactors. Figure 3 shows the optimized PSA cycle sequence and steps. We fabricated a prototype unit that consisted of 4 fixed-bed reactors, which allowed us to generate up to 0.7 kg/hr O₂ on instantaneous basis and 0.1 kg/hr on a continuous basis producing 98+% oxygen (0.2 kg/hr at 90% purity). The system is capable of stand-alone operation, treating up to 12 Nm³/hr air at different inlet pressures. In a series of tests, we carried out parametric tests assessing the impact of absorption time, co-current blowdown steps and steam purge rates. We demonstrated the prototype unit operation for over 1,800 hours producing high purity oxygen. We worked with UCI to update the process simulation model developed previously under DOE contract #DE-FE0024060, integrating the new technology with the GE and E-Gas gasification systems and state-of-the-art and emerging carbon capture technologies (i.e., Selexol and TDA's Warm Gas PSA based carbon capture systems). For all cases, we estimated the process efficiency, COE and cost of CO₂ capture, following the DOE/NETL Cost Guidelines. With the successful completion of the R&D effort, the technology is now ready for a larger pilot-scale demonstration and the technology readiness has been raised from TRL 4 to TRL 6.

We observed that TDA's ASU unit provides significant improvement in overall plant performance increasing the net plant efficiency from 32% to 34.05% for the cold gas cleanup Case for GE gasifier while the improvement is lower for the warm gas cleanup case at 35.33% vs 34.46%. The 1st year Cost of Electricity (COE) and the Cost of CO₂ Capture are also lower for the TDA ASU than that for the cryogenic ASU. For an IGCC power plant integrated with a cold gas cleanup system that uses GE gasifiers, the use of our system instead of a cryogenic unit reduces the COE per MWh from \$142 to \$127.1 while the cost of CO₂ capture including TS&M goes from \$47 to \$37 per tonne. However for an IGCC power plant integrated with a warm gas cleanup system the reduction is much smaller, the COE per MWh is \$134 vs \$121.9 while the cost of CO₂ capture including TS&M is \$41 vs \$30 per tonne.

4.1 Recommendations for Future Work

The results of the DE-FE0026142 project suggest that TDA's sorbent based high temperature ASU merits further research and development. It should be noted that the performance of some of the process units or equipment such as the cryogenic ASU, the Selexol™ and the gas turbine were estimated, and it is recommended that vendors be contacted for both performance and cost data in a more detailed study in the future. A more detailed system simulation and cost analysis is also recommended, including design work and accurate quotes from the suppliers of the major process equipment (e.g., air separation unit, gasifier, CO₂ compressors). Successful completion of this recommended work will provide the basis for the new technology to be employed in potential pilot-scale demonstrations (1-10 MW scale).

5. References

- [1] R. Haghpanah et al. "Multiobjective optimization of a four-step adsorption process for post-combustion CO₂ capture via finite volume simulation". *Ind. Eng. Chem. Res.*, vol. 52, no. 11, pp. 4249-4265, 2013.
- [2] Krishnamurthy et al. "CO₂ capture from dry flue gas by vacuum swing adsorption: A pilot plant study." *AIChE Journal*. Vol. 60. pp. 1830–1842, 2014.
- [3] Rajagopalan A.; Avila A.; Rajendran A. "Do adsorbent screening metrics predict process performance? A process optimization based study for post-combustion capture of CO₂". *International Journal of Greenhouse Gas Control*. Vol. 46, pp. 76-85, 2016.

Appendix A

Final Report from University of California, Irvine

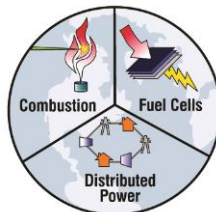
**TDA Project # 2208
DoE Contract No.: DE-FE-0026142**

**Low Cost Air Separation Process for Gasification
Applications**

FINAL REPORT

Prepared By

Advanced Power and Energy Program



**University of California, Irvine
May 2019**

DISCLAIMER

This report was prepared by the Advanced Power and Energy Program of the University of California, Irvine (UCI) as an account of work sponsored by TDA. Neither the Advanced Power and Energy Program, nor any of their employees, makes any warranty, express or implied, or assumes any legal liability or responsibility for the accuracy, completeness, or usefulness of any information, apparatus, product, or process disclosed, or represents that its use would not infringe privately owned rights. The views and opinions of the authors expressed herein do not necessarily state or reflect those of the Advanced Power and Energy Program or any agency thereof.

Table of Contents

1.0	Executive Summary.....	4
2.0	Introduction	5
3.0	Process Design Basis and Methodology.....	6
3.1	IGCC power plant	6
4.0	Process Descriptions.....	7
4.1	Case 1A - IGCC power plant equipped with GE gasifier integrated with TDA's ASU with cold gas cleanup	7
4.1.1	TDA's Sorbent ASU	7
4.2	Case 1B - IGCC power plant equipped with GE gasifier integrated with TDA's ASU with warm gas cleanup	8
4.2.1	TDA's Sorbent ASU	9
4.2.2	Warm Gas Cleanup and Regenerable Sorbent CO ₂ Capture	10
4.2.3	CO ₂ Purification and Pressurization	11
4.3	Case 2A - IGCC power plant equipped with E-Gas gasifier integrated with TDA's ASU with cold gas cleanup	11
4.3.1	TDA's Sorbent ASU	12
4.4	Case 2B - IGCC power plant equipped with E-Gas gasifier integrated with TDA's ASU with warm gas cleanup.....	12
4.4.1	TDA's Sorbent ASU	13
4.4.2	Warm Gas Cleanup and Regenerable Sorbent CO ₂ Capture	14
4.4.3	CO ₂ Purification and Pressurization	15
5.0	Results and Discussion	15
6.0	References and Bibliography.....	16

1.0 Executive Summary

As part of the subcontract work under DE-FE-0026142 project (TDA#2208), the Advanced Power and Energy Program (APEP) of the University of California, Irvine (UCI) is developing simulation models to estimate the performance and cost of the TDA's Advanced air separation concept for:

1. IGCC Plants utilizing the GE type gasifier
2. IGCC Plants utilizing the E-Gas type gasifier

Plant cost estimates and capital requirements are estimated with input provided by TDA for the proprietary air separation unit (ASU) equipment.

Cold Gas Cleanup. The TDA's sorbent ASU in a GE type gasifier based IGCC showed a substantial improvement in the thermal performance of an IGCC with cold gas cleanup, a 7% decrease in overall plant heat rate over the corresponding IGCC designed with a cryogenic ASU (heat rate decreased from 11,297 kJ/kWh to 10,574 kJ/kWh). The TDA ASU in an E-Gas type gasifier based IGCC with cold gas cleanup showed a less substantial improvement in the thermal performance, about 4% decrease in overall plant heat rate over the corresponding IGCC designed with a cryogenic ASU (heat rate decreased from 11,645 kJ/kWh to 11,169 kJ/kWh).

Warm Gas Cleanup. The advantage in overall plant thermal efficiency of using the TDA ASU was lower with warm gas cleanup in IGCC using GE type gasifiers. The TDA ASU in a GE type gasifier based IGCC with warm gas cleanup, showed a 3% decrease in overall plant heat rate over the corresponding IGCC designed with a cryogenic ASU (heat rate decreased from 10,492 kJ/kWh to 10,189 kJ/kWh). Further optimization of this case may possibly improve its heat rate. The TDA ASU in an E-Gas type gasifier based IGCC with warm gas cleanup showed a similar improvement in the thermal performance as seen with cold gas cleanup, a 4% decrease in overall plant heat rate over the corresponding IGCC designed with a cryogenic ASU (heat rate decreased from 10,667 kJ/kWh to 10,228 kJ/kWh).

The advantage seen for the TDA ASU based cases is primarily due to the replacement of the nitrogen injected (typically supplied by a cryogenic ASU) into the gas turbine for NOx control with depleted air from TDA's ASU, thereby saving power associated with the nitrogen compression as well as air compression. Note that the amount of air supplied to the elevated pressure train (in our simulation) of a cryogenic ASU being a larger fraction of the total air supplied to this cryogenic ASU (i.e., air supplied to elevated pressure and low pressure trains combined), the nitrogen being supplied by the elevated pressure train.

The TDA ASU shows a greater improvement in the specific plant cost (\$/kW basis) of an IGCC with cold gas cleanup, as much as 13% and 11% decrease in this cost for cases 1A and 2A over the corresponding cryogenic ASU based IGCC also with cold gas cleanup. Its advantage in the specific plant cost was a bit lower for an IGCC with warm gas cleanup, a 10% and 9% decrease for cases 1B and 2B over the corresponding cryogenic ASU based IGCC also with warm gas cleanup.

The TDA ASU also shows a greater improvement in the 1st year cost of electricity (COE) of an IGCC with cold gas cleanup, as much as 11% and 8% decrease in this cost for cases 1A and 2A over the corresponding cryogenic ASU based IGCC also with cold gas cleanup, this decrease in this cost attributable to the heat rate and specific plant cost advantages. Its advantage in the COE was also significant for the IGCCs with warm gas cleanup; the 1st year COE decreased by as much as 8% and 7% for cases 1B and 2B over the corresponding cryogenic ASU based IGCC also with warm gas cleanup, again this decrease being attributable to the heat rate and specific plant cost advantages.

It should be noted that the performance of some of the process units or equipment such as the cryogenic ASU (reference cases used for comparison), the Selexol™(used in the cold gas cleanup cases) and the gas turbine (all cases) were estimated by us and it is recommended that vendors be contacted for both performance and cost data in a more detailed study in the future. It should be also mentioned that the costs of the TDA sorption based ASUs on a total plant basis were estimated by TDA. These ASU cost estimates are substantially lower than those appearing in the referenced NETL/DoE report for the cryogenic ASUs which were used as the basis for the reference cases (used in the comparisons). This reduced cost of the TDA sorption based ASU over the cryogenic ASU is a major reason for the substantial improvement in the economics presented in this report.

2.0 Introduction

First a detailed system model was developed based on the schematic provided for the air separation system. In the simulation APEP carried out all mass and energy balance calculations using Aspen Plus® simulation software across the major subsystems in the ASU integrated to the overall power plant.

The following lists the cases developed:

1. Case 1A - IGCC power plant equipped with GE gasifier integrated with TDA's sorbent ASU with cold gas capture¹
2. Case 1B - IGCC power plant equipped with GE gasifier integrated with TDA's sorbent ASU and warm gas capture
3. Case 2A - IGCC power plant equipped with E-Gas gasifier integrated with TDA's sorbent ASU with cold gas capture²
4. Case 2B - IGCC power plant equipped with E-Gas gasifier integrated with TDA's sorbent ASU and warm gas capture.

¹ Using Case 2 documented in Cost and Performance Baseline for Fossil Energy Plants Volume 1: Bituminous Coal and Natural Gas to Electricity, Revision 2a, September 2013, DOE/NETL-2010/1397

² Using Case 4 documented in Cost and Performance Baseline for Fossil Energy Plants Volume 1: Bituminous Coal and Natural Gas to Electricity, Revision 2a, September 2013, DOE/NETL-2010/1397

APEP estimated consumables and the plant efficiency, and incorporated TDA's cost estimates for the ASU sorbent system for all cases, and trace component removal and CO₂ PSA separation systems for the warm gas capture cases, into the power plant cost estimates to estimate the overall plant cost, cost of electricity (COE), and cost of CO₂ capture. This effort also included a limited amount of sensitivity analysis on the major design parameters in order to arrive at the desired operating conditions.

The deliverables for this project include:

1. Block flow diagrams and simplified process flow diagrams accompanied by major stream data
2. Overall plant performance estimates taking into account all consumables and the useful by-products
3. Cost estimates for COE and cost of CO₂ capture
4. An analysis of results and recommendations.

3.0 Process Design Basis and Methodology

3.1 IGCC power plant

The process design for the cold gas cleanup cases is based on fully loading (limited by shaft output) two General Electric 7FA type gas turbines where possible when not constrained by the suction air flow rate limit. The overall basis for design is consistent with Case 2 and Case 4 documented in Cost and Performance Baseline for Fossil Energy Plants, Volume 1: Bituminous Coal and Natural Gas to Electricity, Revision 2a, September 2013, DOE/NETL-2010/1397.

Specifically, the following are consistent with the respective referenced cases:

- 1) Feed coal and natural gas analysis
- 2) Site characteristics and ambient conditions
- 3) Environmental controls and performance
- 4) Balance of plant subsystems

The system boundaries for the plant are defined by the following:

- 1) Delivered coal entering the power plant, through high-pressure, high-purity CO₂ stream crossing the plant boundary.
- 2) Plant air intake from the ambient.
- 3) Flue gas to stack inclusive of stack.
- 4) Net electricity conditioned and sent to electric grid.
- 5) Raw make-up water.
- 6) Waste streams generated by the power plant are adequately treated on-site prior to disposal either by landfill or other commercial disposal options.

4.0 Process Descriptions

Figures 1, 3, 5 and 7 present the overall block flow diagram for Cases 1A, 1B, 2A and 2B, the greenfield power plants integrated with capture of CO₂ while Figures 2, 4, 6 and 8 present the process flow diagram for TDA's air separation system for Cases 1A, 1B, 2A and 2B. The stream data for Cases 1A, 1B, 2A and 2B are presented in Tables 1 through 4.

4.1 Case 1A - IGCC power plant equipped with GE gasifier integrated with TDA's ASU with cold gas cleanup

The IGCC plant employing the cold gas cleanup and CO₂ capture technology consists of the following process plant subsystems:

- TDA's Sorbent ASU
- Coal Feed Preparation
- Gasification based on GE type gasifier technology
- High Temperature Syngas Cooling and Scrubbing
- Sour Shifting and Low Temperature Gas Cooling (Cold Gas Heat Recovery)
- Syngas Desulfurization and Decarbonization using a two-stage Selexol™ process (Acid Gas Removal or AGR)
- Claus Sulfur Recovery and Tail Gas Hydrogenation followed by Recycle to the AGR
- CO₂ Dehydration and Pressurization
- Syngas Humidification and Preheating
- Syngas Expansion in Power Recovery Turbo-expander
- Gas Turbines (based on GE F class type technology)
- Heat Recovery Steam Generators (HRSGs)
- Reheat Steam Cycle

The plant also has the necessary utilities (e.g. cooling water supply, make-up water treatment, plant and instrument air) to support the process units. Detailed process description of a similar case but utilizing a cryogenic ASU may be found in the previously referenced DOE/NETL report 2010/1397.

4.1.1 TDA's Sorbent ASU

Initially, a sensitivity analysis was conducted to quantify the impact of the ASU operating temperature on the overall plant performance. As expected, the overall plant heat rate decreased as the operating temperature was reduced since the fraction of syngas diverted to the ASU for the regeneration of the sorbent also decreased. Desorption temperatures used in this analysis were 800°C, 750°C and 650°C. Compared to the 800°C case, the relative plant heat rates decreased by 0.2% for the 750°C desorption temperature, and by 0.6% for the 650°C desorption temperature. Since there will be a significant reduction in cost of

equipment within the ASU due to cheaper materials of construction with the lower desorption temperature, the 650°C design was selected.

Air required by the ASU is partially supplied by extraction from the gas turbine compressor discharge while the remaining is supplied by a dedicated compressor (main air compressor or MAC) located within the ASU. The fraction of air extracted (9.1% based on the gas turbine suction air flow rate) was set by that required to fully load the gas turbine with the suction air flow rate corresponding to that with inlet guide vanes fully opened (this suction air flow being determined from the natural gas case for the same set of ambient conditions). The extracted air is further compressed to a pressure of 17.38 bar and combined with the air discharging the MAC and preheated in a feed/effluent exchanger to a temperature of 598°C against the depleted air leaving the fixed bed O₂ sorption unit at 663°C. The depleted air (96.1 mole % N₂) at a temperature of 448°C is supplied to the gas turbine as a thermal diluent for NO_x control.

Regeneration of the sorbent is accomplished with preheated Low Low Pressure (LLP) steam generated within the ASU. The regeneration pressure of 1.41 bar is such that the ratio of partial pressure of O₂ during the adsorption step to that during the desorption step is 3.0 to provide a reasonable driving force (note that additional regeneration steam could be provided by extraction from the steam turbine to increase the desorption pressure resulting in a reduction in the O₂ compression power but would require piping of LLP steam over a long distance within the plant while also penalizing the steam turbine power output).

Balance of heat required by the regeneration process is met by combusting a small fraction (1.4%) of the desulfurized/decarbonized syngas also preheated along with the LLP steam to a temperature of 630°C against the oxygen stream leaving the regeneration step at a temperature of 650°C. The oxygen stream is further cooled in a series of heat exchange coils to provide heat for the syngas humidifier, LLP steam generation and finally trim cooled against cooling water before it is pressurized in an intercooled compressor. The amount of O₂ required by the Claus Sulfur Recovery Unit is extracted at the required intermediate pressure while the remainder is compressed to the pressure required by the gasifier. This oxygen stream contains 95% by mole O₂.

4.2 Case 1B - IGCC power plant equipped with GE gasifier integrated with TDA's ASU with warm gas cleanup

The IGCC plant employing the sorbent CO₂ capture consists of the following process plant subsystems:

- TDA's Sorbent ASU
- Coal Feed Preparation
- Gasification based on GE type gasifier technology
- High Temperature Syngas Cooling and Scrubbing
- Sour Shifting
- Warm Gas Cleanup similar to Research Triangle Institute (RTI) process including Acid (H₂SO₄) Unit
- Regenerable Sorbent CO₂ Capture (based on TDA technology)

- CO₂ Purification and Pressurization
- Syngas Preheating and Expansion in Power Recovery Turbo-expander
- Gas Turbines (based on GE F class type technology)
- HRSGs
- Reheat Steam Cycle

The plant also has the necessary utilities (e.g. cooling water supply, make-up water treatment, plant and instrument air) to support the process units. Plant subsystems that are significantly different from the Cold Gas Cleanup case are described in the following.

4.2.1 TDA's Sorbent ASU

A sensitivity analysis was also initially conducted for the plant with warm gas cleanup to quantify the impact of the ASU operating temperature on the overall plant performance. As expected, the overall plant heat rate decreased as the operating temperature was reduced since the fraction of syngas diverted to the ASU for the regeneration of the sorbent also decreased. Desorption temperatures used in this analysis were again 800°C, 750°C and 650°C. Compared to the 800°C case, the relative plant heat rates decreased by 0.03% for the 750°C desorption temperature, and by 0.33% for the 650°C desorption temperature. These improvements in heat rate however, are not as significant as those obtained with the cold gas cleanup. Since there will be a significant reduction in cost of equipment within the ASU due to cheaper materials of construction with the lower desorption temperature, the 650°C design was selected.

Air required by the ASU is partially supplied by extraction from the gas turbine compressor discharge while the remaining is supplied by a dedicated compressor (main air compressor or MAC) located within the ASU. The fraction of air extracted (10% based on the gas turbine suction air flow rate) was set by that required to fully load the gas turbine with the suction air flow rate corresponding to that with inlet guide vanes fully opened (this suction air flow being determined from the natural gas case for the same set of ambient conditions). The extracted air is further compressed to a pressure of 17.38 bar and combined with the air discharging the MAC and preheated in a feed/effluent exchanger to a temperature of 598°C against the depleted air leaving the fixed bed O₂ sorption unit at 663°C. Majority of the depleted air (containing 96.1 mole % N₂) at a temperature of 450°C is supplied to the gas turbine as a thermal diluent for NO_x control. A small fraction (1.3%) of the depleted air is cooled by generating LLP steam and compressed to 41.2 bar as required by the H₂SO₄ unit.

Regeneration of the sorbent is accomplished with preheated Low Low Pressure (LLP) steam generated within the ASU. The regeneration pressure of 1.43 bar is such that the ratio of partial pressure of O₂ during the adsorption step to that during the desorption step is 3.0 to provide a reasonable driving force (note that additional regeneration steam could be provided by extraction from the steam turbine to increase the desorption pressure resulting in a reduction in the O₂ compression power but would require piping of LLP steam over a long distance within the plant while also penalizing the steam turbine power output).

Balance of heat required by the regeneration process is met by combusting a small fraction (1.5%) of the desulfurized/decarbonized humidified syngas also preheated along with the LLP steam to a temperature of 630°C against the oxygen stream leaving the regeneration step at a temperature of 650°C. The oxygen stream is further cooled in a series of heat exchange coils to provide heat for MP steam generation, LLP steam generation and finally trim cooled against cooling water before it is pressurized in an intercooled compressor.

The amounts of O₂ required by the H₂SO₄ unit and that required by the catalytic combustor used for CO₂ purification (to combust the residuals amounts of H₂, CO and CH₄) are extracted at the required intermediate pressures while the remainder is compressed to the pressure required by the gasifier. This oxygen stream contains 95% by mole O₂.

4.2.2 Warm Gas Cleanup and Regenerable Sorbent CO₂ Capture

Scrubbed gas is combined with the appropriate amount of steam extracted from the steam turbine after it is attemperated by addition of boiler feed water (BFW) to a temperature such that the syngas - steam mixture is at 215°C. It is then fed to a sour shift reactor similar to the Cold Gas Cleanup case. The partially shifted hot gas (preheated in this shift reactor by the exothermic reaction) is then directly fed to a warm gas desulfurization unit similar to RTI's process utilizing a zinc titanate adsorbent in a fluidized bed. The performance of this unit as well as the production of H₂SO₄ from the SO₂ in the regenerator off-gas was developed utilizing information available in the public domain [Siriwardane et al, 2002]. The regenerator off-gas after particulate removal is depressurized by expansion in a power recovery turbine before feeding it to the H₂SO₄ unit. The on-site ASU provides the small amount of O₂ as required by the H₂SO₄ unit in addition to supplying oxygen to the gasifier and the catalytic combustor used for CO₂ purification (combust the residuals amounts of H₂, CO and CH₄). The hot syngas leaving the desulfurizer is cooled in an intermediate pressure (IP) steam generator followed by a medium pressure (MP) steam generator before being fed to a second adiabatic shift reactor.

The hot syngas leaving the second adiabatic shift reactor is cooled in an IP steam generator followed by a MP steam generator to a temperature of 198°C. Effluent from this exchanger is treated in TDA's expendable warm gas Hg removal system. The design uses lead-lag beds with 3 month change out. Some of the NH₃ and HCN are also removed by this process. The treated syngas is then combined with recycle gas from TDA's PSA unit and then fed to the TDA's warm gas PSA unit for decarbonizing the syngas before it is combusted in the gas turbines. About + 94% of the syngas enters this decarbonizing unit where 98.5% of the CO₂ entering with the syngas is separated on a per-pass basis with the overall carbon capture being 90%. Remainder of the syngas is sent directly to the gas turbine bypassing TDA's CO₂ capture system. Regeneration is accomplished utilizing steam at a desorption pressure of 10.34 barA. Two streams are regenerated, one consisting of "raw CO₂," a mixture of CO₂, steam and small amounts of residual syngas at a temperature of 186°C, and the other recycle gas," with significant amounts of other syngas components (mainly H₂) at a temperature of 235°C for recycle to the CO₂ separation unit.

The decarbonized syngas leaving the CO₂ separation (adsorption) unit at a temperature of 203°C with its accompanying steam is combined with the bypassed syngas. After preheating to 241°C, the gas is supplied to the syngas expander. The small fraction of syngas required by the ASU is taken from the expander discharge, with the remaining supplied to the gas turbines along with the depleted air from the ASU as the thermal diluent for NO_x control. The combined cycle design is similar to the design in the Cold Gas Cleanup case that uses a reheat steam cycle.

4.2.3 CO₂ Purification and Pressurization

The raw CO₂ leaving the CO₂ separation (adsorption) unit is cooled in a series of heat exchangers while generating low pressure (LP) steam, vacuum condensate/makeup BFW heating and finally trim cooled against cooling water before it is compressed, preheated in a feed/effluent exchanger and then fed to a catalytic (noble metal) combustor along with O₂ to oxidize the small amounts of combustibles present in the raw CO₂ stream. The catalyst requirement and size of the reactor were factored from data received from a catalyst vendor on a previous job. The catalyst was 0.1% platinum metal in the form of an oxide deposited onto the surface of a nickel stabilized alumina tablet with a projected catalyst life of 6 years. The effluent from this combustor after generating HP steam is cooled in the feed/effluent exchanger. This is followed by vacuum condensate/makeup BFW heating and finally trim cooled against cooling water. It is then further compressed in an intercooled compressor to the required pressure consistent with the design basis and the Cold Gas Cleanup case.

4.3 Case 2A - IGCC power plant equipped with E-Gas gasifier integrated with TDA's ASU with cold gas cleanup

The IGCC plant employing the cold gas cleanup and CO₂ capture technology consists of the following process plant subsystems:

- TDA's Sorbent ASU
- Coal Feed Preparation
- Gasification based on E-Gas type gasifier technology
- High Temperature Syngas Cooling and Scrubbing
- Sour Shifting and Low Temperature Gas Cooling (Cold Gas Heat Recovery)
- Syngas Desulfurization and Decarbonization using a two-stage Selexol™ process (Acid Gas Removal or AGR)
- Claus Sulfur Recovery and Tail Gas Hydrogenation followed by Recycle to the AGR
- CO₂ Dehydration and Pressurization
- Syngas Humidification and Preheating
- Gas Turbines (based on GE F class type technology)
- Heat Recovery Steam Generators (HRSGs)
- Reheat Steam Cycle

The plant also has the necessary utilities (e.g. cooling water supply, make-up water treatment, plant and instrument air) to support the process units. Detailed process description of a similar case but utilizing a cryogenic ASU May be found in the previously referenced DOE/NETL report 2010/1397.

4.3.1 TDA's Sorbent ASU

Air required by the ASU is partially supplied by extraction from the gas turbine compressor discharge while the remaining is supplied by a dedicated compressor (main air compressor or MAC) located within the ASU. The fraction of air extracted (8.8% based on the gas turbine suction air flow rate) was set by that required to fully load the gas turbine with the suction air flow rate corresponding to that with inlet guide vanes fully opened (this suction air flow being determined from the natural gas case for the same set of ambient conditions). The extracted air is further compressed to a pressure of 17.38 bar and combined with the air discharging the MAC and preheated in a feed/effluent exchanger to a temperature of 598°C against the depleted air leaving the fixed bed O₂ sorption unit at 663°C. The depleted air (96.1 mole % N₂) at a temperature of 448°C is supplied to the gas turbine as a thermal diluent for NO_x control.

Regeneration of the sorbent is accomplished with preheated Low Low Pressure (LLP) steam generated within the ASU. The regeneration pressure of 1.36 bar is such that the ratio of partial pressure of O₂ during the adsorption step to that during the desorption step is 3.0 to provide a reasonable driving force (note that additional regeneration steam could be provided by extraction from the steam turbine to increase the desorption pressure resulting in a reduction in the O₂ compression power but would require piping of LLP steam over a long distance within the plant while also penalizing the steam turbine power output).

Balance of heat required by the regeneration process is met by combusting a small fraction (1.45%) of the desulfurized/decarbonized humidified syngas also preheated along with the LLP steam to a temperature of 630°C against the oxygen stream leaving the regeneration step at a temperature of 650°C. The oxygen stream is further cooled in a series of heat exchange coils to provide heat for the syngas humidifier, LLP steam generation and finally trim cooled against cooling water before it is pressurized in an intercooled compressor. The amount of O₂ required by the Claus Sulfur Recovery Unit is extracted at the required intermediate pressure while the remainder is compressed to the pressure required by the gasifier. This oxygen stream contains 95% by mole O₂.

4.4 Case 2B - IGCC power plant equipped with E-Gas gasifier integrated with TDA's ASU with warm gas cleanup

The IGCC plant employing the sorbent CO₂ capture consists of the following process plant subsystems:

- TDA's Sorbent ASU
- Coal Feed Preparation

- Gasification based on E-Gas type gasifier technology)
- High Temperature Syngas Cooling and Scrubbing
- Sour Shifting
- Warm Gas Cleanup similar to Research Triangle Institute (RTI) process including Acid (H_2SO_4) Unit
- Regenerable Sorbent CO_2 Capture (based on TDA technology)
- CO_2 Purification and Pressurization
- Syngas Preheating
- Gas Turbines (based on GE F class type technology)
- HRSGs
- Reheat Steam Cycle

The plant also has the necessary utilities (e.g. cooling water supply, make-up water treatment, plant and instrument air) to support the process units. Plant subsystems that are significantly different from the Cold Gas Cleanup case are described in the following.

4.4.1 TDA's Sorbent ASU

Air required by the ASU is partially supplied by extraction from the gas turbine compressor discharge while the remaining is supplied by a dedicated compressor (main air compressor or MAC) located within the ASU. The fraction of air extracted (7.1% based on the gas turbine suction air flow rate) was set by that required to fully load the gas turbine with the suction air flow rate corresponding to that with inlet guide vanes fully opened (this suction air flow being determined from the natural gas case for the same set of ambient conditions). The extracted air is further compressed to a pressure of 17.38 bar and combined with the air discharging the MAC and preheated in a feed/effluent exchanger to a temperature of 597°C against the depleted air leaving the fixed bed O_2 sorption unit at 663°C. Majority of the depleted air (containing 96.1 mole % N_2) at a temperature of 450°C is supplied to the gas turbine as a thermal diluent for NO_x control. A small fraction (1.4%) of the depleted air is cooled by generating LLP steam and compressed to 41.2 bar as required by the H_2SO_4 unit.

Regeneration of the sorbent is accomplished with preheated Low Low Pressure (LLP) steam generated within the ASU. The regeneration pressure of 1.42 bar is such that the ratio of partial pressure of O_2 during the adsorption step to that during the desorption step is 3.0 to provide a reasonable driving force (note that additional regeneration steam could be provided by extraction from the steam turbine to increase the desorption pressure resulting in a reduction in the O_2 compression power but would require piping of LLP steam over a long distance within the plant while also penalizing the steam turbine power output).

Balance of heat required by the regeneration process is met by combusting a small fraction (1.4%) of the desulfurized/decarbonized syngas also preheated along with the LLP steam to a temperature of 630°C against the oxygen stream leaving the regeneration step at a temperature of 650°C. The oxygen stream is further cooled in a series of heat exchange coils to provide

heat for MP steam generation, LLP steam generation and finally trim cooled against cooling water before it is pressurized in an intercooled compressor.

The amounts of O₂ required by the H₂SO₄ unit and that required by the catalytic combustor used for CO₂ purification (to combust the residuals amounts of H₂, CO and CH₄) are extracted at the required intermediate pressures while the remainder is compressed to the pressure required by the gasifier. This oxygen stream contains 95% by mole O₂.

4.4.2 Warm Gas Cleanup and Regenerable Sorbent CO₂ Capture

Scrubbed gas is combined with the appropriate amount of steam extracted from the steam turbine after it is attemperated by addition of boiler feed water (BFW) to a temperature such that the syngas - steam mixture is at 215°C. It is then fed to a sour shift reactor similar to the Cold Gas Cleanup case. The partially shifted hot gas (preheated in this shift reactor by the exothermic reaction) is then directly fed to a warm gas desulfurization unit similar to RTI's process utilizing a zinc titanate adsorbent in a fluidized bed. The performance of this unit as well as the production of H₂SO₄ from the SO₂ in the regenerator off-gas was developed utilizing information available in the public domain [Siriwardane et al, 2002]. The regenerator off-gas after particulate removal is depressurized by expansion in a power recovery turbine before feeding it to the H₂SO₄ unit. The on-site ASU provides the small amount of O₂ as required by the H₂SO₄ unit in addition to supplying oxygen to the gasifier and the catalytic combustor used for CO₂ purification (combust the residuals amounts of H₂, CO and CH₄). The hot syngas leaving the desulfurizer is cooled in an intermediate pressure (IP) steam generator followed by a medium pressure (MP) steam generator before being fed to a second adiabatic shift reactor.

The hot syngas leaving the second adiabatic shift reactor is cooled in an IP steam generator followed by a MP steam generator to a temperature of 198°C. Effluent from this exchanger is treated in TDA's expendable warm gas Hg removal system. The design uses lead-lag beds with 3 month change out. Some of the NH₃ and HCN are also removed by this process. The treated syngas is then combined with recycle gas from TDA's PSA unit and then fed to the TDA's warm gas PSA unit for decarbonizing the syngas before it is combusted in the gas turbines. About+ 94% of the syngas enters this decarbonizing unit where 98.5% of the CO₂ entering with the syngas is separated on a per-pass basis with the overall carbon capture being 90%. Remainder of the syngas is sent directly to the gas turbine bypassing TDA's CO₂ capture system. Regeneration is accomplished utilizing steam at a desorption pressure of 10.34 barA. Two streams are regenerated, one consisting of "raw CO₂," a mixture of CO₂, steam and small amounts of residual syngas at a temperature of 186°C, and the other recycle gas," with significant amounts of other syngas components (mainly H₂) at a temperature of 235°C for recycle to the CO₂ separation unit.

The decarbonized syngas leaving the CO₂ separation (adsorption) unit at a temperature of 203°C with its accompanying steam is combined with the bypassed syngas. After preheating to 241°C, the gas is supplied to the syngas expander. The small fraction of syngas required by the ASU is taken from the expander discharge, with the remaining supplied to the gas turbines along with the depleted air from the ASU as the thermal diluent for NO_x control. The combined

cycle design is similar to the design in the Cold Gas Cleanup case that uses a reheat steam cycle.

4.4.3 CO₂ Purification and Pressurization

The raw CO₂ leaving the CO₂ separation (adsorption) unit is cooled in a series of heat exchangers while generating low pressure (LP) steam, vacuum condensate/makeup BFW heating and finally trim cooled against cooling water before it is compressed, preheated in a feed/effluent exchanger and then fed to a catalytic (noble metal) combustor along with O₂ to oxidize the small amounts of combustibles present in the raw CO₂ stream. The catalyst requirement and size of the reactor were factored from data received from a catalyst vendor on a previous job. The catalyst was 0.1% platinum metal in the form of an oxide deposited onto the surface of a nickel stabilized alumina tablet with a projected catalyst life of 6 years. The effluent from this combustor after generating HP steam is cooled in the feed/effluent exchanger. This is followed by vacuum condensate/makeup BFW heating and finally trim cooled against cooling water. It is then further compressed in an intercooled compressor to the required pressure consistent with the design basis and the Cold Gas Cleanup case.

5.0 Results and Discussion

The overall plant performance summaries are presented in Table 5 for the Cold Gas Cleanup Cases 1A and 2A, and in Table 6 for the Warm gas Cleanup Cases 1B and 2B.

Cold Gas Cleanup. The TDA's sorbent ASU in a GE type gasifier based IGCC showed a substantial improvement in the thermal performance of an IGCC with cold gas cleanup, a 7% decrease in overall plant heat rate over the corresponding IGCC designed with a cryogenic ASU (heat rate decreased from 11,297 kJ/kWh to 10,574 kJ/kWh). The TDA ASU in an E-Gas type gasifier based IGCC with cold gas cleanup showed a less substantial improvement in the thermal performance, about 4% decrease in overall plant heat rate over the corresponding IGCC designed with a cryogenic ASU (heat rate decreased from 11,645 kJ/kWh to 11,169 kJ/kWh).

Warm Gas Cleanup. The advantage in overall plant thermal efficiency of using the TDA ASU was lower with warm gas cleanup in IGCC using GE type gasifiers. The TDA ASU in a GE type gasifier based IGCC with warm gas cleanup, showed a 3% decrease in overall plant heat rate over the corresponding IGCC designed with a cryogenic ASU (heat rate decreased from 10,492 kJ/kWh to 10,189 kJ/kWh). Further optimization of this case may possibly improve its heat rate. The TDA ASU in an E-Gas type gasifier based IGCC with warm gas cleanup showed a similar improvement in the thermal performance as seen with cold gas cleanup, a 4% decrease in overall plant heat rate over the corresponding IGCC designed with a cryogenic ASU (heat rate decreased from 10,667 kJ/kWh to 10,228 kJ/kWh).

The advantage seen for the TDA ASU based cases is primarily due to the replacement of the nitrogen injected (typically supplied by a cryogenic ASU) into the gas turbine for NOx control

with depleted air from TDA's ASU, thereby saving power associated with the nitrogen compression as well as air compression. Note that the amount of air supplied to the elevated pressure train (in our simulation) of a cryogenic ASU being a larger fraction of the total air supplied to this cryogenic ASU (i.e., air supplied to elevated pressure and low pressure trains combined), the nitrogen being supplied by the elevated pressure train.

Tables 7 through 9 present the total plant cost by major plant subsections for cases 1A and 2A, and cases 1B and 2B. The TDA ASU shows a greater improvement in the specific plant cost (\$/kW basis) of an IGCC with cold gas cleanup, as much as 13% and 11% decrease in this cost for cases 1A and 2A over the corresponding cryogenic ASU based IGCC also with cold gas cleanup. Its advantage in the specific plant cost was a bit lower for an IGCC with warm gas cleanup, a 10% and 9% decrease for cases 1B and 2B over the corresponding cryogenic ASU based IGCC also with warm gas cleanup.

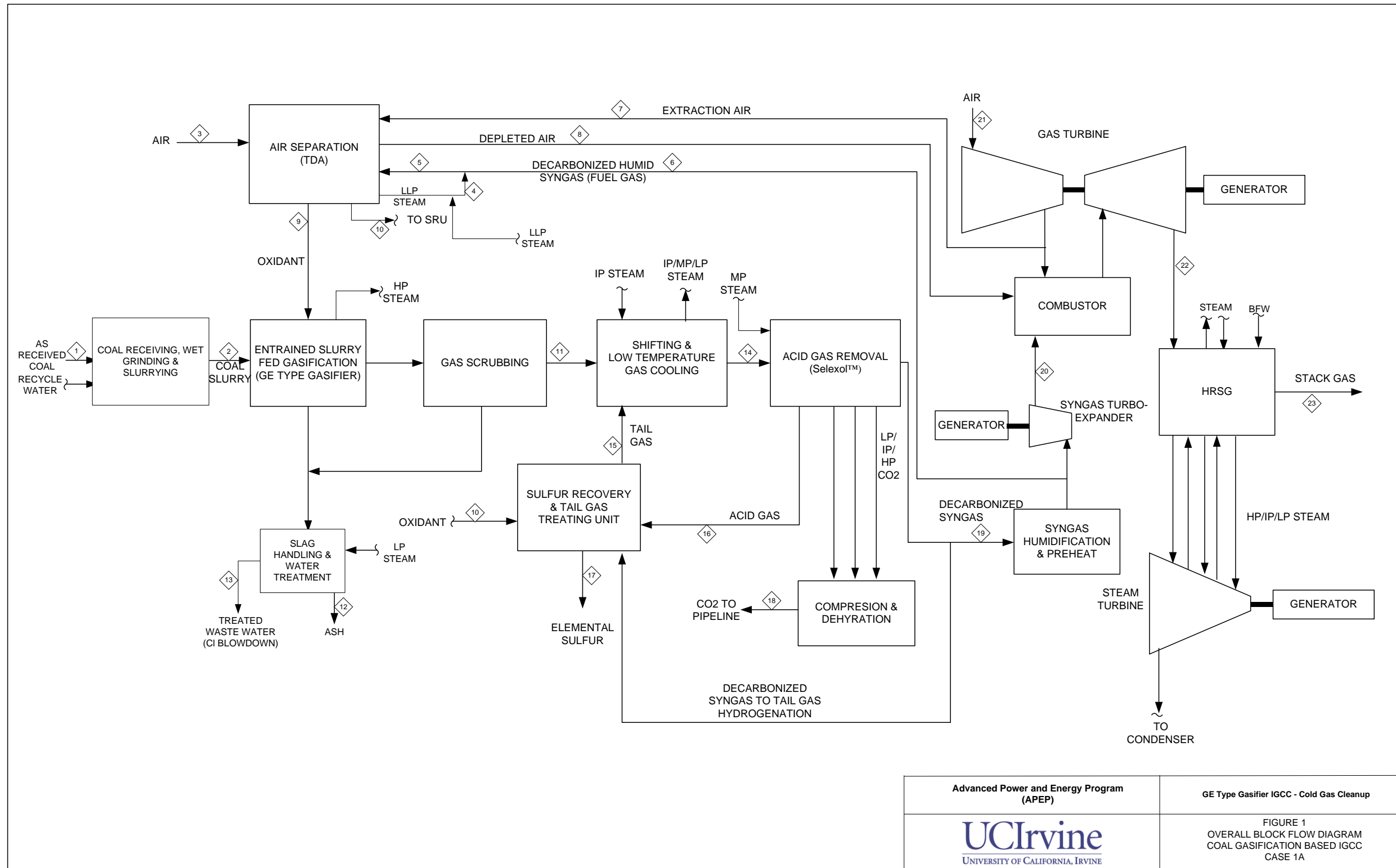
The process economics along with the cost of electricity as well as the cost of capturing and avoiding the CO₂ emissions are summarized in Table 10. The TDA ASU also shows a greater improvement in the 1st year cost of electricity (COE) of an IGCC with cold gas cleanup, as much as 11% and 8% decrease in this cost for cases 1A and 2A over the corresponding cryogenic ASU based IGCC also with cold gas cleanup, this decrease in this cost attributable to the heat rate and specific plant cost advantages. Its advantage in the COE was also significant for the IGCCs with warm gas cleanup; the 1st year COE decreased by as much as 8% and 7% for cases 1B and 2B over the corresponding cryogenic ASU based IGCC also with warm gas cleanup, again this decrease being attributable to the heat rate and specific plant cost advantages.

It should be noted that the performance of some of the process units or equipment such as the cryogenic ASU (reference cases used for comparison), the Selexol™(used in the cold gas cleanup cases) and the gas turbine (all cases) were estimated by us and it is recommended that vendors be contacted for both performance and cost data in a more detailed study in the future. It should be also mentioned that the costs of the TDA sorption based ASUs on a total plant basis were estimated by TDA. These ASU cost estimates are substantially lower than those appearing in the referenced NETL/DoE report for the cryogenic ASUs which were used as the basis for the reference cases (used in the comparisons). This reduced cost of the TDA sorption based ASU over the cryogenic ASU is a major reason for the substantial improvement in the economics presented in this report.

6.0 References and Bibliography

1. *Cost and Performance Baseline for Fossil Energy Plants, Volume 1: Bituminous Coal and Natural Gas to Electricity*, Revision 2a, September 2013, DOE/NETL-2010/1397.
2. *Process Modeling Desin Parameters*. Department of Energy, 2014. DOE/NETL-341/051314.

3. *Quality Guidelines for Energy System Studies: Carbon Dioxide Transport and Storage Costs in NETL Studies.* Pittsburgh, PA : Department of Energy, 2013. DOE/NETL-2013/1614.
4. *Cost Estimation Methodology for NETL Assessments of Power Plant Performance.* Pittsburgh : Department of Energy, 2011. 2011/1455.
5. *Capital Cost Scaling Methodology.* Pittsburgh : Department of Energy, 2013. 341/013113.
6. Siriwardane RV, Cicero DC, Jain S, Raghbir, Gupta P, Turk BS. *Durable zinc oxide-based regenerable sorbents for desulfurization of syngas in a fixed-bed reactor.* In: Fifth international symposium on gas cleaning at high temperature; September 17–20, 2002.



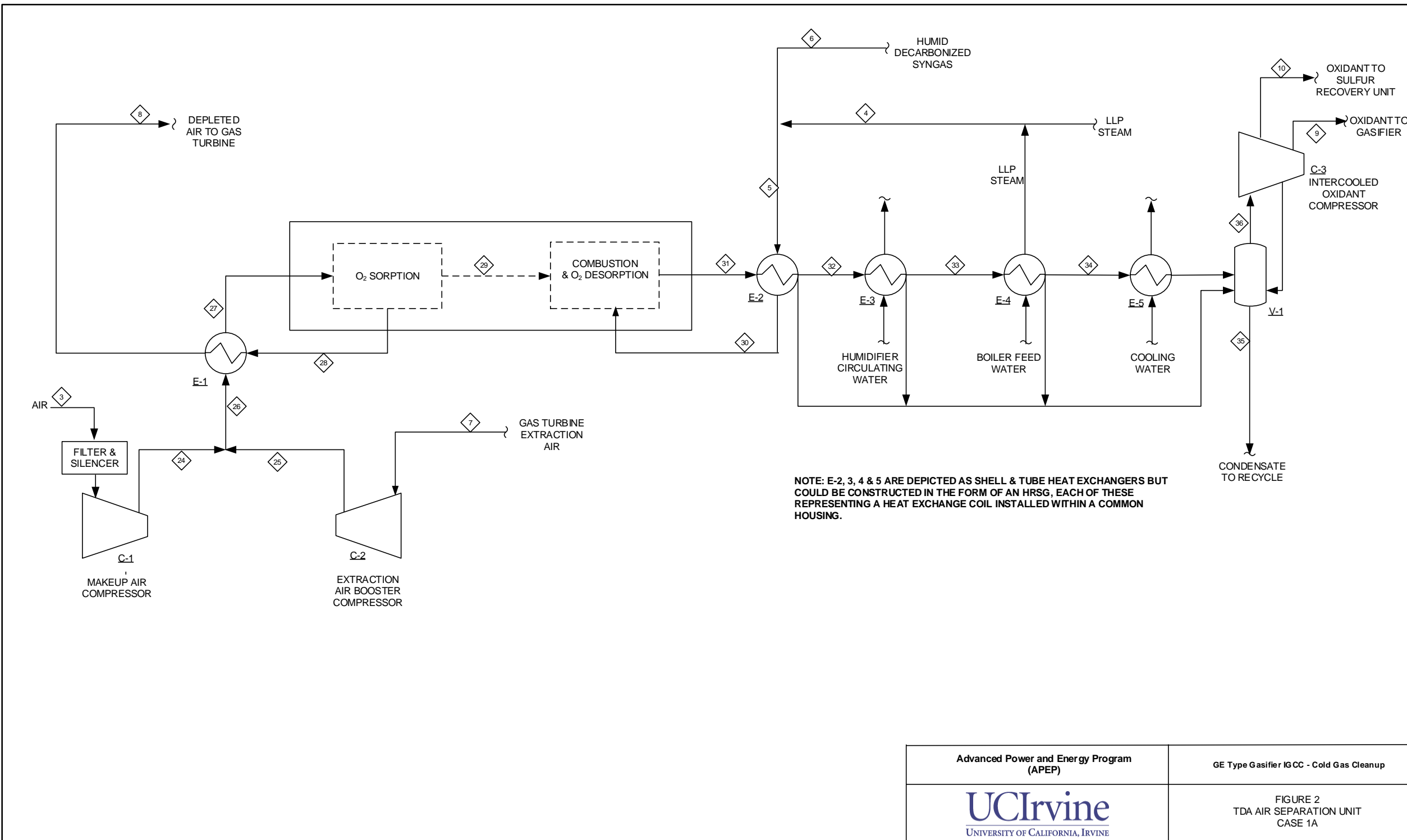
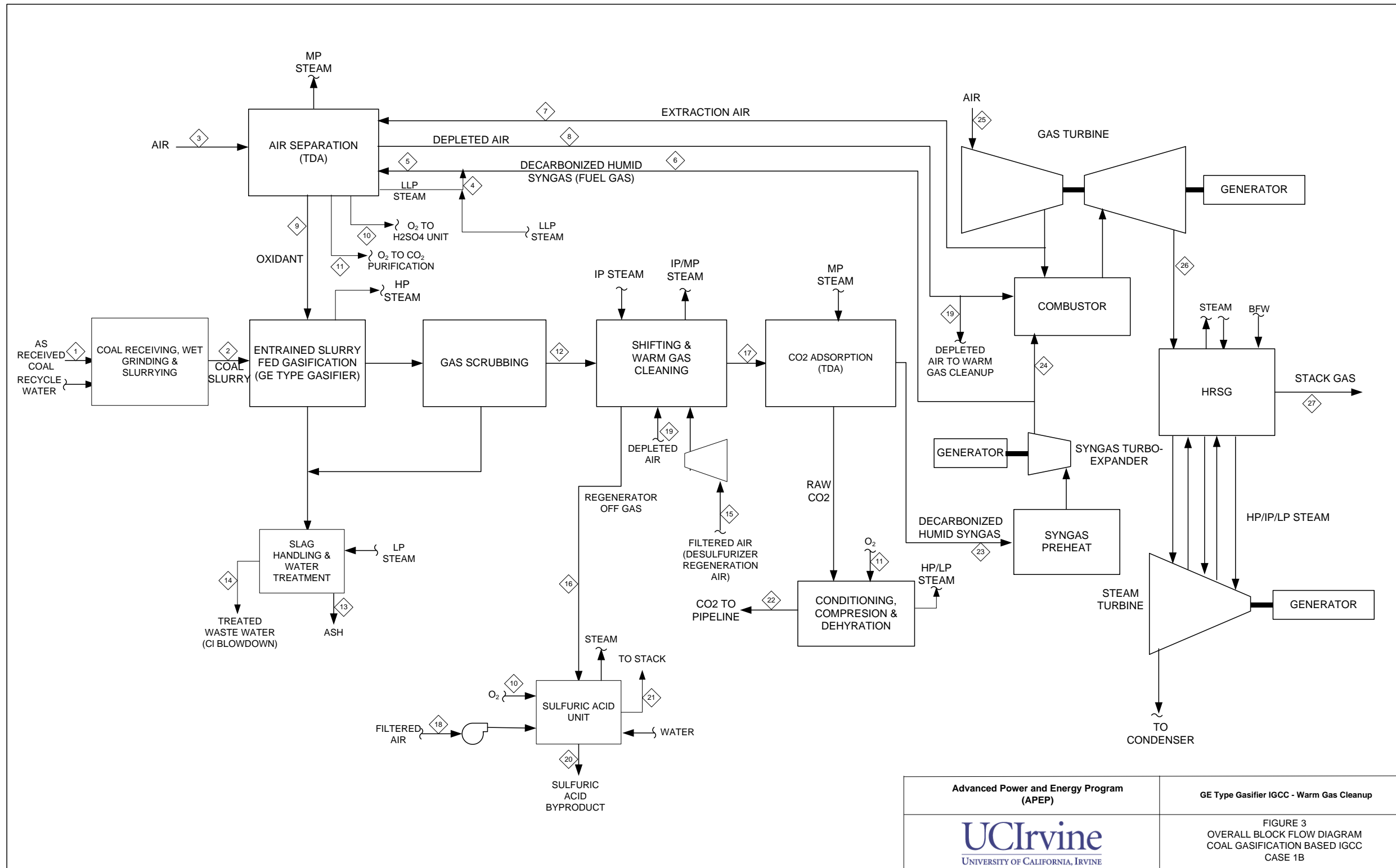


Table 1 – Case 1A Stream Data

Stream No.	1	2	3	4	5	6	7	8	9	10	11	12	13	14	15	16	17	18
Temperature C	15	77	15	115	140	185	429	448	77	19	207	60	57	26	148	48	174	25
Pressure bar	1.01	72.39	1.01	1.66	1.60	31.72	15.99	16.48	64.81	8.58	53.61	1.01	3.10	48.78	66.72	2.45	1.45	152.70
Vapor Frac			1.00	1.00	1.00	1.00	1.00	1.00	1.00	1.00	1.00		0.01	1.00	1.00	1.00	1.00	-
Mole Flow kmol/hr			17,904	367	765	398	10,042	22,174	5,539	140	32,197		1,255	28,271	332	494	87	10,466
Mass Flow kg/hr	221,412	312,420	516,541	6,607	10,552	3,945	289,712	622,573	176,380	4,463	626,991	18,929	28,306	562,826	12,536	17,642	5,550	458,476
Fluid Mole Fractions																		
O2		0.0000	0.2076	0.0000	0.0000	0.0000	0.2076	0.0131	0.9502	0.9486	0.0000		0.0000	0.0000	0.0001	0.0000	0.0000	0.0000
N2		0.0000	0.7719	0.0000	0.0067	0.0129	0.7719	0.9614	0.0457	0.0457	0.0102		0.0000	0.0127	0.0948	0.0016	0.0000	0.0000
AR		0.0000	0.0094	0.0000	0.0001	0.0001	0.0094	0.0117	0.0006	0.0006	0.0001		0.0000	0.0001	0.0003	0.0000	0.0000	0.0000
H2		0.0000	0.0000	0.0000	0.2954	0.5675	0.0000	0.0000	0.0000	0.0000	0.2439		0.0000	0.5613	0.1074	0.1027	0.0000	0.0047
CO		0.0000	0.0000	0.0000	0.0056	0.0108	0.0000	0.0000	0.0000	0.0000	0.2573		0.0000	0.0108	0.0034	0.0031	0.0000	0.0003
CO2		0.0000	0.0003	0.0000	0.0148	0.0285	0.0003	0.0004	0.0028	0.0028	0.1000		0.0000	0.4054	0.7839	0.5218	0.0000	0.9950
H2O		1.0000	0.0108	1.0000	0.6769	0.3792	0.0108	0.0135	0.0007	0.0024	0.3809		0.9851	0.0008	0.0026	0.0158	0.0000	0.0000
CH4		0.0000	0.0000	0.0000	0.0005	0.0009	0.0000	0.0000	0.0000	0.0000	0.0008		0.0000	0.0009	0.0004	0.0004	0.0000	0.0000
H2S		0.0000	0.0000	0.0000	0.0000	0.0000	0.0000	0.0000	0.0000	0.0000	0.0053		0.0000	0.0062	0.0071	0.3540	0.0000	0.0000
NH3		0.0000	0.0000	0.0000	0.0000	0.0000	0.0000	0.0000	0.0000	0.0000	0.0015		0.0003	0.0017	0.0000	0.0000	0.0000	0.0000
COS		0.0000	0.0000	0.0000	0.0000	0.0000	0.0000	0.0000	0.0000	0.0000	0.0001		0.0000	0.0000	0.0000	0.0005	0.0000	0.0000
HCL		0.0000	0.0000	0.0000	0.0000	0.0000	0.0000	0.0000	0.0000	0.0000	0.0000		0.0146	0.0000	0.0000	0.0000	0.0000	0.0000
SO2		0.0000	0.0000	0.0000	0.0000	0.0000	0.0000	0.0000	0.0000	0.0000	0.0000		0.0000	0.0000	0.0000	0.0000	0.0000	0.0000
Total		1.0000	1.0000	1.0000	1.0000	1.0000	1.0000	1.0000	1.0000	1.0000	1.0000		1.0000	1.0000	1.0000	1.0000	1.0000	1.0000

Table 1 (Cont'd) – Case 1A Stream Data

Stream No.	19	20	21	22	23	24	25	26	27	28	29	30	31	32	33	34	35	36
Temperature C	35	185	15	557	127	416	448	428	598	663	598	630	650	592	200	126	40	27
Pressure bar	46.68	31.72	1.01	1.05	0.99	17.38	17.38	17.38	17.17	16.83	17.17	1.53	1.41	1.30	1.28	1.26	1.01	1.01
Vapor Frac	1.00	1.00	1.00	1.00	1.00	1.00	1.00	1.00	1.00	1.00	1.00	1.00	1.00	1.00	1.00	-	1.00	1.00
Mole Flow kmol/hr	17,259	27,378	109,350	140,943	140,943	17,904	10,042	27,947	27,947	22,174	5,773	765	6,423	6,423	6,423	744	5,883	
Mass Flow kg/hr	85,876	271,391	3,154,735	3,759,006	3,759,006	516,541	289,712	806,253	806,253	622,573	183,688	10,552	194,243	194,243	194,243	194,243	13,399	184,526
Fluid Mole Fractions																		
O2	0.0000	0.0000	0.2076	0.0918	0.0918	0.2076	0.2076	0.2076	0.2076	0.0131	0.9547	0.0000	0.8401	0.8401	0.8401	0.8401	0.0000	0.9171
N2	0.0208	0.0129	0.7719	0.6976	0.6976	0.7719	0.7719	0.7719	0.7719	0.9614	0.0441	0.0067	0.0404	0.0404	0.0404	0.0404	0.0000	0.0441
AR	0.0002	0.0001	0.0094	0.0085	0.0085	0.0094	0.0094	0.0094	0.0094	0.0117	0.0005	0.0001	0.0005	0.0005	0.0005	0.0005	0.0000	0.0005
H2	0.9134	0.5675	0.0000	0.0000	0.0000	0.0000	0.0000	0.0000	0.0000	0.0000	0.0000	0.2954	0.0000	0.0000	0.0000	0.0000	0.0000	0.0000
CO	0.0174	0.0108	0.0000	0.0000	0.0000	0.0000	0.0000	0.0000	0.0000	0.0000	0.0000	0.0056	0.0000	0.0000	0.0000	0.0000	0.0000	0.0000
CO2	0.0458	0.0285	0.0003	0.0081	0.0081	0.0003	0.0003	0.0003	0.0003	0.0004	0.0000	0.0148	0.0025	0.0025	0.0025	0.0025	0.0000	0.0027
H2O	0.0009	0.3792	0.0108	0.1940	0.1940	0.0108	0.0108	0.0108	0.0108	0.0135	0.0006	0.6769	0.1164	0.1164	0.1164	0.1164	1.0000	0.0354
CH4	0.0015	0.0009	0.0000	0.0000	0.0000	0.0000	0.0000	0.0000	0.0000	0.0000	0.0000	0.0005	0.0000	0.0000	0.0000	0.0000	0.0000	0.0000
H2S	0.0000	0.0000	0.0000	0.0000	0.0000	0.0000	0.0000	0.0000	0.0000	0.0000	0.0000	0.0000	0.0000	0.0000	0.0000	0.0000	0.0000	0.0000
NH3	0.0000	0.0000	0.0000	0.0000	0.0000	0.0000	0.0000	0.0000	0.0000	0.0000	0.0000	0.0000	0.0000	0.0000	0.0000	0.0000	0.0000	0.0000
COS	0.0000	0.0000	0.0000	0.0000	0.0000	0.0000	0.0000	0.0000	0.0000	0.0000	0.0000	0.0000	0.0000	0.0000	0.0000	0.0000	0.0000	0.0000
HCL	0.0000	0.0000	0.0000	0.0000	0.0000	0.0000	0.0000	0.0000	0.0000	0.0000	0.0000	0.0000	0.0000	0.0000	0.0000	0.0000	0.0000	0.0000
SO2	0.0000	0.0000	0.0000	0.0000	0.0000	0.0000	0.0000	0.0000	0.0000	0.0000	0.0000	0.0000	0.0000	0.0000	0.0000	0.0000	0.0000	0.0000
Total	1.0000	1.0000	1.0000	1.0000	1.0000	1.0000	1.0000	1.0000	1.0000	1.0000	1.0000	1.0000	1.0000	1.0000	1.0000	1.0000	1.0000	1.0000



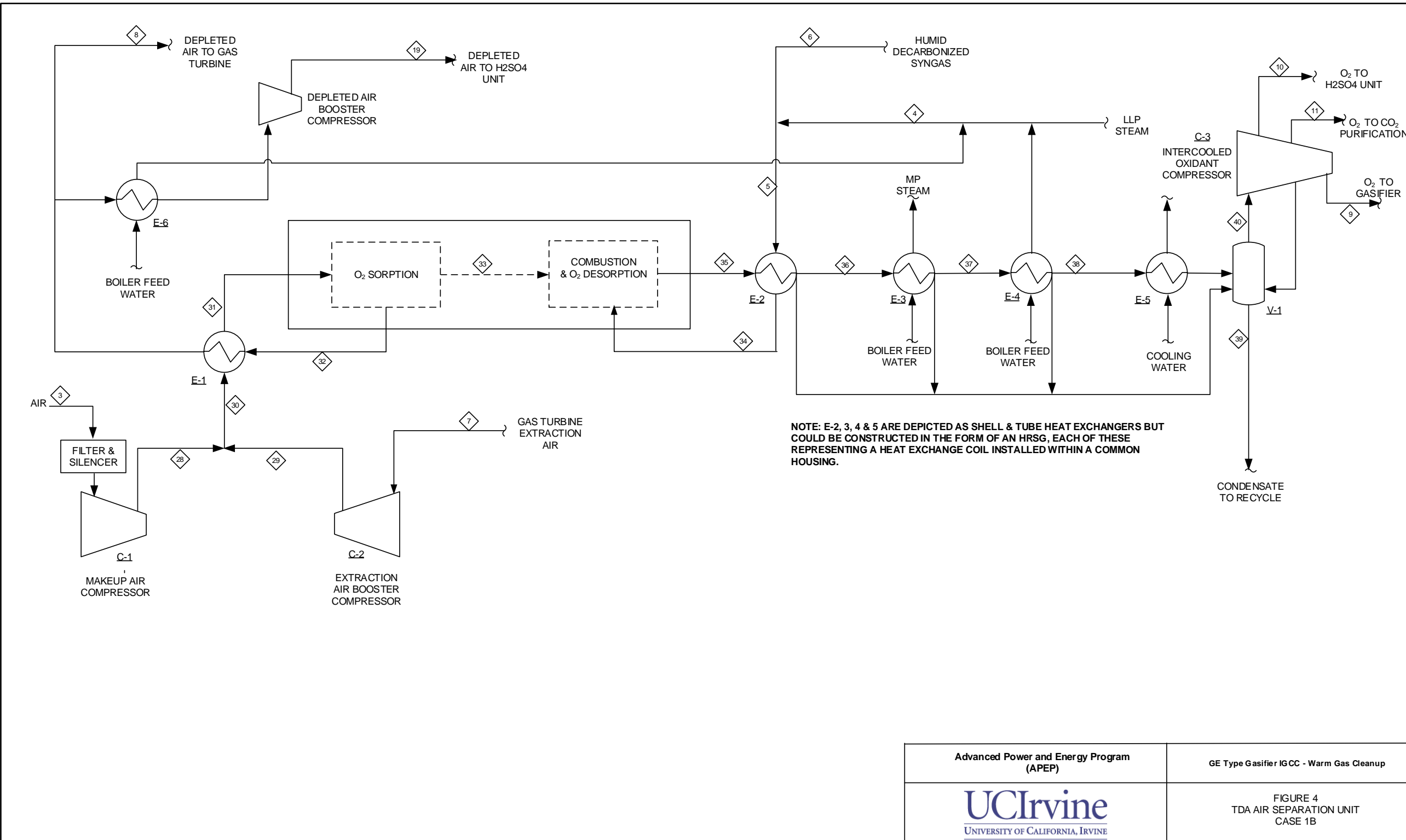
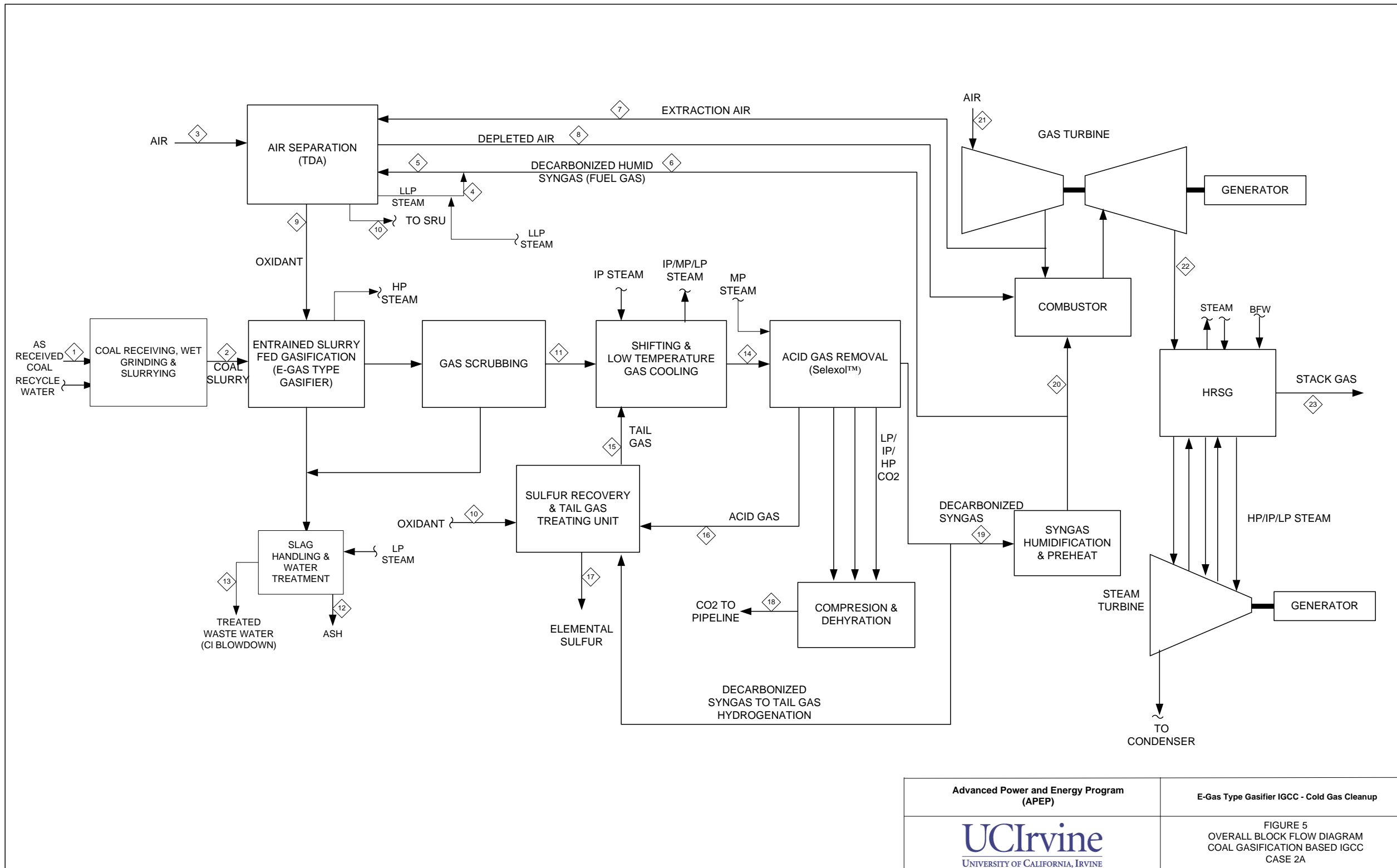


Table 2 – Case 1B Stream Data

Stream number	1	2	3	4	5	6	7	8	9	10	11	12	13	14	15	16	17	18	19	20
Temperature C	15	77	15	115	143	195	430	448	77	19	127	206	0	57	15	417	198	15	281	20
Pressure bar	1.01	72.39	1.01	1.68	1.61	31.72	16.03	16.48	64.81	8.58	20.50	53.61	1.01	3.10	1.01	1.03	49.12	1.01	41.20	1.01
Vapor Frac			1.00	1.00	1.00	1.00	1.00	1.00	1.00	1.00	1.00	1.00		0.01	1.00	1.00	1.00	1.00	0.00	
Mole Flow kmol/hr			17,760	442	868	426	10,908	22,457	5,595	106	112	32,177		1,270	1,314	2,094	39,027	532	303	195
Mass Flow kg/hr	224,171	316,313	512,371	7,966	12,354	4,388	314,700	630,512	178,230	3,368	3,560	627,097	19,165	28,657	37,904	64,997	747,709	15,359	8,510	17,485
Fluid Mole Fractions																				
O2			0.2076	0.0000	0.0000	0.0000	0.2076	0.0131	0.9524	0.9508	0.9508	0.0000		0.0000	0.2076	0.0473	0.0000	0.2077	0.0131	0.0000
N2			0.7719	0.0000	0.0053	0.0108	0.7719	0.9614	0.0434	0.0434	0.0434	0.0099		0.0000	0.7719	0.8279	0.0082	0.7722	0.9614	0.0000
AR			0.0094	0.0000	0.0000	0.0001	0.0094	0.0117	0.0005	0.0005	0.0005	0.0001		0.0000	0.0094	0.0100	0.0001	0.0094	0.0117	0.0000
H2			0.0000	0.0000	0.2668	0.5436	0.0000	0.0000	0.0000	0.0000	0.0000	0.2471		0.0000	0.0000	0.0000	0.4113	0.0000	0.0000	0.0000
CO			0.0000	0.0000	0.0048	0.0097	0.0000	0.0000	0.0000	0.0000	0.0000	0.2606		0.0000	0.0000	0.0000	0.0074	0.0000	0.0000	0.0000
CO2			0.0003	0.0000	0.0147	0.0299	0.0003	0.0004	0.0030	0.0030	0.0030	0.1013		0.0000	0.0003	0.0008	0.2912	0.0003	0.0004	0.0000
H2O			0.0108	1.0000	0.7080	0.4049	0.0108	0.0135	0.0007	0.0024	0.0024	0.3732		0.9851	0.0108	0.0306	0.2803	0.0104	0.0135	0.1040
CH4			0.0000	0.0000	0.0004	0.0009	0.0000	0.0000	0.0000	0.0000	0.0000	0.0008		0.0000	0.0000	0.0000	0.0007	0.0000	0.0000	0.0000
H2S			0.0000	0.0000	0.0000	0.0000	0.0000	0.0000	0.0000	0.0000	0.0000	0.0053		0.0000	0.0000	0.0000	0.0000	0.0000	0.0000	0.0000
NH3			0.0000	0.0000	0.0000	0.0001	0.0000	0.0000	0.0000	0.0000	0.0000	0.0015		0.0003	0.0000	0.0000	0.0009	0.0000	0.0000	0.0000
COS			0.0000	0.0000	0.0000	0.0000	0.0000	0.0000	0.0000	0.0000	0.0000	0.0001		0.0000	0.0000	0.0000	0.0000	0.0000	0.0000	0.0000
HCL			0.0000	0.0000	0.0000	0.0000	0.0000	0.0000	0.0000	0.0000	0.0000	0.0000		0.0146	0.0000	0.0000	0.0000	0.0000	0.0000	0.0000
HCN			0.0000	0.0000	0.0000	0.0000	0.0000	0.0000	0.0000	0.0000	0.0000	0.0000		0.0000	0.0000	0.0000	0.0000	0.0000	0.0000	0.0000
SO2			0.0000	0.0000	0.0000	0.0000	0.0000	0.0000	0.0000	0.0000	0.0000	0.0000		0.0000	0.0000	0.0835	0.0000	0.0000	0.0000	0.0000
H2SO4			0.0000	0.0000	0.0000	0.0000	0.0000	0.0000	0.0000	0.0000	0.0000	0.0000		0.0000	0.0000	0.0000	0.0000	0.0000	0.0000	0.8960
Total			1.0000	1.0000	1.0000	1.0000	1.0000	1.0000	1.0000	1.0000	1.0000	1.0000		1.0000	1.0000	1.0000	1.0000	1.0000	1.0000	1.0000

Table 2 (Cont'd) – Case 1B Stream Data

Stream number	21	22	23	24	25	26	27	28	29	30	31	32	33	34	35	36	37	38	39	40	
Temperature C	43	27	202	195	15	558	126	416	448	428	598	663	598	630	650	586	198	126	41	27	
Pressure bar	1.01	152.70	47.90	31.72	1.01	1.05	0.98	17.38	17.38	17.38	17.17	16.83	17.17	1.54	1.43	1.32	1.30	1.27	1.01	1.01	
Vapor Frac	1.00	0.00	0.95	1.00	1.00	1.00	1.00	1.00	1.00	1.00	1.00	1.00	1.00	1.00	1.00	1.00	1.00	0.00	1.00		
Mole Flow kmol/hr	1,913	10,506	29,146	28,720	109,350	141,673	141,673	17,760	10,908	28,668	28,668	22,760	5,908	868	6,659	6,659	6,659	858	6,022		
Mass Flow kg/hr	53,937	462,241	300,211	295,823	3,154,735	3,766,369	3,766,369	512,371	314,700	827,071	827,071	639,022	188,049	12,354	200,403	200,403	200,403	200,403	15,452	188,926	
Fluid Mole Fractions																					
O2	0.0587	0.0000	0.0000	0.0000	0.2076	0.0899	0.0899	0.2076	0.2076	0.2076	0.2076	0.0131	0.9569	0.0000	0.8313	0.8313	0.8313	0.8313	0.0000	0.9192	
N2	0.9087	0.0009	0.0108	0.0108	0.7719	0.6909	0.6909	0.7719	0.7719	0.7719	0.7719	0.9614	0.0419	0.0053	0.0379	0.0379	0.0379	0.0379	0.0000	0.0419	
AR	0.0110	0.0000	0.0001	0.0001	0.0094	0.0084	0.0084	0.0094	0.0094	0.0094	0.0094	0.0117	0.0005	0.0000	0.0005	0.0005	0.0005	0.0005	0.0000	0.0005	
H2	0.0000	0.0000	0.5436	0.5436	0.0000	0.0000	0.0000	0.0000	0.0000	0.0000	0.0000	0.0000	0.2668	0.0000	0.0000	0.0000	0.0000	0.0000	0.0000	0.0000	
CO	0.0000	0.0000	0.0097	0.0097	0.0000	0.0000	0.0000	0.0000	0.0000	0.0000	0.0000	0.0000	0.0048	0.0000	0.0000	0.0000	0.0000	0.0000	0.0000	0.0000	
CO2	0.0010	0.9991	0.0299	0.0299	0.0003	0.0085	0.0085	0.0003	0.0003	0.0003	0.0003	0.0004	0.0000	0.0147	0.0026	0.0026	0.0026	0.0026	0.0000	0.0029	
H2O	0.0205	0.0000	0.4049	0.4049	0.0108	0.2023	0.2023	0.0108	0.0108	0.0108	0.0108	0.0135	0.0006	0.7080	0.1277	0.1277	0.1277	0.1277	0.1277	0.1000	0.0354
CH4	0.0000	0.0000	0.0009	0.0009	0.0000	0.0000	0.0000	0.0000	0.0000	0.0000	0.0000	0.0000	0.0004	0.0000	0.0000	0.0000	0.0000	0.0000	0.0000	0.0000	
H2S	0.0000	0.0000	0.0000	0.0000	0.0000	0.0000	0.0000	0.0000	0.0000	0.0000	0.0000	0.0000	0.0000	0.0000	0.0000	0.0000	0.0000	0.0000	0.0000	0.0000	
NH3	0.0000	0.0000	0.0001	0.0001	0.0000	0.0000	0.0000	0.0000	0.0000	0.0000	0.0000	0.0000	0.0000	0.0000	0.0000	0.0000	0.0000	0.0000	0.0000	0.0000	
COS	0.0000	0.0000	0.0000	0.0000	0.0000	0.0000	0.0000	0.0000	0.0000	0.0000	0.0000	0.0000	0.0000	0.0000	0.0000	0.0000	0.0000	0.0000	0.0000	0.0000	
HCL	0.0000	0.0000	0.0000	0.0000	0.0000	0.0000	0.0000	0.0000	0.0000	0.0000	0.0000	0.0000	0.0000	0.0000	0.0000	0.0000	0.0000	0.0000	0.0000	0.0000	
HCN	0.0000	0.0000	0.0000	0.0000	0.0000	0.0000	0.0000	0.0000	0.0000	0.0000	0.0000	0.0000	0.0000	0.0000	0.0000	0.0000	0.0000	0.0000	0.0000	0.0000	
SO2	0.0002	0.0000	0.0000	0.0000	0.0000	0.0000	0.0000	0.0000	0.0000	0.0000	0.0000	0.0000	0.0000	0.0000	0.0000	0.0000	0.0000	0.0000	0.0000	0.0000	
H2SO4	0.0000	0.0000	0.0000	0.0000	0.0000	0.0000	0.0000	0.0000	0.0000	0.0000	0.0000	0.0000	0.0000	0.0000	0.0000	0.0000	0.0000	0.0000	0.0000	0.0000	
Total	1.0000	1.0000	1.0000	1.0000	1.0000	1.0000	1.0000	1.0000	1.0000	1.0000	1.0000	1.0000	1.0000	1.0000	1.0000	1.0000	1.0000	1.0000	1.0000	1.0000	



Advanced Power and Energy Program
(APEP)

E-Gas Type Gasifier IGCC - Cold Gas Cleanup

UCIrvine
UNIVERSITY OF CALIFORNIA, IRVINE

FIGURE 5
OVERALL BLOCK FLOW DIAGRAM
COAL GASIFICATION BASED IGCC
CASE 2A

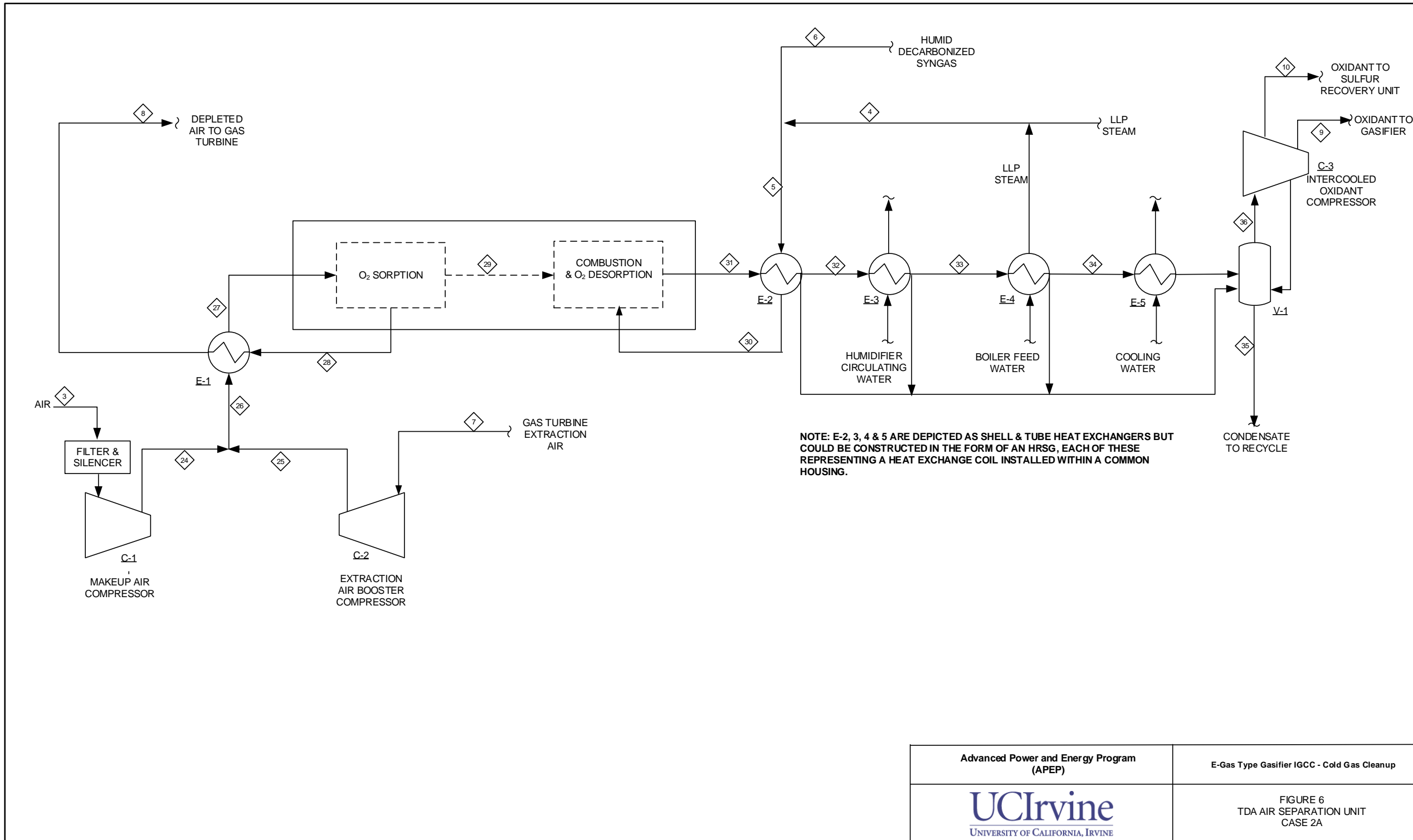
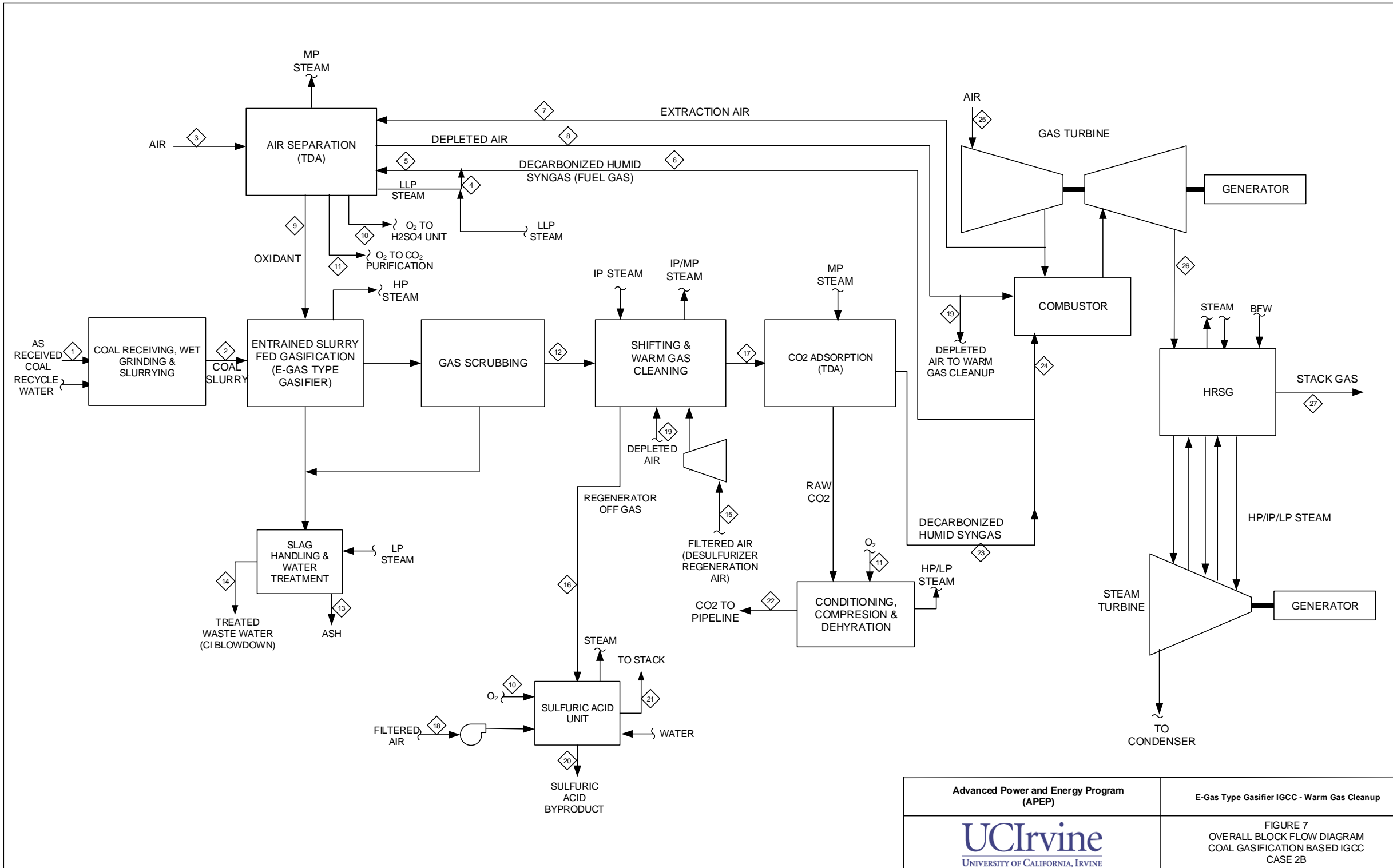


Table 3 – Case 2A Stream Data

Stream No.	1	2	3	4	5	6	7	8	9	10	11	12	13	14	15	16	17	18
Temperature C	15	76	15	114	178	211	430	447	69	19	184	60	58	27	158	48	174	27
Pressure bar	1.01	58.61	1.01	1.61	1.54	30.81	16.04	16.48	50.33	8.58	38.78	1.01	3.10	33.96	52.92	2.45	1.45	152.70
Vapor Frac			1.00	1.00	1.00	1.00	1.00	1.00	1.00	1.00	1.00	0.01	1.00	1.00	1.00	1.00	-	
Mole Flow kmol/hr			17,792	117	510	393	9,578	21,729	5,330	217	30,567		1,249	28,040	978	857	86	10,446
Mass Flow kg/hr	219,679	309,975	513,287	2,104	6,164	4,060	276,326	610,081	169,798	6,906	610,720	17,464	27,791	573,291	29,439	32,993	5,507	457,483
Fluid Mole Fractions																		
O2	0.0000	0.2076	0.0000	0.0000	0.0000	0.2076	0.0131	0.9521	0.9506	0.0000		0.0000	0.0000	0.0000	0.0000	0.0000	0.0000	0.0000
N2	0.0000	0.7719	0.0000	0.0094	0.0121	0.7719	0.9614	0.0435	0.0434	0.0097		0.0000	0.0123	0.0694	0.0008	0.0000	0.0001	
AR	0.0000	0.0094	0.0000	0.0001	0.0001	0.0094	0.0117	0.0005	0.0005	0.0001		0.0000	0.0001	0.0002	0.0000	0.0000	0.0000	0.0000
H2	0.0000	0.0000	0.0000	0.4011	0.5202	0.0000	0.0000	0.0000	0.0000	0.2585		0.0000	0.5299	0.2541	0.0555	0.0000	0.0044	
CO	0.0000	0.0000	0.0000	0.0085	0.0110	0.0000	0.0000	0.0000	0.0000	0.2600		0.0000	0.0113	0.0622	0.0020	0.0000	0.0003	
CO2	0.0000	0.0003	0.0000	0.0127	0.0164	0.0003	0.0004	0.0030	0.0030	0.1286		0.0000	0.4068	0.5264	0.6457	0.0000	0.9944	
H2O	1.0000	0.0108	1.0000	0.5564	0.4248	0.0108	0.0135	0.0008	0.0024	0.3082		0.9820	0.0009	0.0029	0.0093	0.0000	0.0000	
CH4	0.0000	0.0000	0.0000	0.0118	0.0153	0.0000	0.0000	0.0000	0.0000	0.0152		0.0000	0.0159	0.0127	0.0043	0.0000	0.0008	
H2S	0.0000	0.0000	0.0000	0.0000	0.0000	0.0000	0.0000	0.0000	0.0000	0.0057		0.0000	0.0086	0.0711	0.2811	0.0000	0.0000	
NH3	0.0000	0.0000	0.0000	0.0000	0.0000	0.0000	0.0000	0.0000	0.0000	0.0138		0.0035	0.0141	0.0000	0.0000	0.0000	0.0000	
COS	0.0000	0.0000	0.0000	0.0000	0.0000	0.0000	0.0000	0.0000	0.0000	0.0003		0.0000	0.0000	0.0010	0.0014	0.0000	0.0000	
HCL	0.0000	0.0000	0.0000	0.0000	0.0000	0.0000	0.0000	0.0000	0.0000	0.0000		0.0146	0.0000	0.0000	0.0000	0.0000	0.0000	
SO2	0.0000	0.0000	0.0000	0.0000	0.0000	0.0000	0.0000	0.0000	0.0000	0.0000		0.0000	0.0000	0.0000	0.0000	0.0000	0.0000	
Total	1.0000	1.0000	1.0000	1.0000	1.0000	1.0000	1.0000	1.0000	1.0000	1.0000		1.0000	1.0000	1.0000	1.0000	1.0000	1.0000	

Table 3 (Cont'd) – Case 2A Stream Data

Stream No.	20	21	22	23	24	25	26	27	28	29	30	31	32	33	34	35	36
Temperature C	211	15	559	127	416	448	427	598	663	598	630	650	612	150	125	64	27
Pressure bar	30.81	1.01	1.05	0.98	17.38	17.38	17.38	17.17	16.83	17.17	1.47	1.36	1.25	1.23	1.21	1.18	1.01
Vapor Frac	1.00	1.00	1.00	1.00	1.00	1.00	1.00	1.00	1.00	1.00	1.00	1.00	1.00	1.00	1.00	-	1.00
Mole Flow kmol/hr	27,335	109,350	141,576	141,576	17,792	9,578	27,370	27,370	21,729	5,641	510	6,046	6,046	6,046	6,046	499	5,571
Mass Flow kg/hr	282,161	3,154,735	3,770,662	3,770,662	513,287	276,326	789,613	789,613	610,081	179,532	6,164	185,696	185,696	185,696	185,696	8,993	177,132
Fluid Mole Fractions																	
O2	0.0000	0.2076	0.0911	0.0911	0.2076	0.2076	0.2076	0.0131	0.9569	0.0000	0.8735	0.8735	0.8735	0.8735	0.0000	0.9480	
N2	0.0121	0.7719	0.6939	0.6939	0.7719	0.7719	0.7719	0.7719	0.9614	0.0419	0.0094	0.0399	0.0399	0.0399	0.0399	0.0000	0.0433
AR	0.0001	0.0094	0.0084	0.0084	0.0094	0.0094	0.0094	0.0117	0.0005	0.0001	0.0005	0.0005	0.0005	0.0005	0.0005	0.0000	0.0005
H2	0.5202	0.0000	0.0000	0.0000	0.0000	0.0000	0.0000	0.0000	0.0000	0.4011	0.0000	0.0000	0.0000	0.0000	0.0000	0.0000	0.0000
CO	0.0110	0.0000	0.0000	0.0000	0.0000	0.0000	0.0000	0.0000	0.0000	0.0085	0.0000	0.0000	0.0000	0.0000	0.0000	0.0000	0.0000
CO2	0.0164	0.0003	0.0085	0.0085	0.0003	0.0003	0.0003	0.0004	0.0000	0.0127	0.0028	0.0028	0.0028	0.0028	0.0000	0.0030	
H2O	0.4248	0.0108	0.1980	0.1980	0.0108	0.0108	0.0108	0.0108	0.0135	0.0006	0.5564	0.0833	0.0833	0.0833	0.0833	1.0000	0.0051
CH4	0.0153	0.0000	0.0000	0.0000	0.0000	0.0000	0.0000	0.0000	0.0000	0.0118	0.0000	0.0000	0.0000	0.0000	0.0000	0.0000	
H2S	0.0000	0.0000	0.0000	0.0000	0.0000	0.0000	0.0000	0.0000	0.0000	0.0000	0.0000	0.0000	0.0000	0.0000	0.0000	0.0000	
NH3	0.0000	0.0000	0.0000	0.0000	0.0000	0.0000	0.0000	0.0000	0.0000	0.0000	0.0000	0.0000	0.0000	0.0000	0.0000	0.0000	
COS	0.0000	0.0000	0.0000	0.0000	0.0000	0.0000	0.0000	0.0000	0.0000	0.0000	0.0000	0.0000	0.0000	0.0000	0.0000	0.0000	
HCL	0.0000	0.0000	0.0000	0.0000	0.0000	0.0000	0.0000	0.0000	0.0000	0.0000	0.0000	0.0000	0.0000	0.0000	0.0000	0.0000	
SO2	0.0000	0.0000	0.0000	0.0000	0.0000	0.0000	0.0000	0.0000	0.0000	0.0000	0.0000	0.0000	0.0000	0.0000	0.0000	0.0000	
Total	1.0000	1.0000	1.0000	1.0000	1.0000	1.0000	1.0000	1.0000	1.0000	1.0000	1.0000	1.0000	1.0000	1.0000	1.0000	1.0000	



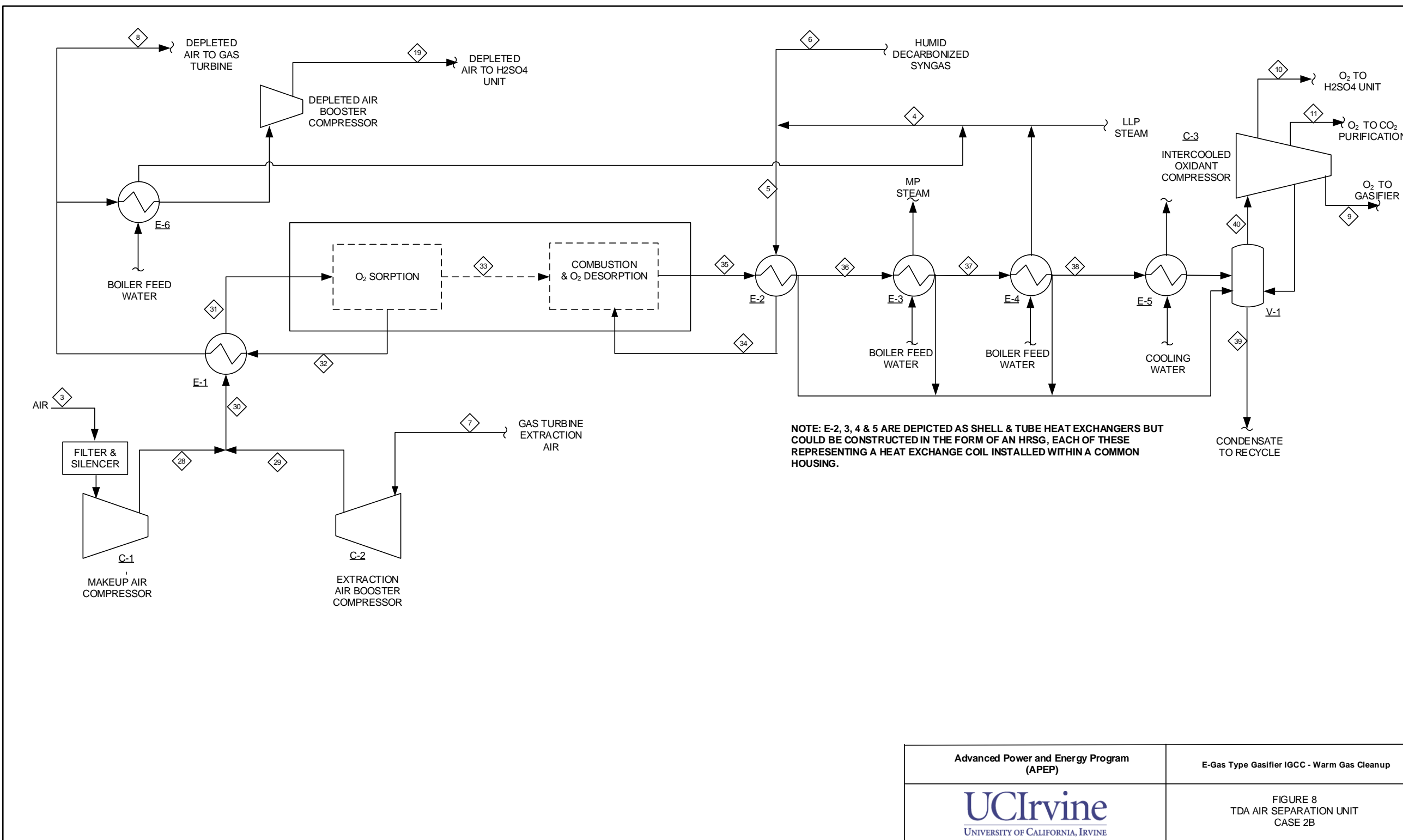


Table 4 – Case 2B Stream Data

Stream number	1	2	3	4	5	6	7	8	9	10	11	12	13	14	15	16	17	18	19	20
Temperature C	15	76	15	115	145	203	430	445	77	19	127	185	60	58	15	459	198	15	281	20
Pressure bar	1.01	58.61	1.01	1.67	1.61	32.89	16.06	16.48	64.81	8.58	20.50	38.78	1.01	3.10	1.01	1.03	34.30	1.01	41.20	1.01
Vapor Frac			1.00	1.00	1.00	1.00	1.00	1.00	1.00	1.00	1.00	1.00	0.01	1.00	1.00	1.00	1.00	1.00	0.00	
Mole Flow kmol/hr			19,058	415	771	356	7,741	20,979	5,253	104	73	29,707		1,247	1,289	2,064	35,014	522	297	195
Mass Flow kg/hr	219,805	310,153	549,826	7,476	11,045	3,569	223,314	589,031	167,335	3,296	2,328	603,235	17,474	27,770	37,194	63,894	691,925	15,063	8,351	17,216
Fluid Mole Fractions																				
O2			0.2076	0.0000	0.0000	0.0000	0.2076	0.0131	0.9524	0.9508	0.9508	0.0000		0.0000	0.2076	0.0443	0.0000	0.2077	0.0131	0.0000
N2			0.7719	0.0000	0.0049	0.0107	0.7719	0.9614	0.0434	0.0433	0.0433	0.0100		0.0000	0.7719	0.8259	0.0080	0.7722	0.9614	0.0000
AR			0.0094	0.0000	0.0000	0.0001	0.0094	0.0117	0.0005	0.0005	0.0005	0.0001		0.0000	0.0094	0.0099	0.0001	0.0094	0.0117	0.0000
H2			0.0000	0.0000	0.2416	0.5229	0.0000	0.0000	0.0000	0.0000	0.0000	0.2447		0.0000	0.0000	0.0000	0.3907	0.0000	0.0000	0.0000
CO			0.0000	0.0000	0.0045	0.0098	0.0000	0.0000	0.0000	0.0000	0.0000	0.2553		0.0000	0.0000	0.0000	0.0073	0.0000	0.0000	0.0000
CO2			0.0003	0.0000	0.0037	0.0081	0.0003	0.0004	0.0030	0.0030	0.0030	0.1348		0.0000	0.0003	0.0006	0.3034	0.0003	0.0004	0.0000
H2O			0.0108	1.0000	0.7326	0.4213	0.0108	0.0135	0.0007	0.0024	0.0024	0.3162		0.9836	0.0108	0.0361	0.2660	0.0104	0.0135	0.1224
CH4			0.0000	0.0000	0.0126	0.0272	0.0000	0.0000	0.0000	0.0000	0.0000	0.0255		0.0000	0.0000	0.0000	0.0203	0.0000	0.0000	0.0000
H2S			0.0000	0.0000	0.0000	0.0000	0.0000	0.0000	0.0000	0.0000	0.0000	0.0059		0.0000	0.0000	0.0000	0.0000	0.0000	0.0000	0.0000
NH3			0.0000	0.0000	0.0000	0.0000	0.0000	0.0000	0.0000	0.0000	0.0000	0.0072		0.0018	0.0000	0.0000	0.0043	0.0000	0.0000	0.0000
COS			0.0000	0.0000	0.0000	0.0000	0.0000	0.0000	0.0000	0.0000	0.0000	0.0003		0.0000	0.0000	0.0000	0.0000	0.0000	0.0000	0.0000
HCL			0.0000	0.0000	0.0000	0.0000	0.0000	0.0000	0.0000	0.0000	0.0000	0.0000		0.0146	0.0000	0.0000	0.0000	0.0000	0.0000	0.0000
HCN			0.0000	0.0000	0.0000	0.0000	0.0000	0.0000	0.0000	0.0000	0.0000	0.0000		0.0000	0.0000	0.0000	0.0000	0.0000	0.0000	0.0000
SO2			0.0000	0.0000	0.0000	0.0000	0.0000	0.0000	0.0000	0.0000	0.0000	0.0000		0.0000	0.0000	0.0831	0.0000	0.0000	0.0000	0.0000
H2SO4			0.0000	0.0000	0.0000	0.0000	0.0000	0.0000	0.0000	0.0000	0.0000	0.0000		0.0000	0.0000	0.0000	0.0000	0.0000	0.0000	0.8776
Total			1.0000	1.0000	1.0000	1.0000	1.0000	1.0000	1.0000	1.0000	1.0000	1.0000		1.0000	1.0000	1.0000	1.0000	1.0000	1.0000	1.0000

Table 4 (Cont'd) – Case 2B Stream Data

Stream number	21	22	23	24	25	26	27	28	29	30	31	32	33	34	35	36	37	38	39	40
Temperature C	43	27	203	203	15	560	125	416	448	425	597	663	597	630	650	589	198	126	41	27
Pressure bar	1.01	152.70	32.89	32.89	1.01	1.05	0.98	17.38	17.38	17.38	17.17	16.83	17.17	1.54	1.42	1.31	1.29	1.27	1.01	1.01
Vapor Frac	1.00	0.00	1.00	1.00	1.00	1.00	1.00	1.00	1.00	1.00	1.00	1.00	1.00	1.00	1.00	1.00	1.00	0.00	1.00	
Mole Flow kmol/hr	1,882	10,426	25,944	25,587	109,350	141,362	141,362	19,058	7,741	26,799	26,799	21,276	5,523	771	6,200	6,200	6,200	781	5,625	
Mass Flow kg/hr	52,971	458,745	259,799	256,230	3,154,735	3,776,702	3,776,702	549,826	223,314	773,140	773,140	597,348	175,787	11,045	186,832	186,832	186,832	14,076	176,478	
Fluid Mole Fractions																				
O2	0.0554	0.0000	0.0000	0.0000	0.2076	0.0931	0.0931	0.2076	0.2076	0.2076	0.0131	0.9569	0.0000	0.8341	0.8341	0.8341	0.8341	0.0000	0.9193	
N2	0.9081	0.0005	0.0107	0.0107	0.7719	0.6994	0.6994	0.7719	0.7719	0.7719	0.9614	0.0419	0.0049	0.0380	0.0380	0.0380	0.0380	0.0000	0.0419	
AR	0.0109	0.0000	0.0001	0.0001	0.0094	0.0085	0.0085	0.0094	0.0094	0.0094	0.0094	0.0117	0.0005	0.0000	0.0005	0.0005	0.0005	0.0000	0.0005	
H2	0.0000	0.0000	0.5229	0.5229	0.0000	0.0000	0.0000	0.0000	0.0000	0.0000	0.0000	0.0000	0.2416	0.0000	0.0000	0.0000	0.0000	0.0000	0.0000	
CO	0.0000	0.0000	0.0098	0.0098	0.0000	0.0000	0.0000	0.0000	0.0000	0.0000	0.0000	0.0000	0.0045	0.0000	0.0000	0.0000	0.0000	0.0000	0.0000	
CO2	0.0008	0.9995	0.0081	0.0081	0.0003	0.0084	0.0084	0.0003	0.0003	0.0003	0.0003	0.0004	0.0000	0.0037	0.0026	0.0026	0.0026	0.0026	0.0026	
H2O	0.0245	0.0000	0.4213	0.4213	0.0108	0.1905	0.1905	0.0108	0.0108	0.0108	0.0108	0.0135	0.0006	0.7326	0.1249	0.1249	0.1249	0.1249	0.1249	
CH4	0.0000	0.0000	0.0272	0.0272	0.0000	0.0000	0.0000	0.0000	0.0000	0.0000	0.0000	0.0000	0.0126	0.0000	0.0000	0.0000	0.0000	0.0000	0.0000	
H2S	0.0000	0.0000	0.0000	0.0000	0.0000	0.0000	0.0000	0.0000	0.0000	0.0000	0.0000	0.0000	0.0000	0.0000	0.0000	0.0000	0.0000	0.0000	0.0000	
NH3	0.0000	0.0000	0.0000	0.0000	0.0000	0.0000	0.0000	0.0000	0.0000	0.0000	0.0000	0.0000	0.0000	0.0000	0.0000	0.0000	0.0000	0.0000	0.0000	
COS	0.0000	0.0000	0.0000	0.0000	0.0000	0.0000	0.0000	0.0000	0.0000	0.0000	0.0000	0.0000	0.0000	0.0000	0.0000	0.0000	0.0000	0.0000	0.0000	
HCL	0.0000	0.0000	0.0000	0.0000	0.0000	0.0000	0.0000	0.0000	0.0000	0.0000	0.0000	0.0000	0.0000	0.0000	0.0000	0.0000	0.0000	0.0000	0.0000	
HCN	0.0000	0.0000	0.0000	0.0000	0.0000	0.0000	0.0000	0.0000	0.0000	0.0000	0.0000	0.0000	0.0000	0.0000	0.0000	0.0000	0.0000	0.0000	0.0000	
SO2	0.0002	0.0000	0.0000	0.0000	0.0000	0.0000	0.0000	0.0000	0.0000	0.0000	0.0000	0.0000	0.0000	0.0000	0.0000	0.0000	0.0000	0.0000	0.0000	
H2SO4	0.0000	0.0000	0.0000	0.0000	0.0000	0.0000	0.0000	0.0000	0.0000	0.0000	0.0000	0.0000	0.0000	0.0000	0.0000	0.0000	0.0000	0.0000	0.0000	
Total	1.0000	1.0000	1.0000	1.0000	1.0000	1.0000	1.0000	1.0000	1.0000	1.0000	1.0000	1.0000	1.0000	1.0000	1.0000	1.0000	1.0000	1.0000	1.0000	

Table 5 - Overall Plant Performance – IGCCs with Cold Gas Cleanup

CASE	1A	2A
GROSS POWER GENERATED (AT GENERATOR TERMINALS), kWe		
GAS TURBINE POWER	464,000	464,000
STEAM TURBINE POWER	258,428	237,948
SYNGAS EXPANDER POWER	8,779	-
TOTAL POWER, kWE	731,207	701,948
AUXILIARY LOAD SUMMARY, kWE		
COAL HANDLING	450	446
COAL MILLING	2,278	2,261
COAL SLURRY PUMPS	792	629
SLAG HANDLING & DEWATERING	1,130	1,114
AIR SEPARATION UNIT MAIN AIR COMPRESSOR	61,024	60,640
GAS TURBINE EXTRACTION AIR COMPRESSOR	1,702	1,560
OXYGEN COMPRESSOR	22,827	20,688
SYNGAS RECYCLE COMPRESSOR	-	1,269
TAIL GAS RECYCLE COMPRESSOR	1,718	5,915
CO2 COMPRESSOR	31,237	31,660
BOILER FEEDWATER & DEMIN PUMPS	4,616	5,746
VACUUM CONDENSATE PUMP	321	425
PROCESS CONDENSATE & SWS SYSTEMS	717	49
HUMIDIFIER & BFW CIRCULATING PUMPS	222	302
COOLING WATER CIRCULATING PUMPS	4,882	4,283
COOLING TOWER FANS	2,465	2,162
SCRUBBER PUMPS	72	396
SELEXOL UNIT	19,125	21,314
GAS TURBINE AUXILIARIES	1,000	1,000
STEAM TURBINE AUXILIARIES	112	104
CLAUS & TAIL GAS TREATING AUXILIARIES	205	203
MISCELLANEOUS BALANCE OF PLANT	2,922	3,042
TRANSFORMER LOSSES	2,708	2,600
TOTAL AUXILIARIES, kWE	162,523	167,807
NET POWER, kWE	568,684	534,141
% NET PLANT EFFICIENCY, % HHV	34.05	32.23
NET HEAT RATE		
KJ/KWH	10,574	11,169
BTU/KWH	10,022	10,587
CONDENSER COOLING DUTY		
10^6 KJ/H	1,455	1,223
10^6 BTU/H	1,379	1,159
CONSUMABLES		
AS-RECEIVED COAL FEED		
KG/H	221,412	219,679
LB/H	488,213	484,392
THERMAL INPUT, KWT HHV	1,669,897	1,656,828
RAW WATER USAGE		
M^3/MIN	20.05	23.16
GPM	5,298	6,120
CARBON CAPTURED, %	90	90

Table 6 - Overall Plant Performance – IGCCs with Warm Gas Cleanup

CASE	1B	2B
GROSS POWER GENERATED (AT GENERATOR TERMINALS), kWe		
GAS TURBINE POWER	464,000	464,000
STEAM TURBINE POWER	264,588	261,787
SYNGAS EXPANDER POWER	10,545	-
TOTAL POWER, kWE	739,133	725,787
AUXILIARY LOAD SUMMARY, kWE		
COAL HANDLING	455	446
COAL MILLING	2,307	2,262
COAL SLURRY PUMPS	756	662
SLAG HANDLING & DEWATERING	1,144	1,123
AIR SEPARATION UNIT MAIN AIR COMPRESSOR	60,532	64,957
OXYGEN & DEPLETED AIR COMPRESSORS	23,731	22,208
GT EXTRACTION AIR COMPRESSOR	1,793	1,243
SYNGAS RECYCLE COMPRESSOR	-	1,234
CO2 PURIFICATION & COMPRESSION	30,011	26,944
BOILER FEEDWATER & DEMIN PUMPS	4,932	5,422
VACUUM CONDENSATE PUMP	372	412
PROCESS CONDENSATE & SWS SYSTEMS	554	84
BFW CIRCULATING PUMPS	86	98
COOLING WATER CIRCULATING PUMPS	4,780	4,531
COOLING TOWER FANS	2,413	2,287
SCRUBBER PUMPS	72	395
DESULFURIZER UNIT	4,978	4,885
GAS TURBINE AUXILIARIES	1,000	1,000
STEAM TURBINE AUXILIARIES	115	114
H2SO4 UNIT	(3,968)	(3,736)
MISCELLANEOUS BALANCE OF PLANT	2,958	3,043
TRANSFORMER LOSSES	2,738	2,688
TOTAL AUXILIARIES, kWE	141,759	142,303
NET POWER, kWE	597,373	583,484
% NET PLANT EFFICIENCY, % HHV	35.33	35.20
NET HEAT RATE,		
KJ/KWH	10,189	10,228
BTU/KWH	9,657	9,694
CONDENSER COOLING DUTY		
10^6 KJ/H	1,589	1,498
10^6 BTU/H	1,506	1,420
CONSUMABLES		
AS-RECEIVED COAL FEED		
KG/H	224,171	219,805
LB/H	494,297	484,670
THERMAL INPUT, KWT HHV	1,690,706	1,657,778
RAW WATER USAGE		
M^3/MIN	23.55	22.78
GPM	6,223	6,018
CARBON CAPTURED, %	90	90

Table 7 - Plant Cost Summary (2011 \$1000) – IGCCs with Cold Gas Cleanup

CASE	1A	2A
ASU	148,622	141,460
Fuel receiving, preparation & feeding	114,692	111,764
Gasifier, syngas cooler & aux (Case 2 A includes syngas scrubber)	308,866	310,217
Gasification foundations	19,027	21,363
Ash handling	55,324	45,055
Soot Recovery + SARU	7,035	
Flare stack system (for Case 1 A, included in gasifier aux above)		3,700
Shift reactor	22,019	16,055
LTGC (Case 1A includes syngas scrubber, Case 2A includes syngas humidifier)	26,304	51,701
Blowback gas systems		1,636
Fuel gas piping	1,741	1,931
Gas cleanup foundations	1,811	1,964
Hg Removal	4,140	3,729
Selexol	256,553	255,802
Claus + TG Recycle	40,641	40,428
CO2 compression, dehydration + pumping	66,545	67,228
Syngas Expander	11,797	
Gas turbine + generator + auxiliaries	159,299	159,009
HRSG, ducting + stack	56,225	56,633
Steam turbine + generator + auxiliaries	83,886	79,887
Surface condenser	5,858	5,273
Feedwater system	19,143	27,648
Water makeup + pretreating	2,220	2,470
Other feedwater subsystems	3,997	4,030
Service water systems	7,191	7,094
Other boiler plant systems	8,154	8,128
Fuel oil system & nat gas	2,315	2,297
Waste water treatment	2,733	2,697
Misc. power plant equipment	3,119	3,043
Cooling water system	39,396	36,007
Accessory electric plant	106,706	105,993
Instrumentation & controls	32,989	32,444
Improvement to site	23,622	23,151
Buildings & structures	22,343	21,683
Total	1,664,315	1,651,517

Table 8 - Plant Cost Summary (2011 \$1000) – IGCCs with Warm Gas Cleanup

CASE	1B	2B
ASU	177,683	177,112
Fuel receiving, preparation & feeding	115,633	111,806
Gasifier, syngas cooler & aux (Case 2B includes syngas scrubber)	311,825	310,355
Gasification foundations	19,145	21,369
Ash handling systems	55,702	45,069
Soot Recovery + SARU	7,079	0
Flare stack system (for Case 1 B, included in gasifier aux above)	0	3,701
Warm gas desulfurization	34,858	34,418
H ₂ SO ₄ unit	76,355	75,537
Shift reactor	22,429	15,335
Syngas scrubber (for Case 2B, included in gasifier aux)	13,387	
Blowback gas systems	0	1,636
Fuel gas piping	2,539	2,694
Gas cleanup foundations	1,844	1,877
Trace contaminant removal	4,418	4,436
CO ₂ separation / recycle	156,969	141,082
CO ₂ purification / heat recovery	27,459	29,867
CO ₂ compression / drying / pumping	66,971	60,911
Syngas Expander	13,413	0
Gas turbine + generator + auxiliaries	159,299	159,009
HRSG, ducting + stack	56,667	56,862
Steam turbine + generator + auxiliaries	85,281	85,406
Surface condenser	6,234	6,091
Feedwater system	25,840	21,697
Water makeup + pretreating	2,489	2,441
Other feedwater subsystems	4,065	4,312
Service water systems	7,254	7,096
Other boiler plant systems	8,296	8,714
Fuel oil system & nat gas	2,315	2,297
Waste water treatment	2,758	2,698
Misc. power plant equipment	3,127	3,068
Cooling water system	38,802	37,493
Accessory electric plant	107,225	107,598
Instrumentation & controls	33,042	32,446
Improvement to site	23,646	23,152
Buildings & structures	22,371	21,685
Total	1,696,417	1,619,271

Table 9 - Process Economics

CASE	1A	1B	2A	2B
Net power, MW	569	597	534	583
Net efficiency, % HHV	34	35.33	32.23	35.20
Capacity factor (CF), %	80	80	80	80
Total plant cost (TPC), \$	1,664,314,918	1,696,416,960	1,651,517,116	1,619,271,109
6 month labor cost	15,663,392	15,992,802	15,621,324	15,412,414
1 month maintenance materials	2,759,060	2,840,628	2,748,643	2,696,913
1 month non-fuel consumables	822,579	1,204,070	882,800	1,154,424
1 month waste disposal	493,094	497,712	489,247	488,054
25% of 1 month fuel cost at 100% CF	3,056,093	3,094,175	3,032,174	3,033,914
2% of TPC	33,286,298	33,928,339	33,030,342	32,385,422
60 day supply of fuel & consumables at 100% CF	25,736,447	26,789,461	25,666,515	26,216,048
0.5% of TPC (spare parts)	8,321,575	8,482,085	8,257,586	8,096,356
Initial catalyst & chemicals cost, \$	23,833,053	21,163,514	23,848,019	19,863,479
Land	900,000	900,000	900,000	900,000
Other owners's costs (15% of TPC)	249,647,238	254,462,544	247,727,567	242,890,666
Financing costs	44,936,503	45,803,258	44,590,962	43,720,320
Total overnight cost (TOC), \$	2,073,770,249	2,111,575,546	2,058,312,295	2,016,129,119
Fixed operating cost for initial year of operation (OCF), \$	64,613,083	65,913,942	64,272,989	63,210,250
Annual feed cost at above CF for initial year (OCV1), \$	117,353,955	118,816,306	116,435,489	116,502,293
Other annual variable operating cost at above CF for initial year (OCV2), \$	39,117,431	43,607,132	39,558,625	41,658,151
Annual CO2 transporting, storing, and monitoring cost at above CF for initial year (OCV3), \$	32,109,618	32,363,737	31,668,370	31,735,198
Annual byproduct revenues at above CF for initial year (OCV4), \$	4,245,347	12,952,498	4,212,050	12,411,871
1st year cost of electricity (COE) w/o CO2 TS&M, \$/MWh	119.1	114.1	126.1	112.4
1st year cost of electricity (COE), \$/MWh	127.1	121.9	134.5	120.1
1st year CO2 capture cost without CO2 TS&M compared to corresponding IGCC (w/o CO2 capture), \$/tonne	22	17	33	18
1st year CO2 capture cost without CO2 TS&M compared to SCPC (w/o CO2 capture), \$/tonne	47	43	53	40
1st year CO2 avoided cost with CO2 TS&M compared to corresponding IGCC (w/o CO2 capture), \$/tonne	37	30	53	32
1st year CO2 avoided cost with CO2 TS&M compared to SCPC (w/o CO2 capture), \$/tonne	64	57	76	55